Pax6-dependent mechanisms in mammalian corticogenesis

Von der Fakultät für Lebenswissenschaften

der Technischen Universität Carolo-Wilhelmina

zu Braunschweig

zur Erlangung des Grades eines

Doktors der Naturwissenschaften

(Dr. rer. nat.)

genehmigte

D i s s e r t a t i o n

von Tran Cong Tuoc
aus Bac ninh / Vietnam

---

1. Referent: Prof. Dr. Hans-Henning Arnold
2. Referent: Prof. Dr. Martin Korte
eingereicht am: 06.06.2007
mündliche Prüfung (Disputation) am: 10.09.2007

Druckjahr 2007

Diese Arbeit wurde am Max Planck Institut für Biophysikalische Chemie
-Karl-Friedrich-Bonhoeffer-Institut-
in Göttingen
in der Abteilung für Molekulare Zellbiologie (Direktor: Prof. Dr. Peter Gruss),
Arbeitsgruppe Molecular Developmental Neurobiology (Gruppenleiter:
Prof. Dr. Anastassia Stoykova)
durchgeführt.

Acknowledgements

This study was performed from January 2004 to May 2007 in the Research Group Molecular Developmental Neurobiology, Department of Molecular Cell Biology in the Max-Planck- Institute for Biophysical Chemistry, under the supervision of Prof. Dr. Anastassia Stoykova.

Upon the accomplishment of my Ph.D. career, I would first like to sincerely acknowledge my supervisor, Prof. Dr. Anastassia Stoykova, who has brought me to the most exciting research field and offered me a great project. I would also like to thank her for her patient supervision as well as extensive support both in this project and in daily life. During the time in her Lab, what I have learned from her is not only the knowledge of neuroscience, but also scientific skills to be a good scientist.

I would like to express my gratitude to the following people for their support and assistance in my study:

- Martina Daniel, Silke Schlott, Silke Eckert for their outstanding technical assistance.
- Heike Fett, Sigurd Hille, Sharif Mahsur, Dr Bernd Föhring, BTL teams for their technical support.
- The members in department, especially, Dr. Kamal Chowdhury, Dr. Lingfei Luo, Prof. Dr. Michael Kessel, Dr. Mara Pitulescu, Sven Pilarski, Dr. Joachim Berger, Dr. Patrick Collombat, Dr. Ahmet Ucar, Andreas Zembrzycki, Dr. Gundula Griesel, Dr. Ulrike Teichmann for their valuable suggestions and discussions.
- B. Anderson, D. Anderson, I. Bach, R. Benezra, G. Bernier, D. Bohmann, C. Kaznovski, R. Klein, J. Liu, T. Niikura, H. Okano, M. Price, J. Rubenstein, V. Tarabykin for their generosities in providing experimental materials.
- Collaborative scientists: Dr. Konstantin Radyushkin (MPI Göttingen), Dr. Maria Carmen Piñon (University of Oxford), Prof. Dr. Zoltan Molnar (University of Oxford), Prof. Dr. Michail Davidoff (University of Hamburg) for providing me their unpublished data in the frame of the

project “Layer-specific defects and behavioral abnormalities in the cortex-specific Pax6 knock out mouse”
- Dr. Matthew Holt for his comments and correction of this script.
- Prof. Dr. Hans-Henning Arnold (TU Braunschweig) and Prof. Dr. Martin Korte (TU Braunschweig) for their kind acceptance to grade this thesis and to be involved in the thesis committee.

I sincerely say thanks to my wife and my brother for their persistent warm support. When I was almost exhausted by experiments, they gave me most of the consolations and motivation. They also shared with me many knotty duties of the Asiatic traditional culture. Without their support, I would not have finished my Ph.D. career successfully. Finally I am greatly indebted to my parent for their moral and intellectual supports and their encouragements. This thesis book is dedicated to my beloved parent.

Table of contents

1. Introduction

Each behavioral phenomenon in man, such as the perception of sensory input, performance of motor output and cognitive function, is controlled by the central nervous system (CNS). These processes are dependent on the precise interaction of billions of neurons, which are generated during embryonic development. While classical series of anatomical studies over a century ago helped us to understand the structure and organization of the nervous system, modern studies on the development of this most complex organ are expanding the knowledge on the cellular and molecular processes underlying the wonderful complexity of the mature nervous system.

1.1. Morphological organization of the central nervous system during embryogenesis and at maturity

After the closure of the neural tube at late gastrulation the caudal part forms the spinal cord, while anteriorly, three vesicles are formed: the rhombencephalon, mesencephalon, and prosencephalon. The rhombencephalon (hindbrain) gives rise to the pons, cerebellum and medulla oblongata, its cavity becomes the fourth ventricle. The dorsal part of the mesencephalon (midbrain) forms the tectum where colliculi superiores (the rostral tectum) and colliculi inferiores (the caudal tectum) are formed, and tegmentum where several nuclei are located. The cavity of the mesencephalon develops into the mesencephalic duct or cerebral aqueduct in the adult brain. The prosencephalon (forebrain) subdivides into the telencephalon and diencephalon (see also Table 1; Kandel et al., 2002). The dorsal part of telencephalon forms the cortex (pallium), connected with the olfactory bulb, while the ventral telencephalon (subpallium) gives rise to the basal ganglia (striatum). In the diencephalon, the territory of the pretectum, dorsal thalamus (with epithalamus), the ventral thalamus and hypothalamus are distinguished (Table 1; Fig.1; Kandel et al., 2002).

Spinal cord			
Brain	Brain stem	Rhombencephalon (Hindbrain)	Pons, Cerebellum, Medulla oblongata
		Mesencephalon (Midbrain)	Tectum, Cerebral peduncle, Pretectum, Mesencephalic duct
	Prosencephalon (Forebrain)	Diencephalon	Epithalamus, Thalamus, Hypothalamus, Subthalamus, Pituitary gland, Pineal gland, Third ventricle
		Telencephalon	Basal ganglia, Amygdala, Olfactory bulb, Hippocampus, Neocortex, Lateral ventricles

Table 1. Organization of the CNS

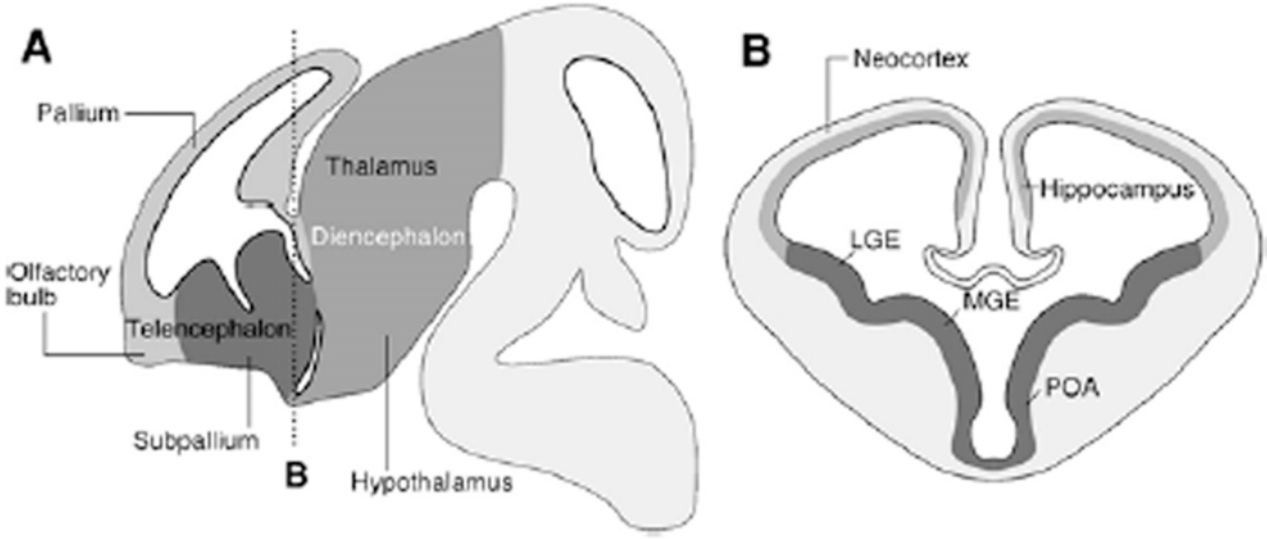

Figure 1. General organization of the mammalian telecephalon

The schema represents the major subdivisions of the embryonic telecephalon in sagittal (A) and coronal (B) views. LGE, Lateral Ganglionic Eminence, MGE: Medial Ganglionic Eminence, POA: Preoptic Area. (Adapted from Marin, 2003).

1.2. Patterning of the CNS during development

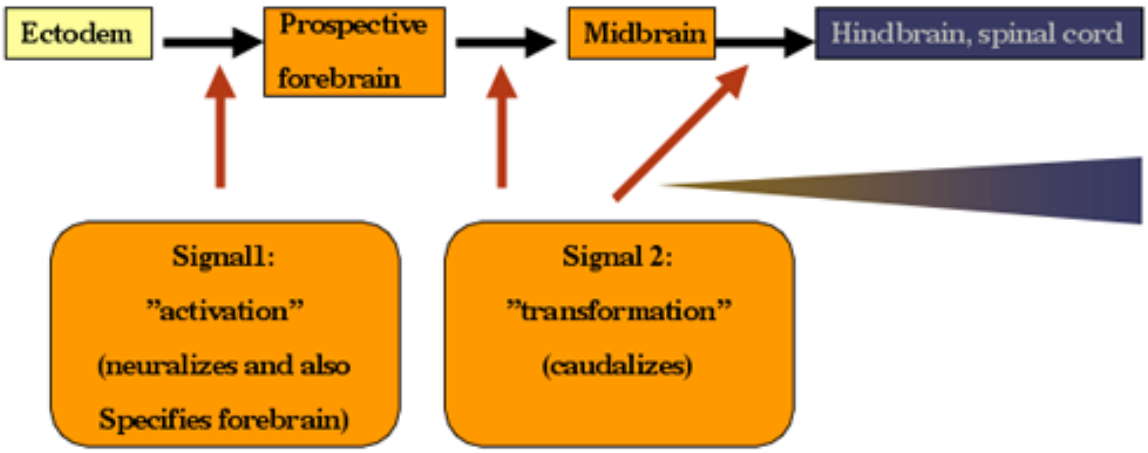

Figure 2. Activation-transformation model for establishment of the AP axis of developing CNS

In the first step (before the beginning of gastrulation), the hypoblast (in chick)/anterior visceral endoderm (AVE) (in vertebrates) specifies the prospective forebrain, "pre-forebrain state". During gastrulation, signals from the node and the early involuting mesoderm stabilize the induced neural fate with anterior characteristics. During the second step, signals from the lately involuting mesoderm cause transformation that leads to acquisition of posterior neural fate characteristics. (Adapted from Stern, 2001).

Patterning of the developing CNS is a process of spatiotemporal differentiation that ensures generation of cells of distinct fate in the correct number, time and location. Establishment of CNS patterning is a long and complex process that starts during gastrulation. Classical experiments in *Xenopus* demonstrated that the neural fate is the "defaults state" of the ectoderm, suppressed by BMP signaling between ectodermal cells. Inhibition of BMP function by molecules (activin, noggin, follistatin), secreted by the "organizer", abrogates BMP signaling and leads to the induction of neural fate with anterior characteristics (Wilson & Hemmati-Brivanlou, 1997; Streit & Stern, 1999). The decisive role in this process

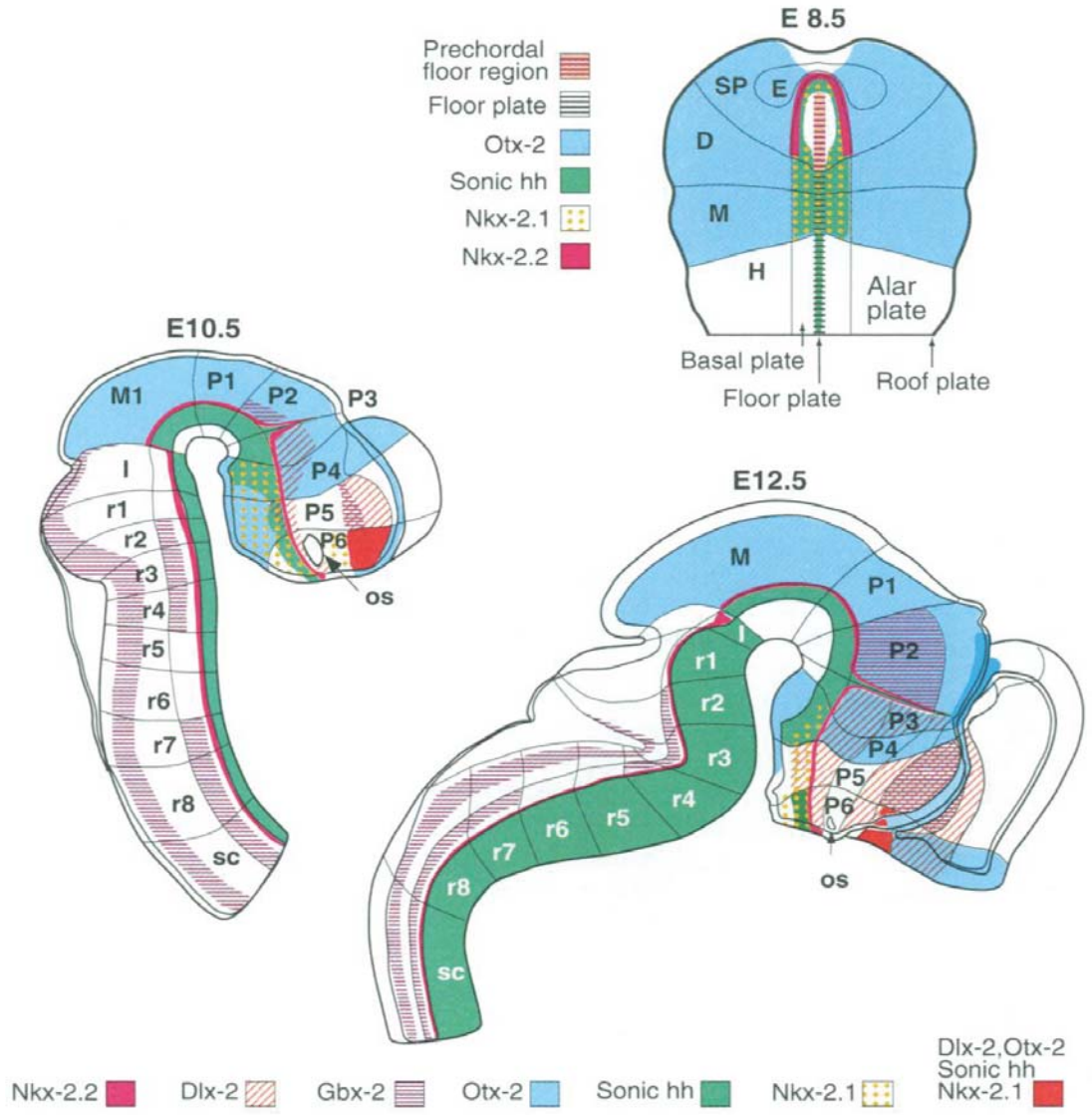

Figure 3. Prosomeres are defined by the expression of genes

The expression of six genes Dlx-2, Gbx-2, Nkx-2.1, Nkx-2.2, Otx-2, and sonic hedgehog (sonic hh) in the neural plate (E8.5) and the neural tube (E10.5 and E12.5) of the embryonic mouse brain are indicated. The fate map of the neural plate and neural tube are based on the studies of gene expression pattern (reviewed by Rubenstein et al., 1994). Neuroepithelium with molecularly specified expression of transcription factors defines prosomeres. The forebrain is organized accordingly to the prosomeres. The provisional transverse and longitudinal boundaries are shown as thin black lines. D, diencephalon; E, eyes; H, rhombencephalon-hindbrain; I, isthmus; M, mesencephalon-midbrain; os, optic stalk; p, prosomere; r, rhombomere; sc, spinal cord; SP, secondary prosencephalon. (Adapted from Rubenstein et al., 1994).

has the organizer (in *Xenopus*), named the Hensen node (in chicken) or the node (in mouse), representing the rostralmost part of the early involuting mesoderm with self-organizing and inductive properties (Stern et al., 2001). Recent evidence indicate that neural induction starts even before gastrulation during which the hypoblast (in chick) or the anterior visceral endoderm (AVE) in mouse induces the earliest neural fate (pre-neural stage) with anterior characteristics (pre-forebrain). Thus, it is assumed that during gastrulation inhibition of BMP signaling between ectodermal cells stabilizes and maintains the neural induction (Fig.2; Stern et al., 2001,). According to the activation/transformation model, the fate of the initially generated neural tube with anterior characteristics is transformed into posterior neural fate as a result of inductive interactions with the lately involuting mesoderm. Secreted factors belonging to the Wnt, FGF and RA (retinoic acid) pathways are involved in this process (Kudoh et al., 2002). As a result, the AP axis of the embryo body including CNS is established.

The development of the CNS depends on the spatiotemporal expression of sets of genes. In the hindbrain, the proliferative NE is subdivided into transverse segment territories (called rhombomeres) with distinct molecular properties and identities (Kiecker & Lumsden, 2005). In *Drosophila,* mouse and man the restricted expression of homeobox-containing homeotic genes (Hox genes) along the AP axis of the body (in the vertebrae, mesoderm, and CNS) generate the so-called HOX-Code that defines the functional identity of corresponding domains of the body (Kessel and Gruss, 1991; Krumlauf, 1992). Evidence from analysis of the expression pattern of more that 100 transcription factors (most of which belonging to the homeobox-containing genes) and regulatory molecules in the rostral brain indicated that their expression domain, respect longitudinal and transverse borders in the developing forebrain (Puelles & Rubenstein, 1993). This was the basis for proposing the “prosomeric model” of forebrain organization, according to which the prosomeres are transverse regions of the forebrain neuroepithelium, molecularly specified by the expression of sets of transcription factors (Fig.3; Rubenstein et al., 1994). The model was proven

and is widely used as a convenient morphological framework for the interpretation of expression patterns in the developing CNS.

1.3. Neurogenesis in mammalian telencephalon

The generation of different neuronal types in the developing telencephalon involves the coordinated programs of anterior-posterior (AP), dorso-ventral (DV) patterning of progenitors in two proliferative zones, the ventricular (VZ) and subventricular zone (SVZ) and their spatiotemporal specification.

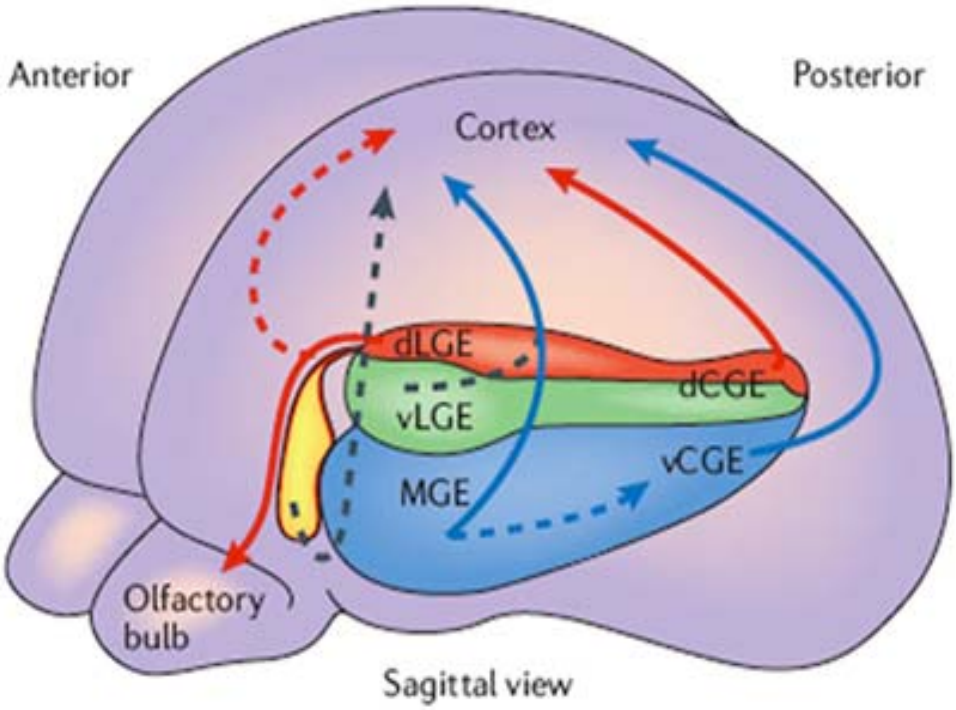

Figure 4. Migration pathways of cortical interneuron subgroups orginating in the ventral telecephalon

Schematic illustration shows distinct established (solid arrows) and possible (dashed arrows) pathways of migration of cortical interneurons from subdivisions of the ventral telecephalon to different places in the telecephalon. (Adapted from Wonders & Anderson, 2006).

Based on the expression patterns of homeobox and other transcription factors, the pallium is divided into four subdivisions: the medial, dorsal, lateral and ventral palliums (MP, DP, LP, VP, respectively). The subpallium contains

three main subdivisions: the lateral ganglionic eminence (LGE), subdivided into the dorsal (dLGE) and ventral (vLGE), medial (MGE) and caudal ganglionic eminences (CGE) (Fig.1; 4; Molnar et al., 2006; Puelles et al., 2000; Marin & Rubenstein, 2001). In mouse, the domains of the pallium and subpallium are specified by the differential expression of a number of transcriptional factors in the proliferative NE already by the E8.5 (reviewed by Rubenstein et al., 1994). While the progenitors of the dorsal telencephalon generate a six-layered structure, in the ventral telencephalon they produce several big nuclei. The main progeny of the pallial progenitors are the projection pyramidal neurons, which are excitatory and glutamatergic. After their generation in the ventricular zone (VZ), the neurons migrate radially along the extended process of the RG cells to their final destination into different cortical layers of the cortical plate (CP), a migratory process that is accomplished only in the postnatal period (P7 in mouse). In contrast, the progenitors in the ventral telencephalon produce GABAergic interneurons and stellate neurons of the basal ganglia. The interneurons (INs) migrate tangentially to contribute to the formation of the distinct cortical layers (Fig.4) (Marin & Rubenstein, 2001; Gorski et al., 2002; Wonders & Anderson, 2006).

1.4. Neurogenesis in mammalian cortex

During development of the mammalian cortex, neurons and glia cells (astrocytes and oligodendrocytes) are subsequently generated from neural stem cells, thereby allowing the establishment of functional neural circuitry (Bayer & Altman, 1991). In mouse cortex, neurons are generated largely from embryonic day 10 (E10) to E17, astrocytes start to appear at around E16, with their numbers peaking in the neonatal period, while differentiated oligodendrocytes are first seen postnatally (Bayer & Altman, 1991). Cultured E10–E12 cortical primary cells (considered as neural stem cells) generate only neurons for the first few days, followed by the sequential genesis of astrocytes and oligodendrocytes, indicating that an intrinsic program controls the temporal cell differentiation of the cortical progenitors (Qian et al., 2000). Studies in the last decade defined an intrinsic mechanism of epigenetic status, transcription factors and an intrinsic influence of environmental cues in establishing this fascinating and complex cell genesis, as well as the

neurogenic-to-gliogenic switch in the developing cortex (reviewed by Miller & Gauthier, 2007).

This introduction will focus mainly on the commitment of neural stem cells to a neuronal fate and differentiation. Other steps of neurogenesis (from neuronal maturation to synaptic integation of the newborn neurons in neuron circuits) and gliogenesis are reviewed comprehensively elsewhere (Ming & Song, 2005; Liedo et al., 2006, Ge et al., 2007; Miller & Gauthier, 2007).

1.4.1. Neural stem cells

In the mammalian telecephalon there are three different populations of progenitors that generate neurons, namely the neuroepithelial (NE or stem cells), radial glial (RG) and basal progenitor cells (BP, named also intermediate progenitors, IP) (Fig.5). Before the beginning of neurogenesis, NE forms a single layer of cells. The neural stem cells have the capacity of self-renewal, which is achieved by symmetric or asymmetric cell divisions, generating two daughter cells with stem cell properties, or one “renewed” stem cell and a pluripotent (or partially fated progenitor), respectively (Guillemot et al., 2006; Gotz & Huttner, 2005). The mechanisms involved in self-renewal of neural stem cells, and maintenance of their undifferentiated state is largely unknown. Findings in the last decade implicated a number of signaling pathways like Notch, Fgf, Wnt and factors such as Emx2, REST, Numb, Numb-like, Tlx, Bmi-1 is essetial in this process (reviewed by Alvarez-Buylla & Lim et al., 2004).

At the onset of the neurogenesis, the NEs give rise to ealiest-borned neurons of the cortex (the Cajal-Retziuz cells) and the RG cells (Fig.5). The majority (more than 90%) of the cortical progenitors are RG cells expressing immunoreactivity for RC2, Nestin, Vimentin, GFAP, astrocyte-specific glutamare transporter (GLAST) and brain lipid binding protein (BLBP), (Misson et al., 1988; Parnavelas & nadarajah, 2001; Campbell & Gotz, 2002). Because shortly before birth the RG cells transform into astrocytes, the classical view until recently was that the RG cells are progenitors of the glial cell lineage only. Novel evidence, however, challenged this view. It turned out that RG cells with long radial processes and expressing glial-specific markers

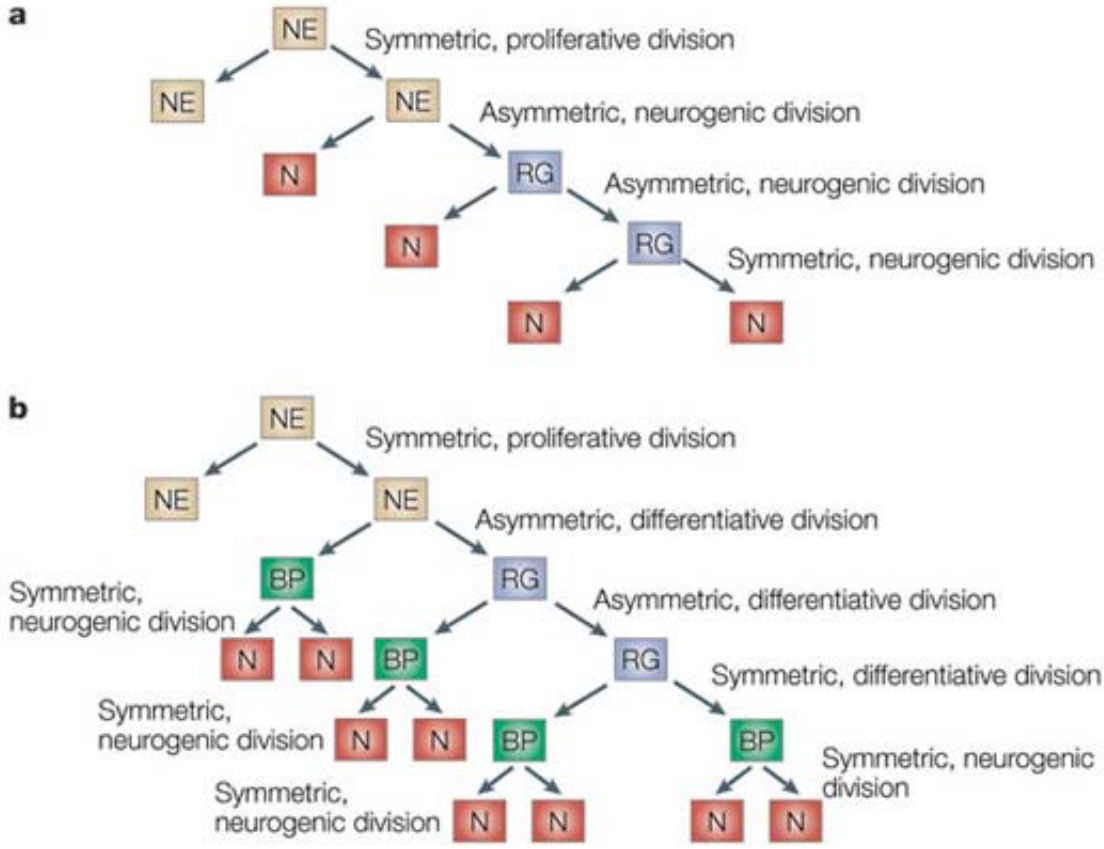

Figure 5. The lineage trees show a simplified view of the relationship between neuroepithelial cells (NE), radial glial cells (RG) and neurons (N), without (a) and with (b) basal progenitors (BP) as cellular intermediates in the generation of neurons and the types of cell division involved. (Adapted from Gotz & Huttner, 2005).

are actually pluripotent cortical progenitors that can generate both, neuronal and glial cells. The RG cells divide at the apical surface of the telencephalic vetricle and generate either directly or indirectly the majority of the cortical neurons. In contrast to RG, the BPs undergo mitosis at the basal side of VZ, where after stage E13.5 in mouse, a second proliferative zone is formed (the subventricular zone, SVZ) (reviewed by Campbell & Gotz, 2002; Guillemot, 2005).

1.4.2. Neuronal differentiation

In vertebrates, the transition of stem cells into committed neuronal progenitors involves a highly coordinated switch in the transcriptional program. This switch is regulated by basic helix-loop-helix (bHLH) transcriptional activators, such as the proneural genes *Ngn1* and *Ngn2*. The activation of proneural genes has the capacity to initiate a full program for neuronal differentiation of the neural stem cells (Ma et al., 1996; Farah et al., 2000; Mizuguchi et al., 2001). Analysis of mouse null mutants revealed the determinant role of proneural genes in the commitment of neural stem cells to a neuronal fate in the cortical development (Fode et al., 2000; Nieto et al., 2001; Schuurmans et al., 2004). In single or double mouse mutants for *Ngn1* and *Ngn2,* there are severe defects in the neuronal differentiation program, including the specification of the cortical neuronal layer identity and the acquisition of proper transmitter phenotype (Fode et al., 2000; Schuurmans et al., 2004). Interestingly, the reduced neurogenesis in the absence of function of these proneural genes is accompanied by an increase in the gliogenesis, demonstrating their importance in promoting the choice of a a neuronal fate and inhibiting the alternative glia cell fate (Nieto et al., 2001; Sun et al., 2001). Notably, the progression from neural stem cells to committed neuronal progenitors and subsequent differentiation involves not only transcriptional activators (like the proneural proteins) but also transcriptional repressors. In fact REST/NRSF, a factor well known to repress neuronal genes in non-neuronal cells was recently discovered as an important modulator of neurogenesis (Ballas et al., 2005). This important study revealed that a progressive reduction in the binding affinity of REST to neuronal promoters is crucial for the transition from pluripotent stem cells to neural stem cells and then to neurons. Strikingly Gage ´s laboratory identified a small modulatory RNA (smRNA) with a similar binding sequence to REST/NRSF and which acts as a competitor of REST/NRSF. Results from gain-of-function (GOF) and dominant-negative experiments demonstrated the important role of this new class of non-coding RNA in cell-lineage commitment and neurogenesis (Kuwabara et al., 2004).

1.4.3. Epigenetic factors in neurogenesis

It has also been demonstrated that the maintenance of pluripotetial stem cells and their transition towards progenitors of different cell lineages such as neurons and glial cells are also tightly controlled at a global level. These studies provided evidence that chromatin-remodeling factors and modification factors of the histone “code” are involved in switching on or switching off genes in an “inactive” state in stem cells and an “active” state in differentiated cells (Kaeser & Emerson, 2006). In fact, Xi & Xie, (2005) demonstrated that distinct chromatin-remodelling complexes regulate the response to signals in neurogenic zones that control the self-renewal of different stem cell types. Recently, the examination of the role of Brg1, a catalytic subunit of SWI-SNF involved in tissue-secific development, revealed that this chomatin remodelling factor is required for neuronogenesis. Interestingly, interactions between Brg1, Ngn and NeuroD implicate a coupling of chromatin remodeling factors with neuronal commitment and neuronal differentiation factors in regulating the neurogenesis (Seo et al., 2005a). Geminin, another factor with high expression in neural progenitors, controls the progression from neural proliferation to differentiation. Geminin was shown to interact with Brg1 and antagonizes its function during neurogenesis (Seo et al., 2005b).

1.4.4. Adult neurogenesis

Neurogenesis was traditionally believed to occur only during embryonic stages in the mammalian CNS (Ramon y Cajal, 1913). Only recently it become generally accepted the existence of neural stem cells with limited neurogenic capacity in few neurogenic zones of the mature brain, namely the SVZ of the lateral ventricle and the subgranular layer (SGL) of the dentate gyrus (DG) of hippocampus (Gross, 2000, Alvarez-Buylla & Lim et al., 2004; Liedo et al., 2006). Understanding of adult mammalian neurogenesis has considerable progress since one discoveries of the distribution of neural stem cells, proliferation, specification of neuronal progenitors, neuronal maturation, migration, nerve guidance, to synaptic integration of newborn neurons in the adult neuron circuits (Gross, 2000, Alvarez-Buylla & Lim et al., 2004; Ming & Song, 2005; Liedo et al., 2006). The common appearance of intrinsic and external factors supporting neurogenesis in active zones of both the

embryonic and adult brain suggest that there is (at least in part) a conserved genetic program of neurogenesis in both stages of development (Hevner, et al., 2006; Liedo et al., 2006). The main distinguishable feature of adult and embryonic neuronogeneses is that in the adult brain, neurogenesis is taking place in an environment that does not favor the generation of new neurons. Therefore, neurogenesis in the adult forebrain needs a protection from the anti-neurogenic influences of the surrounding environment and requires the maintenance of permissive niches (Kempermann et al., 2004; Alvarez-Buylla & Lim et al., 2004; Liedo et al., 2006). The demonstration of active adult neurogenesis opens possibilities for repairing of the adult CNS after injury or degenerative neurological diseases in the future.

1.5. Introduction of the mammalian cortical development

In the mammalian cortex, billion of neurons with distinct morphologies, connectivities, molecular and physiological properties are organized radially in six layers and in numerous tangential functional domains. The study of corticogenesis before 1990 formulated two general hypotheses: the protomap (Rakic, 1988) and protocortex (O´Leary, 1989). The former proposed that the cortical progenitor zone contains the information that determines the cortical areas identity, whereas the later theory postulated that thalamic afferent axons impose the cortical area identity through activity-dependent mechanism.Abundant recent evidence indicates, however that cortical regionalization includes interplay of intrinsic as well as extrinsic mechanisms (reviewed by Sur & Rubenstein, 2005). The intrinsic mechanisms seem to have a more decisive role in the molecular patterning and establishment of cortical area identity, while the thalamocortical projections contribute to the final delineation and maintenance of the area size (O´Leary, 1989; O´Leary and Nakagawa, 2002; Sur & Rubenstein, 2005).

The neurons of distinct cortical layers are generated according to an inside-first/outside-last program. In this way, the early-born neurons (during the period E10-E14 in mouse) populate the lower layers 6 and 5 (L6, L5,

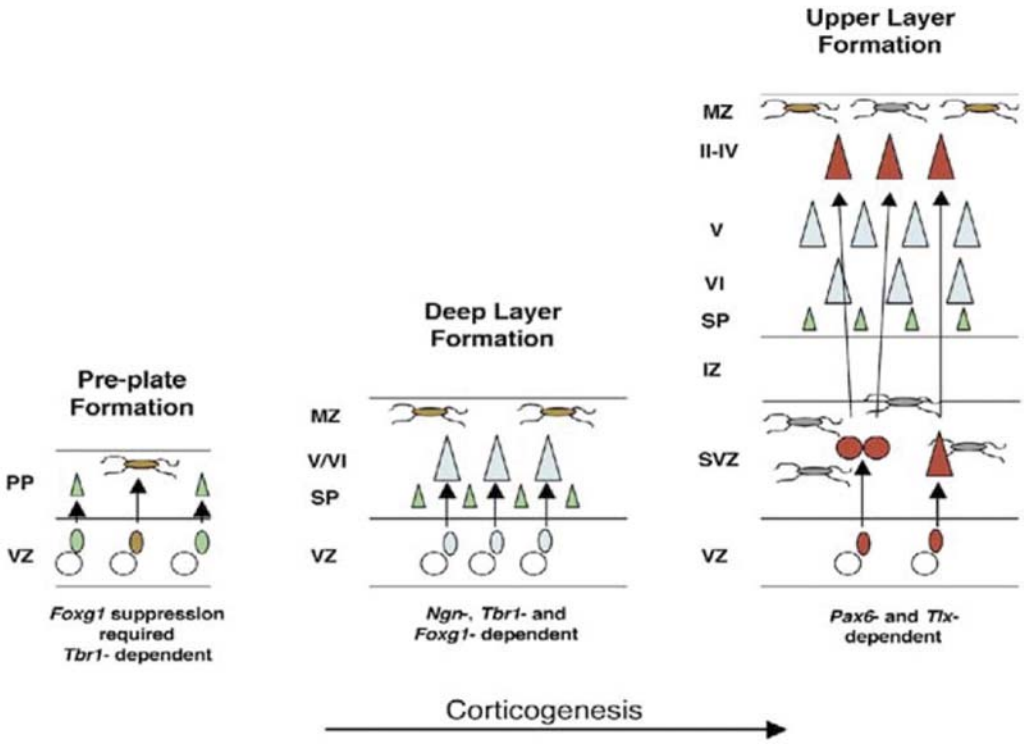

Figure 6. Schema showing the three progressive stages of corticogenesis: preplate formation, lower and upper layer formation

The formation of the preplate (PP) requires the expression of *Tbr1*, whereas the generation of Cajal-Retzius (CR) neurons (brown cells) involves the suppression of *Foxg1* at the earliest stages of corticogenesis. Deep layer neurons (light blue cells) are generated and require the function of both *Ngns* (for L6, L5) and *Tbr1* (for L6). When upper layer cortical neurons (L4-2, red cells) are generated, *Ngns* and *Tbr1* appear to be dispensable, but the functions of *Pax6* and *Tlx* are absolutely required. II-VI, layer 2-6; IZ, intermediate zone; MZ, marginal zone; PP, pre-plate; SP, subplate; SVZ, subventricular zone; VZ, ventricular zone; (Adapted from Campbell, 2005).

named also infragranular layers, IGLs). The neurons generated by the late progenitors (E14.5 – E18.5) form the upper layer (L4, L3, L2, also named supragranular layers, SGLs) (Rakic, 1988). Results form classical transplantation experiments in ferret revealed that the acquiry of distinct neuronal layer fate is dependent on environmental cues after the S phase of the last mitotic cycle of the progenitors (McConnell & Kaznowski, 1991). Furthermore recent data indicates that specification of layer identity in the cortical neurons depends on the function of different transcription factors

during, a specific developmental time window. For instance, telencephalic transcription factor Foxg1 is required to suppresse the earliest born neurons, the Cajal-Retzius (CR) cells and thereby restricts the developmental potential of cortical progenitors (Hanashima et al., 2004). In addition to Foxg1, T-box transcription factor (Tbr1) has been shown to be a genetic determinant for preplate formation, including the differentiation of early-born glutamatergic neurons, CR cells (Fig.6, Hevner et al., 2001; Cambpell, 2005; O´Leary and Nakagawa, 2002).

1.6. Transcription factor Pax6

1.6.1. Conserved function of Pax6 in evolution

Pax6 is a member of the evolutionary conserved Pax gene family (reviewed by Callaerts et al., 1997; Mansouri et al., 1999; Simpson & Price, 2002; Kozmik, 2005). Pax6 was first cloned from human and subsequently from other vertebrate and invertebrate species (reviewed by Callaerts et al., 1997). Pax6 orthologues are highly conserved in both their protein sequence and function. Therefore it is likely that the downstream targets of Pax6 are also highly conserved among species (reviewed by Gehring & Ikeo, 1999).

Mutation of *Pax6* in humans causes the inherited disease *aniridia* (Heyman et al., 1999; Malandrini et al., 2001; Sisodiya et al., 2001), characterized by multiple ocular defects and some neurological and behavioral disabilities (e.g. deficiency in learning). A point mutation between PD and HD of *Pax6* leads to the generation of a premature stop codon and therefore to premature termination of the translation, thus producing a protein without any functional activity (Hill et al., 1991). The homozygous *Sey/Sey* mice die at birth without eyes and severe brain abnormalities (see below). Heterozygous mice show defects in the optic cup (Hill et al., 1991).

Of the four *Drosophila* Pax6 orthologues, it is thought that the *eyeless* (*ey*) and *twin of eyeless* (*toy*) gene products share functional homology with the vertebrate canonical Pax6 isoform. Two other *Drosophila* Pax6 orthologues, *Eye gone (Eyg) and Twin of Eyegone (Toe),* lack the amino-terminal PAI domain and rely only on the RED and HD domain for their

binding capacity. The sequence specificity of Eyg has been studied and found to be very similar to that of Pax6(5a) (Jun et al., 1998; Kozmik, 2005). Similarly, homologue Pax6 mutant, *ey* in the *Drosophila* shows ocular defects analogous to those found in humans and mice (Quiring et al., 1994). By targeted expression of the *ey, toy*, mouse or human Pax6 in various imaginal disc primordia of *Drosophil*a, ectopic eye structures were induced on the wings, the legs, and on the antennae (Czerny et al., 1999; Halder et al., 1995). Reciprocally, vertebrate eye-like structures can be generated by the ectopic expression of *ey* or *toy* in *Xenopus* (Onuma et al., 2002). These data demonstrate that the function of Pax6 is conserved during eye development in animal phyla (reviewed Gehring & Ikeo, 1999; Gehring, 2002).

In addition to its role in eye genesis, *Pax6* is also important in development of the brain and olfactory organs. The *Sey/Sey* embryos lack nasal structures and die at birth with serious brain abnormalities, including forebrain patterning and growth defects. *Aniridia* patients, heterozygous for mutations of *Pax6*, also show defects in cerebral cortex and olfactory organs (Sisodiya et al., 2001, see below). The *drosophila* Pax6 homologues *ey* and *toy* are also expressed in the central nervous system, particularly in the mushroom bodies (Callaerts et al., 2001; Kurusu et al., 2000), which are higher-order brain centers for olfaction associated with learning and elementary cognitive functions in the fly (reviewed by Heisenberg, 1998). *Ey* has been shown to have an important function during axonal differentiation of neurons in the mushroom bodies (Callaerts et al., 2001; Kurusu et al., 2000).

Evidence has been also presented for the evolutionary conservation of *Pax6* gene regulatory elements. Tp date multiple distinct promoters and regulatory elements of mouse *Pax6* have been identified (Kammandel et al., 1999; Anderson et a., 2002; Griffin et al., 2002; Morgan, 2004; Kleinjan et al., 2004; Kim & Lauderdale, 2006). Kammandel et al (1999) reported the identification of three conserved transcription start sites (P0, P1, alpha) in the murine *Pax6* locus. By using transgenic mouse, independent cis-regulatory elements controlling the tissue-specific expression of Pax6 were defined. Specifically, the 4.6-kb region upstream of exon 0 is required to mediate Pax6 expression in the lens, cornea, lacrimal gland and pancreas. Another 530-bp

enhancer fragment located downstream of the Pax6 translational start site in exon 0 is required for expression in the neural retina, the pigment layer of the retina and the iris. Finally, a 5-kb fragment located between the promoters P0 and P1 can mediate expression in the dorsal telencephalon, hindbrain, and the spinal cord (Kammandel et al., 1999). Interestingly, an enhancer of *Drosophila ey* inserted in front of either P0 or P1, is able to reproduce features of the endogenous expression pattern of mouse Pax6 in transgenic mice (Xu et al., 1999). In a reciprocal experiment, the mouse P1 element is also able to drive lacZ reporter gene expression in the eye of *Drosophila* (Xu et al., 1999). This further suggests that Pax6 is preserved during evolution not only at the nucleotide level but also at the functional level.

1.6.2. Pax6 in the mammalian forebrain

In the developing mouse brain, the expression of Pax6 is detected as early as E8.5, confined to the progenitors in the VZ of the dorsal telencephalon, the anlage of the cortex (Walther and Gruss, 1991; Stoykova and Gruss, 1994). The majority (88%) of the E13.5 cortical progenitors represent the RC2-positive radial glial progenitors that also express Pax6 (Gotz et al., 1998). In absence of Pax6, the RG progenitors have morphological defects and abnormalities in their mitotic cycle and expression patterns, indicating that Pax6 is an intrinsic determinant of RG progenitors (Gotz et al., 1998).

1.6.2.1 Pax6 in the regional patterning of the forebrain

Studies on the function of *Pax6* last decade demonstrated an essential role of Pax6 in the patterning of the telecephalon. The expression of *Pax6* and the homeobox transcription factor Gsh2 is restricted to the progenitors of the pallium and subpallium, respectively, governing cortical and striatal development by regulating genetically opposing programs (reviewed by Guillemot et al., 2006). In the *Sey/Sey* mutant mice where Pax6 is not functional (Hill et al., 1991), there is a severe defect in dorsoventral (D/V) molecular patterning at the pallial-subpallial border (PSPB), seen as a down-regulation of the expression of pallial markers and a shifting of the expression of ventral molecular markers into more dorsal pallial domains (Stoykova et al., 1996; 2000;Toresson et al., 2000; Yun et al., 2001; Muzio et al., 2002; Kroll

and O´Leary, 2005). As a result of the progressive ventralization of patterning at the PSPB, during development a portion of the pallial progenitors acquire subpallial identity that leads to increase of ectopically located GABAergic INs in the pallium (Kroll and O´Leary, 2005).

In the cortical progenitors, the expression of Pax6 shows a gradient, being strongly expressed rostrolaterally and only faintly in the caudomedial domains. In contrast, the homeobox transcription factor Emx2 exerts a complimentary gradient in developing cortex, expressed at a high level in caudomedial and at low level in the rostrolateral cortex. By comparing the expression patterns of molecular markers in these two mutants, opposite defects in cortical arealization were detected, suggesting that Pax6 and Emx2 might be able to regulate their own specific expression profiles that have a role in specification of the rostral or caudal cortical identity, respectively (Bishop et al., 2001, 2002, Muzio et al., 2002; reviewed by Mallamaci, Stoykova, 2006). Notably, in absence of the function of both Emx2 and Pax6 proteins, the entire cortex acquires morphological and molecular features reminiscent of those of the striatum (Muzio et al., 2002a; Muzio et al., 2002b). It should be noted however that due to severe defects in the diencephalons found in the *Sey/Sey* embryos (Stoykova et al., 1996; Warren and Price, 1997), the thalamocortical axons do not reach the cortex (Jones et al., 2002). This limits the analysis of effect of the abolishment of the Pax6 function on the cortical area identity, normally throught studying the axonal projections between distinct cortical areas and their corresponding target s within sensory nuclei of the diencephalon. Thus function of Pax6 in the cortical identity is still remaining to be investigated.

1.6.2.2 Pax6 in neuronal specification and cortical layers

As already noted Pax6 is expressed in the radial glial cells (RG), a majority of the dorsal pallium progenitors generating both neurons and glial cells (Malatesta et al., 2000; 2003; Miyata et al., 2001; Anthony et al., 2004; Noctor et al., 2004). In the *Sey/Sey* mutant mice the cortical RG progenitors show alterations of their morphologies, proliferation parameters and expression patterns (Götz et al., 1998; Warren et al., 1999; Estivill-Torrus et al., 2002) and they generate no more than 50% of the normal neuronal progeny of the

cortex (Malatesta et al., 2000). Recent results from retrovirus-mediated overexpression of Pax6 in cortical primary cultures demonstrated an enhancement of the neurogenesis in primary cortical cultures *in vitro* (Heins et al., 2002). Similarly, conditional overexpression of Pax6 in the cortical progenitors of transgenic mice in *vivo* indicated a limited enhancement of neurogenesis especially by the progenitors in the ventral pallium (Berger et al., 2007). Together, these data indicate that the expression of Pax6 in cortical progenitors endows them with neuronal ability (Heins et al., 2002).

Analysing the cortical phenotype of *Sey/Sey* embryos revealed severe defects in neuron generation especially of the upper cortical layers, which might be involved in migratory deficits of the SGL neurons (Caric et al., 1997). The expression of the specific markers, *Svet1, Cux1/2* and *Satb2,* both in the pallial progenitors of the subventricular zone (SVZ) and in the upper layers, is abolished in the *Sey/Sey* cortex (Tarabykin et al., 2001, Nieto et al., 2004; Britannova et al., 2005), suggesting a Pax6-dependent mechanism for generating the upper cortical layers mediated by the progenitors located in the SVZ (reviewed by Cambpell, 2005; Guillemot et al., 2006). Recently analyses of mutants for cortical layer determinants suggested the idea that the generation of the lower and upper cortical layers is controlled largely by the Ngn1/2-dependent and Pax6-depentdent mechanisms, respectively (Fig.6, Cambpell, 2005, Shuurman et al., 2004*).*

However, because *Sey/Sey* embryos die at birth while the final neuronal allocation in distinct cortical layers is accomplished only postnatally. Therefore the final conclusion about the layering defects in the *Sey/Sey* mutant is still an open question.

1.6.3. Molecular properties of the Pax6 protein

In vertebrates the *Pax6* gene encodes two protein isoforms, Pax6 and Pax6(5a) (Fig.7; Carriere et al., 1995; Richardson et al., 1995; Zaniolo et al., 2004). Knowledge about the molecular structure of Pax6 proteins is critical to their biological activity. The paired domain (PD) can be structurally and functionally separated into two independent DNA-binding sub-domains, PAI

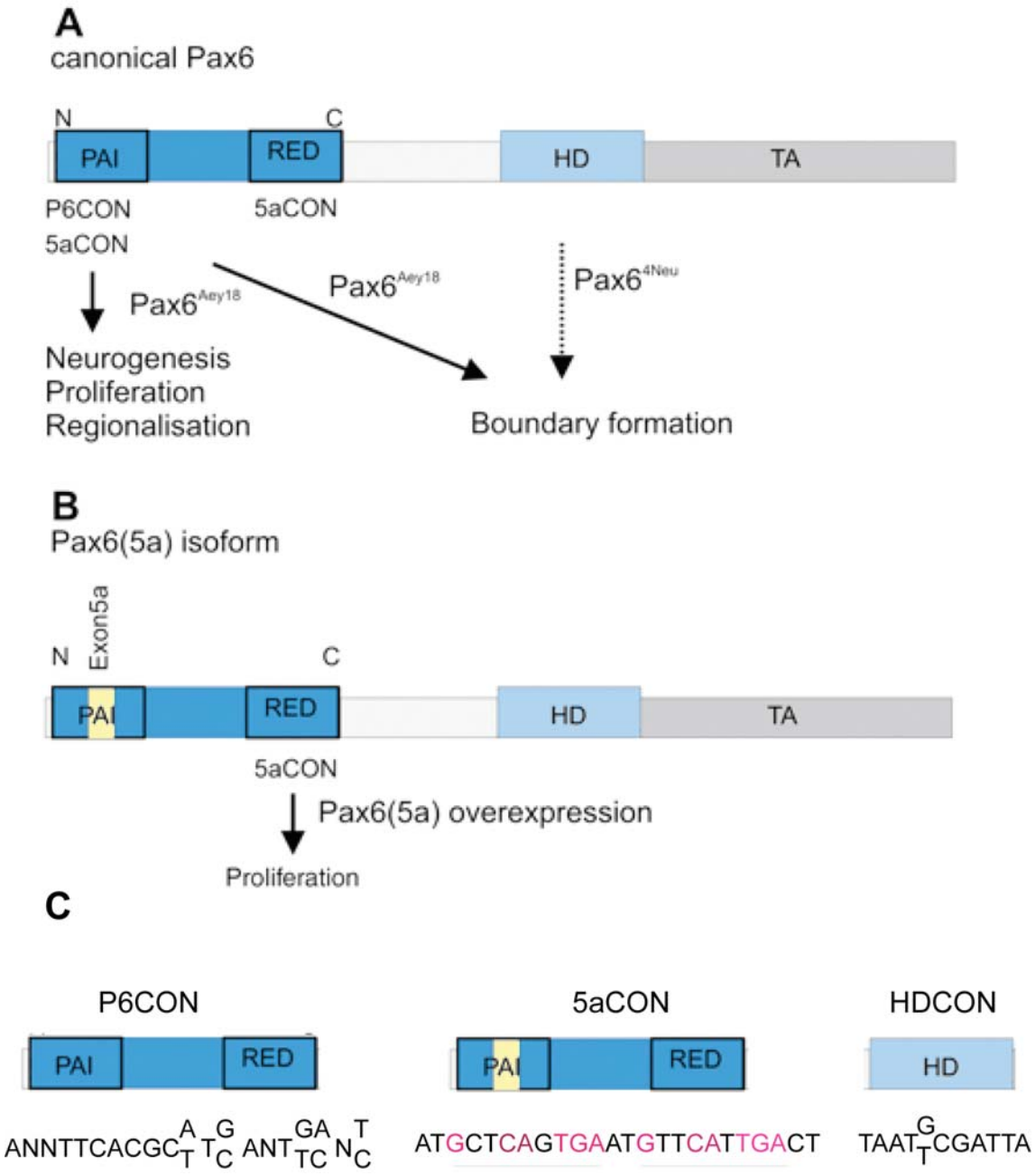

Figure 7. Structure and DNA-binding domains of Pax6

(A/B) In vertebrates Pax6 genes encode two Pax6 isoforms, Pax6 (A) and Pax6(5a) (B) with two different DNA-binding domain, PD and HD. PD can be structurally and functionally separated into two DNA-binding subdomains, PAI and RED. Analyses of mouse Pax6 mutants with defects either in PD or HD showed that the PD of Pax6 is important for the regulation of neurogenesis, proliferation and regionalization in the developing telencephalon, while both PD and HD are required for the formation of the pallio-subpallial boundary (A). Retroviral overexpression revealed the anti-

proliferative role of the Pax6(5a) isoform in cortical cells (B). (C) Distinct domains of Pax6 and Pax6(a) can bind specifically to DNA sequences. Transactivation domain (TA) is required for the full activity of Pax6. PD, Paired Domain; HD, Homeobox Domain; TA, Transactivation Domain; P6CON, Consensus Pax6 Binding Site; 5aCON, Consensus Pax6(5a) Binding Site; HDCON, Consensus Binding Site of Pax6 HD (Adapt from Haubst et a., 2004).

and RED (Fig.7; Czerny et al., 1995; Epstein et al., 1994b; Jun et al., 1998). Mouse Pax6 contains 128 amino acids (Epstein et al., 1994a). In contrast, Pax6(5a) contains a 14 amino acid insertion within the PAI domain forming a distinct paired domain, PD-5a. This insertion eliminates the DNA-binding capacity of the PAI subdomain, leaving the RED subdomain and HD responsible for DNA recognition.

Consequently, these two Pax6 variants recognize different DNA sequences (Fig.7; Epstein et al., 1994b; Kozmik et al., 1997). This initial study showed that the Pax6-binding sequence (known as P6CON) is a bipartite region of 20 base pairs with its 5'-half and 3'-half recognized by the PAI and RED sub-domains, respectively (Fig.7; Epstein et al., 1994a; Czerny et al., 1995). P6CON was derived as a perfect binding site deduced from a series of enrichments for high affinity binding oligonucleotides from an initial pool of random oligonucleotides (Epstein et al., 1994a). Similarly, perfect binding sites were identified for PD(5a) and HD, called 5aCON and HDCON (Fig.7), respectively (Epstein et al., 1994b; Czerny et al., 1995). Evidence for cooperation between Pax6 PD and HD has been shown in the promoter of the neural cell adhesion molecule L1 (Chalepakis et al., 1994). Thus, the DNA–binding properties of the functional Pax6 domains implies that distinct Pax6 binding domains, alone or in cooperation, could regulate different classes of downstream target genes. In fact, a recent analysis of several mouse Pax6 mutants with distinct defects either in PD or HD, combined with gain-of function studies, demonstrated that while the Pax6 PD is necessary for regulation of Pax6-dependent neurogenesis, cell proliferation and patterning, both PD and HD are required for boundary formation at the PSPB. Furthermore retrovirus-mediated overexpression of the Pax6(5a) isoform

inhibits cell proliferation without affecting cell fate. Therefore these results demonstrate a key role for the functional domains of Pax6 in different features of brain development (Fig.7; Haubst et a., 2004).

Molecular studies have also shown that the entire C-terminal region of Pax6 is an activation domain, essential for full activity of the protein (Glaser et al., 1994; Tang et al., 1998; Singh et al., 1998; Duncan et al., 2000a; Mikkola et al., 2001). This activation domain is phosphorylated by kinases, including ERK, p38 kinases and HIPK2 (Carriere et al., 1993; Mikkola et al., 1999; 2001; Kim et al., 2006). The principal residue, serine 413, is evolutionary conserved. If this serine is mutated to alanine, the transcriptional activity of Pax6 is significantly reduced (Mikkola et al., 2001). O-glycosylation of Pax6 was reported (Lefebrve et al., 2002) that might modulate protein-protein interaction between Pax6 and other proteins. Future studies about posttranslational modifications of Pax6 might elucidate further the function of Pax6 in development.

1.6.4. Targets of Pax6 in development

Genes whose expression are modulated by direct interactions between transcriptional factors and their regulatory elements, referred to direct targets. Identification of genes regulated by Pax6 is an essential issue in understanding its biological function. To show the molecular mechanisms of Pax6-dependent gene regulation, the data have to pass a series of tests (Chalepakis et al., 1992). The expression pattern of the Pax6 protein has to precede and overlap the expression pattern of the mRNA of its target gene. The expression level of the target gene must be modulated in response to the activation and inactivation of Pax6 *in vivo*. Regulatory regions of target genes have to contain at least one Pax6 binding site. Binding of Pax6 to this region has furthermore to be demonstrated both *in vitro* using footprinting or gel shift assays and *in vivo* using chromatin immunoprecipitations (ChIPs). Trans-activation assays of the regulatory regions with a reporter gene (e.g. luciferase, LacZ, or GFP) in cell culture, *in ovo* experiment or *in vivo* transgenic mice, give the final proven that activation of a candidate gene is under direct control of Pax6.

Studies have revealed that Pax6 regulates a diverse range of genes (reviewed by Simpson and Price, 2002), including transcription factors: Ngn2, Six3, c-Maf, Prox1, Brg1, Pitx3 and Etv6 (Scardigli et al., 2003; Ashery-Padan et al., 2000; Goudreau et al., 2002; Sakai et al., 2001; Chauhan et al., 2002) and specific adhesive molecules: Integrins, R-cadherin and L1-CAM (Duncan et al., 2000b; Andrews and Mastick, 2003).

Recently new methods that utilize high throughput techniques such as cDNA microassay (Chauhan et al., 2002; Holm et al., 2007) and chromatin immunoprecipitation on chip (ChIP-on chip; Weinmann and Farnham, 2002) are speeding up the identification of downstream genes of Pax6.

1.7. Post-translation modification and ubiquitination of protein

The proteins that underlie the behaviour of any cell type are produced by selective gene expression. However, cells respond continuously to cues from their external and internal environments. The cellular response to changing conditions is frequently mediated by numerous post-translational modifications (PTMs) of the proteins, including phosphorylation, ubiquitination, sumosylation, methylation, acetylation or glycosylation (see review by Walsh & Jefferis, 2006). PTMs are chemical modifications of proteins, one of the later steps in the protein biosynthesis for many proteins. A crucial point for understanding the cellular regulation of PTMs is to define mechanisms by which they exert alterations in cellular phenotype. One mechanism by which PTMs can alter the function of protein is to directly induce a new conformational state. Thus, if PTMs occur with proteins that act as regulatory determinants, this might cause changes in the cellular phenotypes of those proteins (Walsh & Jefferis, 2006). Alternatively, PTMs could modify histon proteins or chromatin remodeling factors. In this way PTMs could modulate either the transcription machinery at a global level or the cell lineage-specific expression of genes (Li et al., 2007)

Among PTMs, protein ubiquitination mediates various mechanisms in control of the protein activity. Initially protein ubiquitination is though to have an exclusive function in labeling the target protein for the ubiquitin-

proteasome system (UPS)-mediated degradation. In this mechanism, ubiquitination is a sequence of reactions catalyzed by at least three classes of enzymes. Ubiquitin is first activated by the ubiqutin-activating enzymes (E1), delivered to the ubiquitin-conjugating enzymes (E2), and then transferred to or mediated by the ubiquitin ligases (E3). Among these, the E3 ligase defines the specificity of substrates (Hochstrasser, 2006). The E3 ligases are categorized into three distinct classes based on the domain with E3 ligase activity: HECT, U-box and RING finger-containing E3 ligases. During protein ubiquitination, RING finger-containing E3 ligases interact with both E2 enzymes and substrates to bring them into a close proximity, allowing the transfer of the ubiquitin moiety from E2 enzymes to substrates (Hochstrasser, 2006). However recent studies reported that protein ubiqutination is also involved in controlling the epigenetic, gene–silencing and transcriptional programs (Li et al., 2007). Future studies are necessary to understand additional PTMs, their mechanisms and the protein targets of PTMs during different cellular responds.

1.8. The aims of study

Our understanding of *Pax6* function in the mammalian corticogenesis relied so far largely on analysing the phenotype of mice with the natural mutation of Pax6 in the *Sey* mice or in mice after a conventional knockout of *Pax6* (*Pax6KO* mice) (St-Onge et al., 1997; Hill et al., 1997). However both of these Pax6 deficient mice in homozygosity die at birth, thus making impossible to study cortical layering, because the allocation of cortical neurons in their final positions in the distinct cortical layers is accomplished only during the second postnatal week (in mouse). The analysis of the role of pax6 in cortical area identity is also not possible because of severe defects of the sensory thalamus. The main aim of this project was to use the Cre-LoxP recombinantion system in order to generate a cortex-specific knock out of the Pax6 function only in the pallial progenitors at the beginning of the neurogenesis thus possibly allowing to avoid the lethality of embryos of the Pax6 mutant. With this system one expects to gain understandings of the role of *Pax6* in different aspects of the postnatal cortex. Given that the determinant role of *Pax6* in the corticogenesis, the second aim of this study was to search for cofactors that modulate the neurogenic activity of Pax6.

2. Results

2.1. Transgenic system for the conditional inactivation of *Pax6* in cortical progenitor

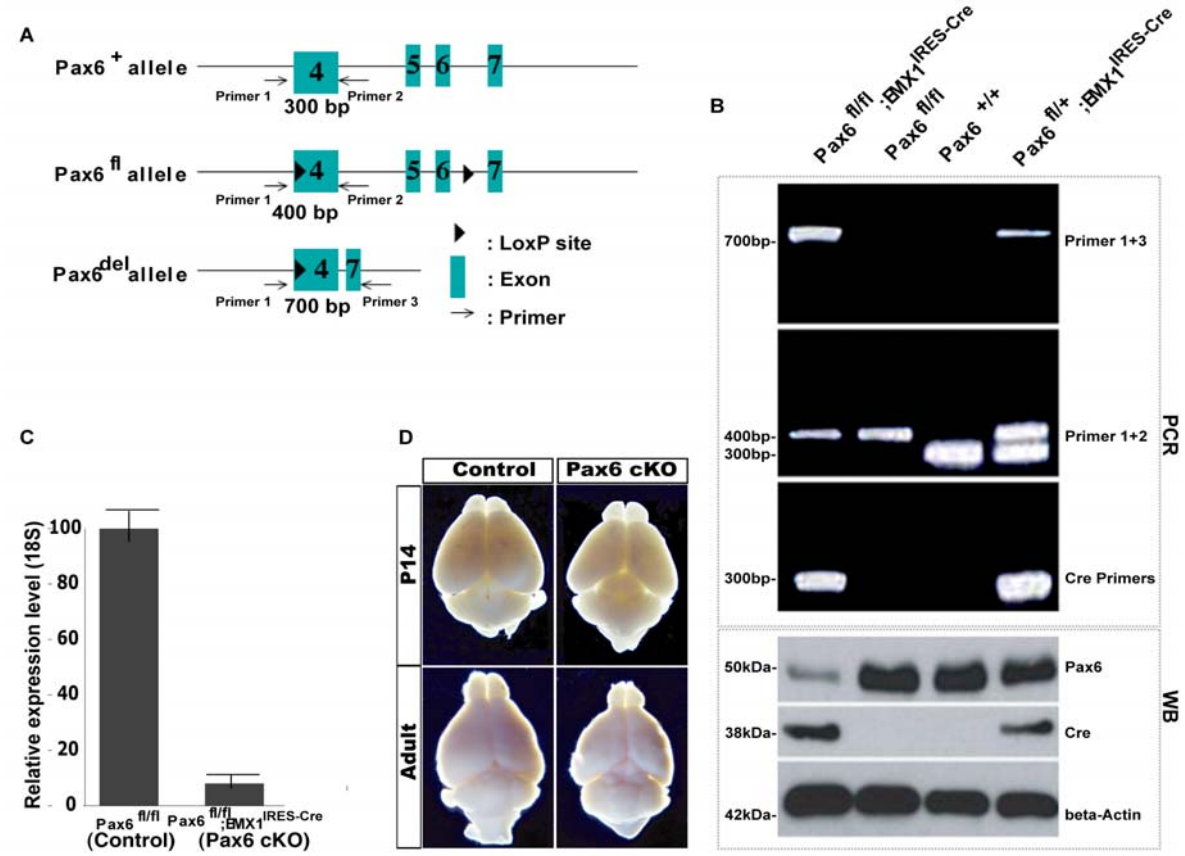

Figure 8. The targeted inactivation of *Pax6* in cortical progenitors

(A) The schema represents the relative positions of exons, loxP sites and primers for genotyping in WT allele (*Pax6*$^{+}$ allele), floxed *Pax6* allele (*Pax6*$^{fl/fl}$ allele) and Cre-mediated deletion of floxed Pax6 allele (*Pax6del* allele) (Ashery-Padan et al., 2000). (B) Combinations of primers with sizes of PCR products for genotyping of embryos and mice in the targeted inactivation system of *Pax6* in cortical progenitors are indicated. The quantification by WB (B) and qPCR (C) showed a diminishing at protein and RNA level of *Pax6cKO* as compared to the control. (D) The comparison revealed *Pax6cKO* mice have a smaller brain at both P14 and adult than those of WT. qPCR, Quantitative RT-PCR; WB, Western blot.

In order to perform inactivation of *Pax6* only in the cortical progenitors, we applied the Cre-LoxP recombination strategy (Sauer & Henderson, 1989; Rajewsky et al., 1996; reviewed by Kwan, 2002). This technique has proved to be a very useful tool for activation and inactivation of specific genes in a "conditional" manner in spatially and temporally restricted patterns. This helps to circumvent the limitations of conventional gene inactivation, particularly, when a given gene has multiple roles at different times and in different tissues. The Cre-LoxP systems consist of two basic elements (two transgenic mouse lines). One line carries the conditional allele, in which a gene segment (or the entire gene) is flanked by the two recognition target sites (loxP). LoxP, a 34-bp consensus sequence, consists of two 13-bp inverted repeats, flanking an 8-bp non-palindromic core. Another transgenic line provides a spatially and temporally controlled expression of the recombinase enzyme (Cre). The Cre recombinase catalyzes recombination to bring about the deletion of the associated DNA in between the two LoxP sites (Sauer & Henderson, 1989; Rajewsky et al., 1996; reviewed by Kwan, 2002).

In this study, we used two transgenic mouse lines: *Pax6* ^{flox} mice (Ashery-Padan et al., 2000) and *Emx1* $^{IRES\text{-}Cre}$ mice (Gorsky et al., 2002). In the *Pax6*^{flox} mice the wild type (wt) allele (*Pax6*$^{+}$ allele) is replaced by gene targeting with a modified *Pax6* allele (*Pax6* ^{flox} allele), in which the partial exon 4 and exons 5, 6 (covering the paired domain), are flanked by two loxP sites (Fig.6A; Ashery-Padan et al., 2000). In the *Emx1*$^{IRES\text{-}Cre}$ mice, the expression of Cre recombinase is controlled by the promoter of the gene *Emx1,* thus being active only in the pallial progenitors, driving effective recombination strating at stage E9.5, and reaching full recombination at stage E12.5 (Gorski et al., 2001). Thus by crossing the *Pax6* ^{flox} and *Emx1* $^{IRES\text{-}Cre}$ mice, we generated a double transgenic mouse line in which the function of *Pax6* is conditionally inactivated only in the pallial progenitors at the onset of neurogenesis. The system for the cortex–specific inactivation of Pax6 was verified by using set of primer pairs for the genotyping allowing to identify the floxed (400bp), wild type (WT, 300bp) or the deletion (700bp) fragment of the corresponding alleles (Fig.8A/B). The western blot and qPCR analyses of extracted proteins and RNA from E12.5 cortices furthermore revealed no

more that 8% residual level of Pax6, both at protein and RNA level, in the *Pax6*$^{fl/fl}$*; Emx1*$^{IRES\text{-}Cre}$ pallium (named thereafter *Pax6cKO*) (Fig.8B/C). The generated *Pax6cKO* mice are healthy, fertile, and reach adulthood. The only obvious malformation of the isolated *Pax6cKO* brain was its smaller size as compared to WT at both juvenile (P10-P15) and adult (3-7 months old) stage (Fig.8D).

2.2. Pax6 specifies the upper cortical layer neurons

Previous data suggested that in the *Sey/Sey* embryos the upper cortical layers are misbuilded (Schmahl et al., 1993; Caric et al., 1997; Stoykova et al., 2000, Schuurman et al., 2004). Two mechanisms have been proposed to be involved in this defect: either a failure in specification of the upper layer neuronal fate (Tarabykin et al., 2001; Schuurmans et al., 2004) or migratory deficiency specifically affecting the late-born neurons (Caric et al., 1997). As already mentioned, the early prenatal lethality of the *Sey/Sey* embryos seriously hampers the study of these processes, because cortical neurons reach their final location into the CP not earlier than stage P8 in mouse.

We took advantage of the *Pax6cKO* mice to examine this issue. We studied the specification of the SGL neurons at postnatal stage P10 (when the neurons are already located at their final position) by using different molecular markers such as *Cux2* (for L4-2; Iulianella et al., 2003), *EphA4* (for L4-2, Garel et al., 2002), *RZRß* (for L4; Nakagawa & O'Leary, 2003), *Svet1* (Tarabykin et al., 2001), *Lmo4* (mostly L4-2, Bulchand et al., 2003). The results showed that *Cux2*+ neurons were entirely missing in the rostroparietal mutant CP (Fig.9A/A´) as well as in progenitors of SVZ at E16.5 (data not shown). Only a few CP cells in the mutant expressed *Eph4* (Fig.9B/B´), *RZRß* (Fig.9C/C´), and *Svet1* (Fig.9F/F´). Similarly, the expression of *Lmo4* was down regulated in the SGLs of the mutant frontal cortex (Fig.9D/D´). Interestingly, transcription factor Id2, normally expressed in the neurons of L5 as well as in the SGL neurons (Neuman et al., 1993; Jen et al., 1997) was specifically down regulated only in the upper

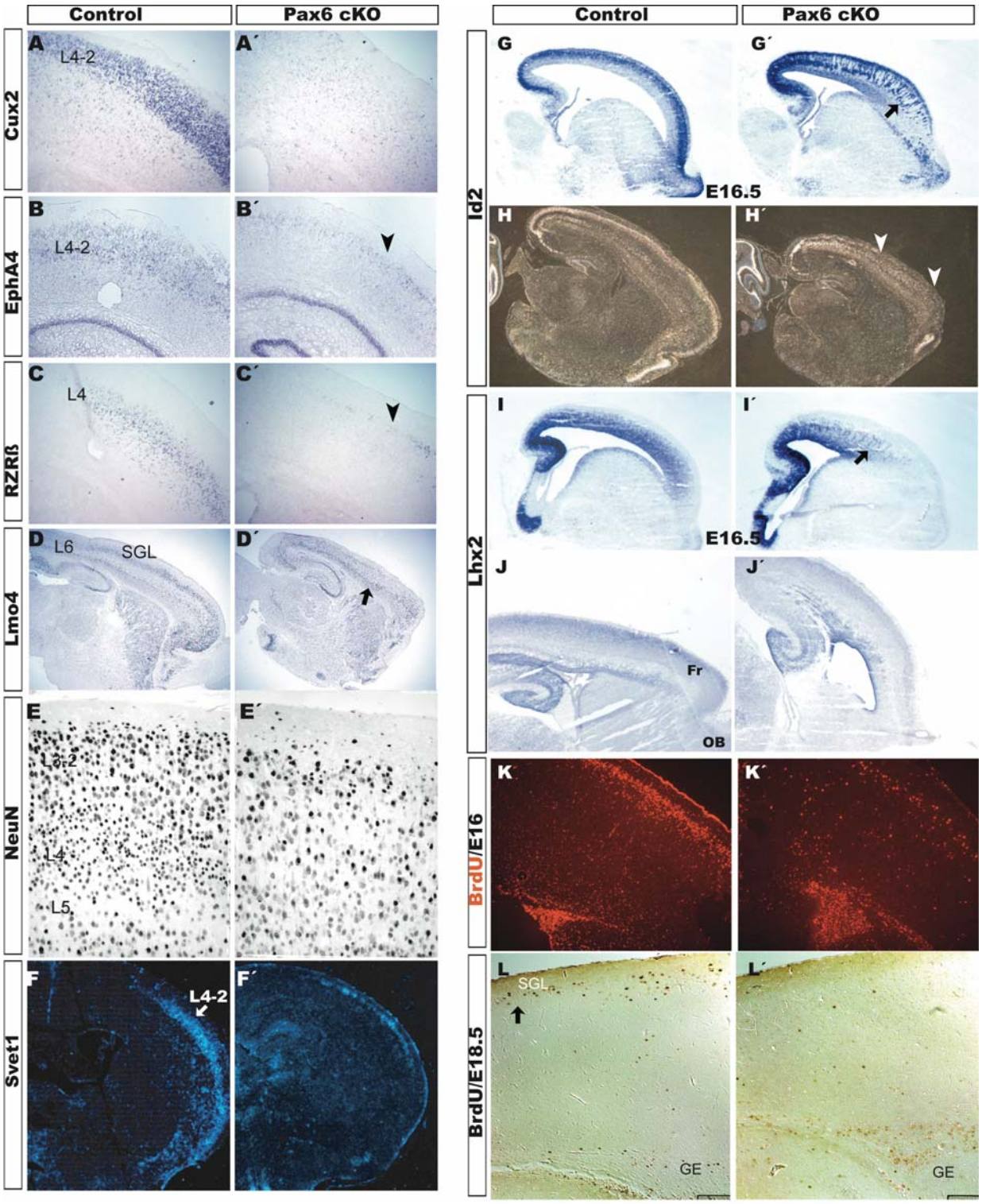

Figure 9. Pax6 specifies the upper cortical layers neurons

ISH and IHC on sections from E16.5 brains (G/G´, I/I´) and from P10 (the others) with markers as indicated. The results showed a complete loss in the expression of *Cux2* (A/A´) or severe attenuation in expression of *EphA4, RZRß, Lmo4* (B/D´, pointed with arrowheads). Note that the expression of *Lmo4* in SGL is lost in the rostral cortex, however a thicker band is seen in the position of the IGL neurons (arrow, D/D´).

(G/H´) Id2 expression is not seen in the rostral SGL neurons at P10, while at E16.5, big expression gaps were detected. (I/J´) Similarly, such complete loss in rostral SGL neurons at P10 and expression gaps at E16.5 was observed in the expression of Lhx2 in Pax6 mutants as compared to the control. (E/E´) Immunostaining with neuN antibody revealed only a few neurons in the position of the SGLs. After BrdU birthdating at stage E16.5 (K/K´) and E18.5 (L/L´), BrdU+ cells are missing at SGL and kept in excess in GE of the *Pax6cKO* cortex at P10 (K/L´). GE, Germinative epithelium; SGL, Subgranular layer.

cortical layers of the rostral cortex (Fig.9H/H´). Analysis of the expression of *Id2* at stage E16.5 (when the generation of the upper layer neurons is at maximum) showed big expression gaps rostrally (Fig.9G/G´) suggesting that proportion of these progenitors are not specified towards the *Id2*+ neuronal fate in absence of *Pax6*. Likewise, the strong expression of TF Lhx2 in the superficial L4-2 at P10 (Bulchand et al., 2003) was abrogated in the mutant (Fig.9J/J´) at P10. Interestingly, similarly to *Id2*, also the expression of *Lhx2* at E16.5 exhibited big expression gaps in the progenitors of the rostral cortex (Fig.9I/I´), suggesting a failure of the specification of this neuronal sub-lineage as well. In addition and consistent with the results from the in situ hybridization analysis, immunostaining with NeuN, a marker for postmitotic neurons revealed only few neurons at the position of the SGLs in *Pax6cKO* brains (Fig.9E/E´).

To study whether the lack of SGL neurons at their normal location might be a result of migratory problems, we traced the SGL neurons in the postnatal *Pax6cKO* cortex by BrdU-pulse labeling at E16.5 (when the generation of SGL peaks) and at E18.5 (when predominantly L3-2 are born). We noticed a severe depletion of BrdU+ cells in the SGLs in both stages along with an increased number of BrdU+ cells in the GE at the PSPB (Fig.9K/L´). The migration defect hypothesis implies that SGL cells were specified correctly, but remain near their origin in the GE. However, despite using numerous SGL markers, we were unable to detect any correctly differentiated SGL neurons either in ectopic lower positions of the CP or in the enlarged VZ/SVZ of the *Pax6cKO* cortex at P10 or 3 months after birth.

Together these, results indicate that late RG progenitors in the *Pax6cKO* do not transition into distinct SGL neuronal subpopulations in a region-specific manner and furthermore indicates that *Pax6* has an intrinsic role in the specification of the upper cortical layer neurons.

2.3. The lack of Pax6 affects normal neuronal outcome and the migration of subpopulations of IGL neurons

Recent data from mutant analyses supports the view that different genetic mechanisms are involved in the cortical layer specification in which the generation of IGL is largely dependent on the function of *Ngn1/2*, while the production of the SGL appears to depend on *Pax6* and *Tlx* function (Fig.6; Schuurmans et al., 2004, reviewed by Campbell, 2005). However, during development Pax6 shows strong expression in the early RG progenitors (generating the IGL neurons) and Pax6 directly controls the expression of *Ngn2*, especially in the rostrolateral pallium (Stoykova et al., 2000; Scardigli et al., 2003). This motivated us to reexamine the question whether *Pax6* might be involved in the patterning of the IGL neurons.

Initial results from immunohistochemistry with NSE (neuron specific enolase) antibody strongly suggested that the number of the pyramidal neurons in the *Pax6cKO* cortex was enhanced, and NSE+ cells appeared trapped within corpus callosum (CC) above the hippocampus (Hi, Fig.10C/C´). In addition, the *Pax6cKO* cortex showed an intensified immunoreactivity for SMI-32 antibody that predominantly labels large pyramidal neurons of layer 5 (L5, Voelker et al., 2004) at P10 (Fig.10E/E´) and in the adult brain (Fig14D/D´).

To assess IGL neuronal identities of the pyramidal neurons from distinct layers, we performed in situ hybridization analyses with layer specific probes on sections from *Pax6cKO* and control mice at P10. The gene *Vglut1* (vesicular glutamate transporter 1) is expressed in all pallial glutamatergic neurons, most strongly in L5 pyramidal neurons (Fremeau et al., 2000). In the mutant, the darker stained band of such neurons was displaced to the uppermost position of the CP and *Vglut1*+ cells were stranded in the lowest

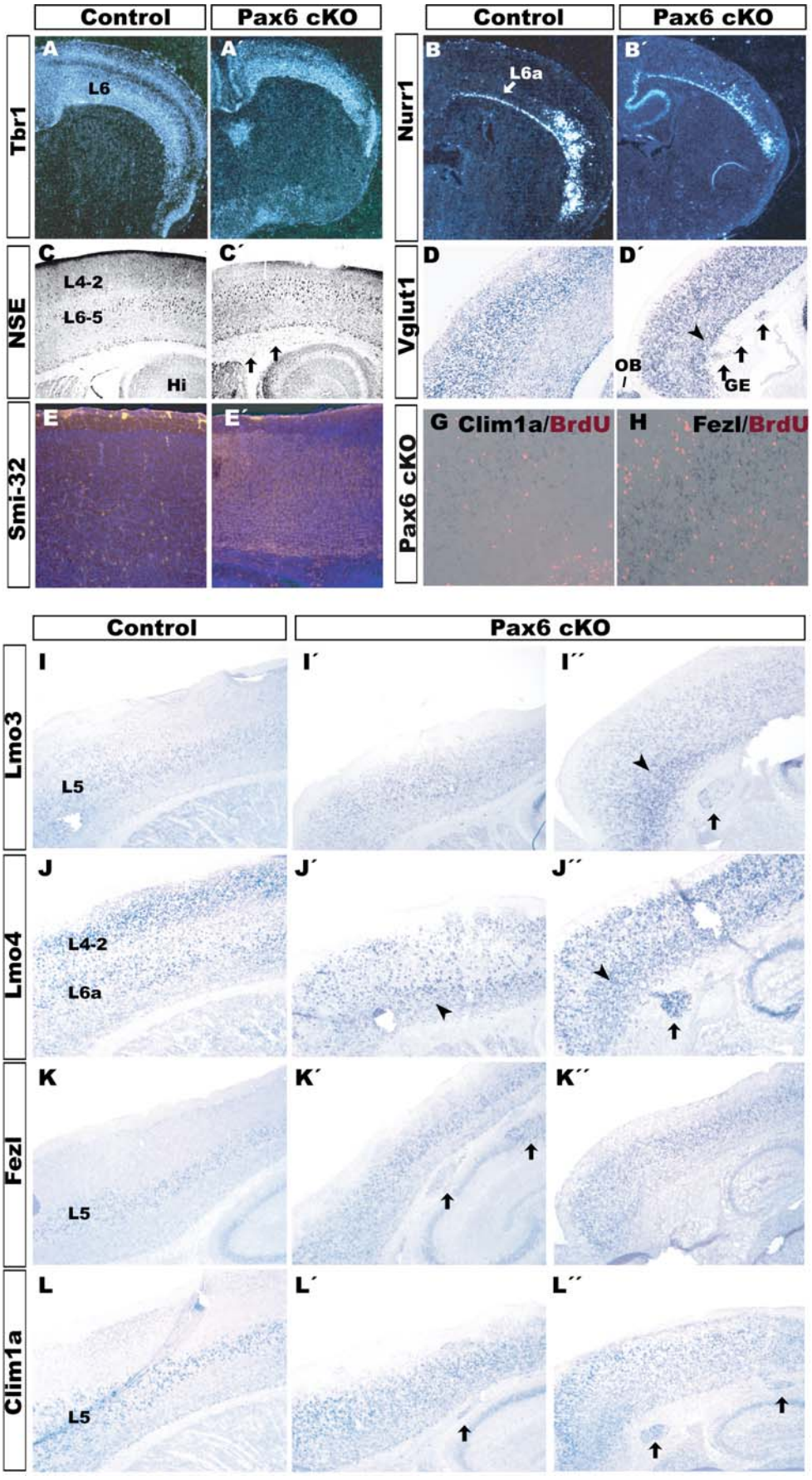
Control
Pax6 cKO
Control
Pax6 cKO
Tbr1
A
L6
A´
Nurr1
B
L6a
B´
NSE
C
L4-2
L6-5
Hi
C´
Vglut1
D
D´
OB
GE
Smi-32
E
E´
Pax6 cKO
G Clim1a/BrdU
H Fezl/BrdU
Control
Pax6 cKO
Lmo3
I
L5
I´
I´´
Lmo4
J
L4-2
L6a
J´
J´´
Fezl
K
L5
K´
K´´
Clim1a
L
L5
L´
L´´

Figure 10. Defects in the migration and pool-size of subsets of IGL neurons of *Pax6cKO* cortex

ISH and IHC analyses revealed defects in the migratory properties of subpopulations of IGL neurons, labeled by *NSE* (C/C´), *Vglut1* (D/D´), *Lmo3* (I/I´´), *Lmo4* (J/J´´), *Fezl* (K/K´´), *Clim1a* (L/L´´), *Slap1* (data not shown). In the mutant, an augmented pool of subsets of IGL neurons, expressing *NSE* (C/C´), Smi-32 (E/E´), *Fezl* (K/K´´), *Clim1a* (L/L´), also *Lmo4* (Fig.9D/D´) was detected. Arrows point to ectopic mis-locations of cell populations in the mutant cortex. After BrdU labeling at E16.5, the double IHC/ISH analysis with BrdU antibody and ISH markers for L5 neurons, *Clim1a* (G) or *Fezl* (H) showed no co-localization of BrdU with these two markers. No change in the expression pattern of two other IGL markers for L6, *Tbr1* (A/A´), *Nurr1* (B/B´) was found in the mutant cortex. GE, Germinative epithelium; OB, ofactory buld;

portion of the CP as well as in the enlarged rostral GE (Fig.10D/D´). Similar cell aggregates were also observed along the CC, hippocampal SVZ (HiSVZ), and posterior periventricular zone (pPv; data not shown). However, the expression of transcription factors *Tbr1* in L6 (Fig.10A/A´) and *Nurr1* in L6a (Fig.10B/B´) appeared not affected in the mutant. The two members of the LIM-only gene family *Lmo3* and *Lmo4* are expressed in subsets of IGL and SGL neurons (Bulchand et al., 2003). The broad and faint expression zone of *Lmo3* that includes most of L5 and L6a neurons was displaced to a more superficial position in the mutant CP (Fig.10I/I´), while rostromedially, *Lmo3*+ cells accumulated in the lowest CP or formed aggregates along the white matter (WM) (Fig.10I´´). In contrast to Lmo3 (accepted mostly as an IGL neuronal marker), *Lmo4* labels a small subset of L6a neurons and a portion of L4-2 neurons (Bulchand et al., 2003). In the mutant cortex, more *Lmo4*+ L6a neurons appeared at lower than their normal position, while *Lmo4* expression of the SGLs of the frontal cortex was almost completely abolished (Fig.10J/J´, Fig.9D/D´).

We extended further our analysis by examining the expression of two specific markers for L5 neurons, *Clim1a,* a cofactor for LIM-HD transcription factors that labels only the deeper position of L5 neurons (Bulchand et al., 2003) and *Fezl,* (*Zfp312, Fez1*), a putative TF containing a zinc-finger domain (Inoue et al., 2004), and recently proposed to be involved in specification of

the corticospinal motor neurons (CSMN, Ariotta et al., 2005; Molyneaux et al., 2005). *Fezl* transcripts appeared to be enhanced in *Pax6cKO* cortex and *Fezl*+ cell clumps were detected in CC above Hi (Fig.10K/K´´). Remarkably, we found that the pool of *Clim1a*+ L5 neurons was clearly enlarged in the *Pax6cKO* cortex at P10 (Fig.10I/I´´) as well as in the adult brain (Fig.14C/C´). In addition, on almost adjacent sagittal sections at medial level, *Clim1a*, *Lmo3* and *Lmo4* label similar cell aggregates ectopically located in the WM and RMS (Fig.10I´´/L´´). Thus, when Pax6 is not functional, subpopulations of molecularly correctly specified IGL neurons (*NSE*+*, Vglut*+*, Clim1a*+*, Lmo3*+*, Lmo4*+ and *Fezl*+*)* have migratory deficits, and the pool of subsets of IGL neurons (*Clim1a*+*, Fezl*+*, Lmo4*+, Smi32+*)* appears to be enlarged. One possibility that might explain the detected enhancement of subpopulations of IGL neurons could be a failure in the specification of the late RG progenitors, keeping on to produce neurons with early (IGL) identity even at late in neurogenesis. To investigate this possibility, we performed BrdU labelling at E16.5 (to label late-born neurons of SGLs) and studied the expression of early IGL markers (*Fezl* and *Clim1a*) in the BrdU+ cells at stage E18.5 by double ISH/IHC (Fig.10G/H). Remarkably, no co-localization of these layer 5 markers with BrdU was found indicating that the increase of IGL neuronal subtypes in *Pax6cKO* cortex is not due to a extended capacity of the late RG to produce early neurons.

All together, our findings indicate that Pax6 plays an important role in modulating the progenitor pool size and migratory ability of specific sub-lineages of IGL neurons.

2.4. Er81 acts downstream of Pax6 in a subpopulation of L5 neurons in the rostral cortex

When applied as a L5 neuronal marker, the expression of the ETS transcription factor *Er81* (Brown and McKnight, 1992) was also altered in the *Pax6cKO* brain. One characteristic was a severe attenuation of *Er81* expression in the parietal domain of the mutant cortex at P10 (Fig.11B/B´). Analysis at E17.5 indicated that *Er81* expression was markedly decreased in the pallial VZ and CP (Fig.11D/E´). We identified potential binding sites for

Pax6 (Epstein et al., 1994) in location -1190 to –1225 in the mouse *Er81* promoter (Coutte et al., 1999). Thus next we investigated direct binding of Pax6 to this sequence by using Electromobility Shift Assay (EMSA). Results of EMSA indicated that Pax6 protein binds to the *Er81* promoter with a low affinity as compared to a sequence of perfectly consensus binding site for Pax6 (Fig.11G, lane 3 and 6). The specificity of the binding was controlled by incubation with anti-Pax6 antibody, which super shifts the DNA-Pax6 protein-Pax6 antibody complex (Fig.11G lane 7). Binding of Pax6 was completely abolished after mutation of the binding site sequence (Fig.11G lanes 9, 10). To determine whether the binding site in the *Er81* promoter is indeed occupied by Pax6 protein in vivo, the chromatin immunoprecipitation (ChIP) assay was performed using mouse tissues of E15.5 WT cortex. In the chromatin that was precipitated with Pax6 antibody, a fragment of 282 bp in location –1322 to –1040 of the *Er81* promoter covering the Pax6 binding sites was detected, while region from –431 to –164 of the *Er81* promorter (used as an external control) was not amplified (Fig.11H). Together, this data indicate that Pax6 protein binds both in vitro and in vivo to the *Er81* promoter.

To study whether Pax6 can activate the *Er81* transcription, we transfected cell lines (Hela, NIH3T3) with a construct containing the *Er81* promoter fused with a luciferase reporter (Er81-Luc) alone or together with the Pax6 expressing plasmid CMV-Pax6 (Fig.11I). Control transfected cells displayed a very low basal level of luciferase activity, whereas co-transfection of Er81-Luc with an increasing amount of *CMV-Pax6* led to robust luciferase activity in a concentration-dependent fashion (Fig.11I). To examine whether *Pax6* is able to activate the *Er81* promoter in a live embryo, we performed *in ovo* coelectroporated chick embryos with *Er81-Luc* plus *CMV-Pax6* and this resulted in marked luciferase expression in contrast to the control co-electroporations of *Er81-Luc* plus *CMV-Gfp* (empty vector) (Fig.11G/k´´). These results indicate that pax6 could activate trans-activity of Er81 promoter at both culture and *in ovo* experiment.

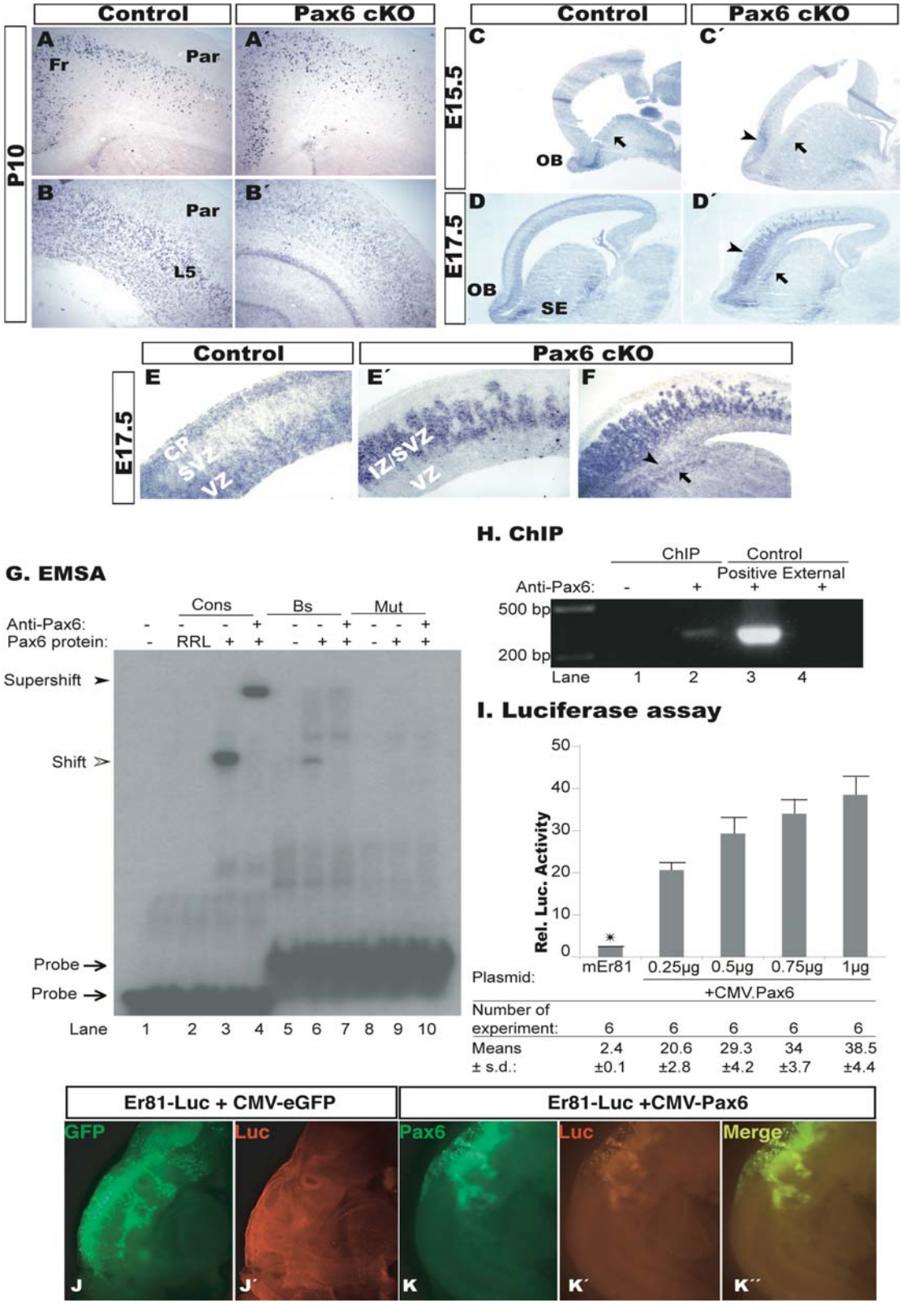
Control
Pax6 cKO
P10
A
Fr
Par
A´
B
Par
L5
B´
E15.5
C
OB
C´
E17.5
D
OB
SE
D´
Control
Pax6 cKO
E17.5
E
CP
sVZ
VZ
E´
iZ/sVZ
VZ
F
G. EMSA
Cons
Bs
Mut
Anti-Pax6:
Pax6 protein:
RRL
Supershift
Shift
Probe
Probe
Lane 1 2 3 4 5 6 7 8 9 10
H. ChIP
ChIP
Control
Positive External
Anti-Pax6:
500 bp
200 bp
Lane 1 2 3 4
I. Luciferase assay
Rel. Luc. Activity
50
40
30
20
10
0
Plasmid:
mEr81
0.25µg
0.5µg
0.75µg
1µg
+CMV.Pax6
Number of experiment: 6 6 6 6 6
Means 2.4 20.6 29.3 34 38.5
± s.d.: ±0.1 ±2.8 ±4.2 ±3.7 ±4.4
Er81-Luc + CMV-eGFP
Er81-Luc +CMV-Pax6
GFP
Luc
Pax6
Luc
Merge
J
J´
K
K´
K´´

Figure. 11. Pax6 directly regulates the activity of *Er81* in pallial progenitors

(A/B´) ISH analysis on cross sections at P10 reveals inhibition of *Er81* expression in L5 of the parietal (Par) cortex, but not in the medial frontal (Fr) cortex. (C/D´) showed the expression of *Er81* on sagittal sections of brains at E15.5 (C/C´) and E17.5 (D/D´). The arrows point to the expression of *Er81* along the pallial-subpallial border, while the arrowheads point to a strong ectopic expression of *Er81* in the pallial SVZ/IZ making connections with the olfactory bulb (OB) (C/D´). Higher magnifications of the images (D/D´) are presented in (E/F). In (D/D´) and (E/E´) note the abrogation of *Er81* expression in the progenitors of the pallial VZ and in the cortical plate (CP), and the robust expression of *Er81* in cell masses all along the SVZ/IZ in the E17.5 mutant cortex. (F) is a more lateral sagittal section of E17.5 *Pax6cKO* brain than that shown in E´ demonstrating the enhanced *Er81* expression in two streams that extend across the LGE towards the OB, within the putative territory of dLGE (arrow) and the ventral pallium (arrowhead). (G) EMSA of ^{32}P labelled probes for the potential Pax6 binding site in the mouse *Er81* promoter and Pax6 protein (see Supplementary Table 2). The arrowheads, the open arrow and the close arrow show the free probes, the complex of probes with protein and the complex of probes, protein with antibody, respectively. The difference between the control probes (lane 1-4) and the others (lane 5-10) is due to the difference in lengths of probes. Clear binding is detected for Pax6 to its potential binding site (lane 6). The binding is not observed with the probe with the TNT rat reticulocyte (RRL) as a protein control (lane 2). The specificity of the binding is controlled by incubation with anti-Pax6 antibody, which makes DNA-Pax6 protein-Pax6 antibody complex to be supershifted (lane 7). Binding of Pax6 was completely abolished after mutation of the binding site sequence (lane 9, 10). (H) ChIP assay was performed to confirm the direct interaction of Pax6 and Er81 promoter *in vivo*. Pax6 antibodies precipitate chromatin, covering the region -1322 to –1040 of the *Er81* promoter with the Pax6 binding site (lane 2), but not in the region –431 to –164 that is outside of the Pax6 binding site (lane 4). No binding is detected in absence of Pax6 antibody (lane 1). (I) Pax6 activates the *Er81* promoter-controlled reporter in co-transfected Hela cells. The combinations and the amounts of plasmids used for co-transfections in the performed six independent experiments are indicated. Error bars illustrate the standard deviations (s.d.) of the relative luciferase activity in each assay. (J/K´´) The activation of *Er81* promoter-controlled reporter by Pax6 is also confirmed by ovo electroporation in chick. Combinations of plasmids used for the experiment are indicated. ChIP, Chromatin immunoprecipitation; CP, Cortical plate; EMSA,

Electrophoretic mobility shift assay; Fr, Frontal cortex; Par, Parietal cortex; IZ, Intermediate zone; SVZ, Subventricular zone; VZ, Ventricular zone;

Finally, to get additional proof that the identified regulatory sequences in the *Er81* regulatory element could correctly drive the endogenous expression of *Er81*, we produced a transgenic mouse line (*Er81Cre* line). A DNA construct was generated, containing a 2.0 kb NheI/Not fragment of the *Er81* promoter, which was placed upstream of a human ß-globin minimal promoter was generated, followed by a Cre recombinase DNA sequence, IRES and GFP reporter sequence (Fig.12A). The *Er81Cre* transgenic mice were crossed with double-reporter mouse line, Z/AP reporter mice (Lobe et al., 1999). Throughout all embryonic and adult stages, the Z/AP reporter mice express the lacZ reporter gene before Cre-mediated excision occurs. Cre excision, however, removes the lacZ gene, allowing expression of the second reporter, the human alkaline phosphatase gene (hPLAP). This double-reporter transgenic line is able to indicate the occurrence of Cre excision and to trace the promoter-driven Cre activity in an extremely widespread manner from early embryonic to adult lineages (Lobe et al., 1999). The analysis of hPLAP activity in different founders of double transgenic line (*Er81Cre*, Z/AP) revealed a similar expression pattern in L5, corresponded to that of the endogenous Er81 in the cortex (arrowheads in Fig.12B/B´). Thus the 2.0 kb fragment used in this study is indeed controls the expression of *Er81* in mouse cortex.

Together, these results indicate that Pax6 directly regulate the Er81 activity in pallial progenitors, possibly specifying a subpopulation of the L5 neurons of IGLs. This finding furthermore supports our proposal that the transcription factor *Pax6* may directly regulate the output of subsets of early born IGL neurons. Noteworthy, the *Er81*+ expression was found also affected in the rostral cortex of the *Ngn1/Ngn2* mouse mutant cortex (Schuurmanns et al., 2004). Because the endogenous level of Pax6 is highest in the progenitors of VP and LP (Stoykova et al., 1997), *Pax6* appears to control the generation of *Er81*+ L5 neurons strictly in a region-specific manner, a phenomenon dually reported in *Pax6* regulation of *Ngn2* (Scardigli et al., 2003).

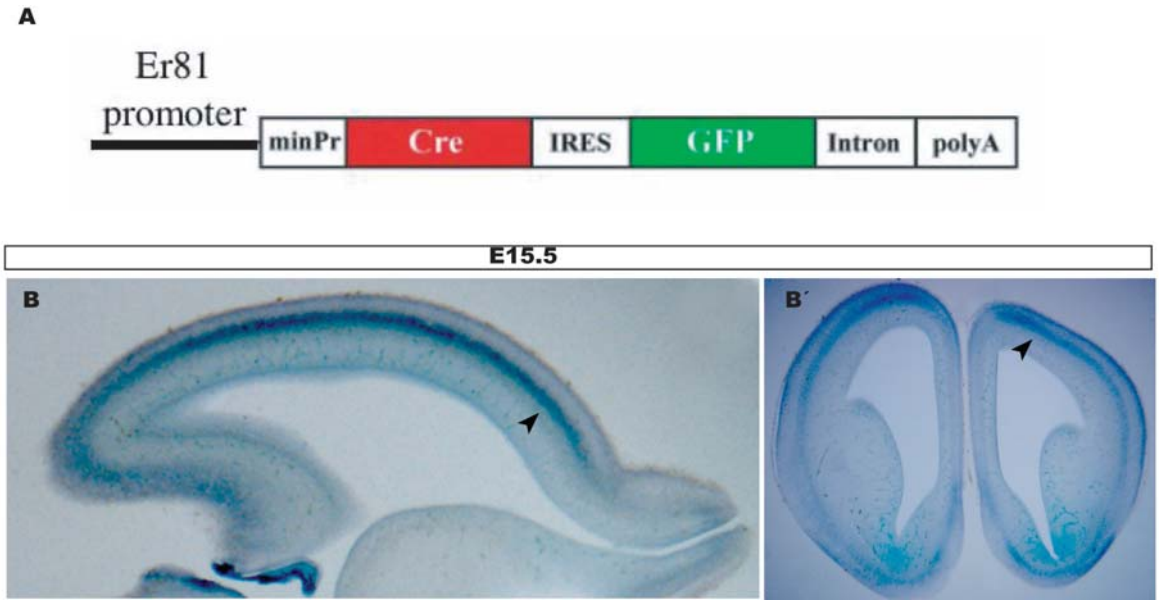

Figure 12. The generation *of Er81Cre* transgenic mice

(A) The *Er81* promoter was subcloned in the upstream position of the ß-globin minimal promoter (minPr) in a backbone plasmid, containing a DNA fragment encoding Cre (Berger et al., 2004). This construct allows the Er81 promoter to simultaneously drive expression of Cre and, via an IRES sequence, GFP reporter sequence. (B/B´) After crossing with Z/AP reporter mice (Lope et al., 1999), hPLAP staining of *Er81Cre* forebrains at E15.5 showed recombination in the L5 of the cortex (B, view of cross section; B´, view of sagital section).

2.5. Pattern defect of the frontal cortex in *Pax6cKO*

In mouse corticogenesis, subventricular zone (SVZ) is a proliferative zone and intermediate zone (IZ) is zone, where postmitotic neurons migrate towards the cortical plate (CP). SVZ and IZ are formed at around E13 and E15, respectively. In addition, tangentially migrating cells were generated in the LGE cross the corticostriatal boundary and enter the SVZ/IZ of the neocortex (DeDiego et al., 1994; Marin & Rubenstein, 2001; Wonders & Anderson, 2006; Kriegstein et al., 2006). Most intriguingly we observed that the inhibition of *Er81* expression in VZ of the rostrolateral *Pax6cKO* cortex at E17.5

occurred together with a strikingly strong ectopic *Er81* expression in the pallial SVZ/IZ, making connection with SVZ of the olfactory bulb (OB, Fig.11D/D´) and becoming visible already from E15.5 (Fig.11C/C´). Importantly, the expression of *Er81* in VP and dLGE of the mutant was enhanced (Fig.11F, arrowhead and arrow, respectively), reflecting the widely documented ventralization of the DV molecular patterning at PSPB in absence of *Pax6* as demonstrated for the *Sey/Sey* brain (Stoykova et al., 2000; Torresson et al., 2000; Yun et al., 2001; Kroll and O´Leary, 2005). The expression of *Er81* and *Dlx1/2* in VZ of the dorsal lateral ganglionic eminence (dLGE) specify progenitors that join the rostral migratory stream (RMS) to reach OB where they differentiate into GABAergic INs (Wichterle et al., 2001; Stenman et al., 2003). As recently demonstrated by Long et al (2007), the expression of *Er81* in SVZ at the level of the prefrontal cortex (PFC) is continuous between the pallial and subpallial domain, thus possibly allowing cell migration of putative cortical INs into the pallium (Wonders and Anderson, 2006). We studied the distribution of *GAD67*+ INs in this particular forebrain region and found that even at P10, more *GAD67*+ cells seem to delaminate from the enlarged SVZ at the transition zone between OB and PFC (Fig.13M/M´´). Furthermore, the enlarged GE at the PSPB in the mutant produced rostral ventricular protrusions that abundantly express both *Dlx1* and *Er81* (Fig.13K/L). In addition, while the expression of *Er81* in L5 neurons of parietal cortex in the mutant was substantially diminished, the MP and the dorsofrontal cortex displayed a similar or even stronger *Er81* signal (Fig.11A/A´). We presently have no a direct evidence for the cell identity of the *Er81*+ cells in the frontalmost *Pax6cKO* cortex. However based on our findings, we can propose that an enlarged set of *Er81*+ INs might migrated from the rostralmost subpallium during development, and/or *Er81*+ cells could be generated postnatally by pallial progenitors with altered identity by the GE of the rostral *Pax6cKO* cortex.

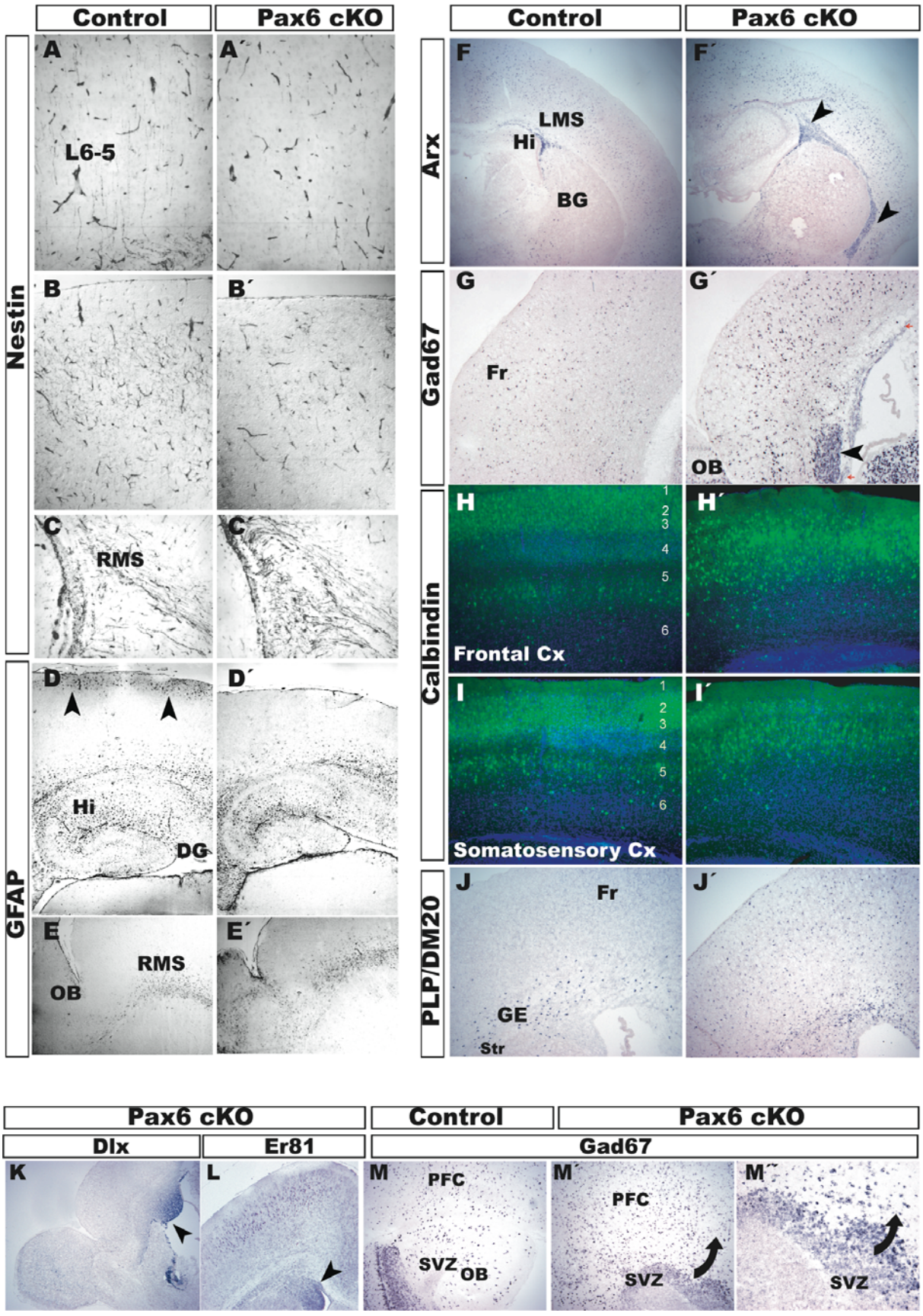
Control
Pax6 cKO
Nestin
A
A´
L6-5
B
B´
C
C´
RMS
GFAP
D
D´
Hi
DG
E
E´
RMS
OB
Control
Pax6 cKO
Arx
F
F´
LMS
Hi
BG
Gad67
G
G´
Fr
OB
Calbindin
H
H´
Frontal Cx
I
I´
Somatosensory Cx
PLP/DM20
J
J´
Fr
GE
Str
Pax6 cKO
Dlx
Er81
Control
Pax6 cKO
Gad67
K
L
M
PFC
SVZ
OB
M´
PFC
SVZ
M´´
SVZ

Figure 13. Defects in the differentiation of the late RG progenitors in *Pax6cKO*
(A/E´) In collaborative study with Dr. M. Davidoff, University of Hamburg, we used a combination of PAP- and ABC techniques to enhance the intensity of the immunostaining with Nestin and GFAP antibodies. (A/C´) IHC with Nestin antibody on cross sections from P10 brains showed Nestin+ RG cells with extending processes towards pia (A/´A), but containing increased number of such cells along RMS (C/C´). (B/B´) Nestin+ cells with astrocytic appearance are only scarcely seen in SS cortex of the mutant. (D/E´) Labelling with GFAP antibody reveals absence of differentiated astrocytes at uppermost position of the neocortex (D/D´, arrowheads), and an enhanced presence of GFAP+ cells along the RMS (E/E´). (F/G´) Cross sections were hybridized with *Arx* (F/F´) and *Gad65* (G/G´) in situ probes. Note that the mutant cortex contains enlarged sets of cells expressing the interneuronal markers *Arx* and *Gad67* in the germinative neuroepithlium (arrowheads) and in the cortex. (H/I´) IHC for Calbindin28 antibody on sagittal sections shows enhanced presence of Calbindin+ cells at uppermost position of the frontal *Pax6cKO* cortex. (J/J´) The germinative epithelium (GE) and the Fr cortex contain enlarged set of *PLP/DM20*+ oligodendrocytes in the *Pax6cKO*. (K/L) The ventricular protrusions of GE of the Fr Pax6cKO cortex abundantly express Dlx1+ (K) and Er81+ (L). (M/M´´) Cross sections at the level of the prefrontal cortex (PFC) brains hybridized with Gad67 in situ probe. Note the enlarged SVZ of the OB in the mutant from which Gad67+ cells appear to delaminate and populate the frontalmost cortex. BG, basal ganglia; DG, Dentate girus; Fr, Frontal cortex; Hi, Hippocampus; RMS, LMS, rostral or lateral migratory stream; Hi, hippocampus; OB, olfactory bulb; PFC, prefrontal cortex; Str, Striatum; SVZ, Subventricular zone.

2.6. Defect of the differentiation of the pallial late RG progenitors in *Pax6cKO* mice

Next we took the advantage of the *Pax6cKO* mice to examine whether the previously reported lack of SGL neurons in the prenatal *Sey/Sey* cortex is due to a delay of the RG differentiation. Late RG cells (E16-E19) generate neurons for SGLs, and astrocytes, while a small population of RG maintains progenitor properties at early postnatal stages. When tested at P10 for the expression of the progenitor cell marker Nestin, it was possible to visualize

Nestin+ RG cells extending their processes towards the pial surface in the control cortex, while the *Pax6cKO* cortex was depleted of such cells (Fig.13A/A´). Nestin+ cells with an astrocytic morphology were abundant in parenchyma of the somatosensory and occipital cortex in the control, but not in the mutant mice (Fig.13B/B´; and data not shown). However, an excess of Nestin+ astrocyte-like cells was seen along the lateral migratory stream (LMS) and rostral migratory stream (RMS) (Fig.13C/C´) in the *Pax6cKO* brain. Immunostaining with anti-GFAP antibody in the *Pax6cKO* brain showed defective distribution of GFAP+ cells with astrocyte-like appearance as these cells were severely diminished or virtually absent at the position of SGLs (Fig.13D/D´), which however appeared more abundant along the SVZ/LMS and RMS (Fig.13E/E´). Furthermore, a substantial portion of the cells in the enlarged RMS of the mutant brain clearly showed a strong expression of *Arx* and *GAD67*, two markers that specifically label migratory subpallial GABAergic INs (Fig.13F/G´). Consequently, the frontal cortex of *Pax6cKO* contains enlarged sets of GABAergic INs of both *Arx*+ and *GAD67*+ types as well as enlarged set of Calbindin 28+ cells, probably representing migrating INs from the subpallium (Fig.13H/I´).

In the rodent forebrain the majority of oligodendroglial progenitors arise during late embryogenesis and early postnatal development from multipotent cells of the SVZ of the lateral ventricles. SVZ cells migrate away from these germinal zones to populate both developing white and gray matter, where they differentiate and mature into myelin-forming oligodendroglia (Levison and Goldman, 1993). Given the enhanced expression of progenitor markers in the enlarged GE the postnatal Pax6cKO brain, we probed the expression of the two oliogodendroglial markers, *Olig2* and *PLP/DM20*. We found a profoundly enhanced expression of both these markers in the *Pax6cKO* as compared to the control cortex (Fig.13J/J´, data not shown).

In summary, these results demonstrate severe defect in the differentiation of late RG cells in *Pax6cKO*: the differentiation of late RG is blocked, leading the abrogation of generation of neurons of SGL projection neurons, in expense of an enhanced pool of cells with progenitor/stem-like

properties in neurogenic zones of the postnatal brain that produce more INs and oligodendrocytes, possibly even postnatally.

2.7. Cytoarchitecture of the *Pax6cKO* cortex at maturity

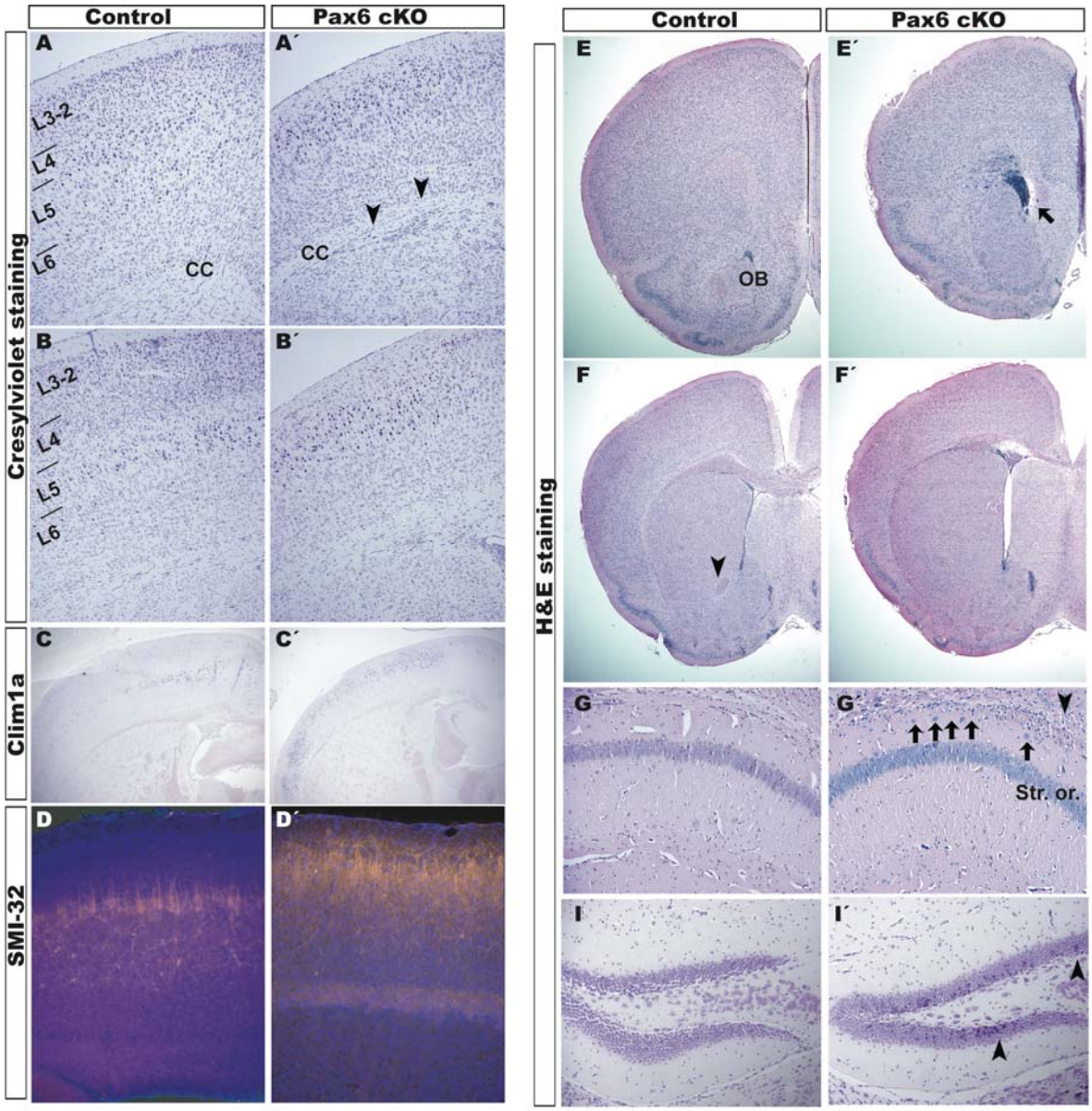

Figure 14. Cortical abnormalities in the adult *Pax6cKO* mice

(A/B´) Cresylviolet staining of cross sections of adult (7 months old) brains confirmed the dysgenesis of SGL neurons and revealed an increased number of cells with the pyramidal morphology at the uppermost position in the *Pax6cKO* cortex. Trapped cells are kept along the corpus callosum (CC) in the mutant brain (A´, pointed by arrowheads). (C/D´) ISH with *Clim1a* probe (C/C´) and IHC with *Smi-32* antibody (D/D´) support the observation that more cells with the pyramidal morphology are

present in the *Pax6cKO* cortices. (E/E´) Haematoxilin & eosin (H&E) staining showed a large population of dark-stained cells are accumulated within the germinative neuroepithelium of the rostral cortex of *Pax6* mutant (pointed with arrow). (F/F´) *Pax6cKO* brain at maturity also showed an absence of the anterior commissure (the commissure is pointed with arrow). (G/G´) Higher magnification of the CA1 region showed the densely accumulated cells in the periventricular zone (pPv) above Hi (arrowheads). The big cells in str. oriens (small arrows) seem to delaminate from pPv towards CA1 in the mutant. (I/I´) The subgranular layer of dentate girus (DG) in the mutant contains a larger set of cells (arrowheads) with appearance of progenitors possibly supplying more newborn neurons in the adult mutant DG and Hi suggested also by the results after immunolabelling with SMI-32 antibody (see Fig. 16G/H´). CC, Corpus callosum; OB, Olfactory buld; Str.or, Stratum oriens;

The observed defects in the cortical layer formation and neuronal differentiation in *Pax6cKO* brains are preserved at adulthood. Morphological analysis of haematoxilin & eosin (H&E) and cresylviolet staining of sections from adult (3-7 months old) brains of the *Pax6cKO* mice revealed a reduced thickness of SGL in the entire cortex (Fig.14A/B´). The thinning of the neocortex in *Pax6cKO* was more profound in the frontoparietal areas, where the cortex appears to contain at a most upper position cells with the pyramidal morphology. Indeed, immunostainig with SMI-32 antibody and ISH with *Clim1a* probe (general markers for L5 pyramidal projection neurons) revealed a superficial location of a large pool of *SMI-32+, Clim1a+* pyramidal neurons in the *Pax6cKO* cortex (Fig.14C/D´). Small dark cells, abundantly populate the germinative neuroepithelium of the rostral cortex (Fig.14E/E´). In consistence with the discovered dysgenesis of the SGLs, the corpus callosum (a thick axonal tract that connects the left and right cerebral hemispheres) was severely underdeveloped in the *Pax6cKO* mutant (Fig.14F/F´). The mutant Hi appeared enlarged with higher cell density in the str. pyramidale, while the pPv above the Hi contained a dense population of progenitor-like cells from where large cells with a pyramidal appearance seem to migrate towards the CA1 (14H/I´).

2.8. Defects of the neuronal differentiation of *Pax6cKO* hippocampus

In the adult hippocampus, neurons are generated from progenitor cells located in the subgranular zone (SGZ) of the dentate gyrus (Kempermann et al., 2004, Ming and Song, 2005 and Lledo et al., 2006). The expression of *Pax6* in cell lineages in hippocampus has been studied previously. Similar to VZ of the cerebral cortex, *Pax6* shows a co-expression with GFAP and Nestin, markers of astrocyte-like and progenitor cells in SGZ of the hippocampus (Maekawa et al., 2005 and Nacher et al., 2005).

The expression patterns of *Vglut1* at P10 (Fig.15A/A´) and the morphological analysis of the adult (Fig.15G/G´) revealed the presence of a thicker str. pyramidale in the Hi of *Pax6cKO*, suggesting augmentation of this cell population. The subbiculum, CA1-CA3 domains, and DG in *Pax6cKO* brain at P10 showed a stronger immunoreactivity with the Smi-32 antibody, although at this stage only a few of the labeled neurons were differentiated, extending processes (Fig.15C/D´). Interestingly, the Hi of 7-months old mutants, displayed a striking increase of the cell number of Nestin+ cells in str. oriens, PSA-NCAM+ newly born neurons in CA1-CA3 and str. radiatum, and Smi-32+ highly differentiated pyramidal neurons in all these three regions (Fig.15E/H´). Further experiments are needed to study the exact origin of the enlarged set of PSA-NCAM+ young and Smi-32+ differentiated pyramidal neurons in Hi of *Pax6cKO.* It is also interesting to note that after a BrdU-pulse labeling at E16.5 and E18.5, more BrdU+ cells were detected in *Pax6cKO* as compared with the control in both the enlarged GE at PSPB as well the HiSVZ and in the depth of DG and CA1 (Fig.9K/L´). Parentally they generate granule neurons of DG and astrocytes. At older stages derivatives of HiSVZ migrate into the pyramidal and molecular layers of CA1-CA3 where they adopt non-pyramidal morphology (Navarro-Quiroga et al., 2006). Thus, our present findings suggest that the enhanced presence of PSA-NCAM+ and Smi-32+ pyramidal neurons in the Hi of *Pax6cKO* possibly involves a postnatal neurogenesis

from progenitors kept in the adult HiSVZ and/or pPv zone (see discussion; also Nakatomi et al., 2002).

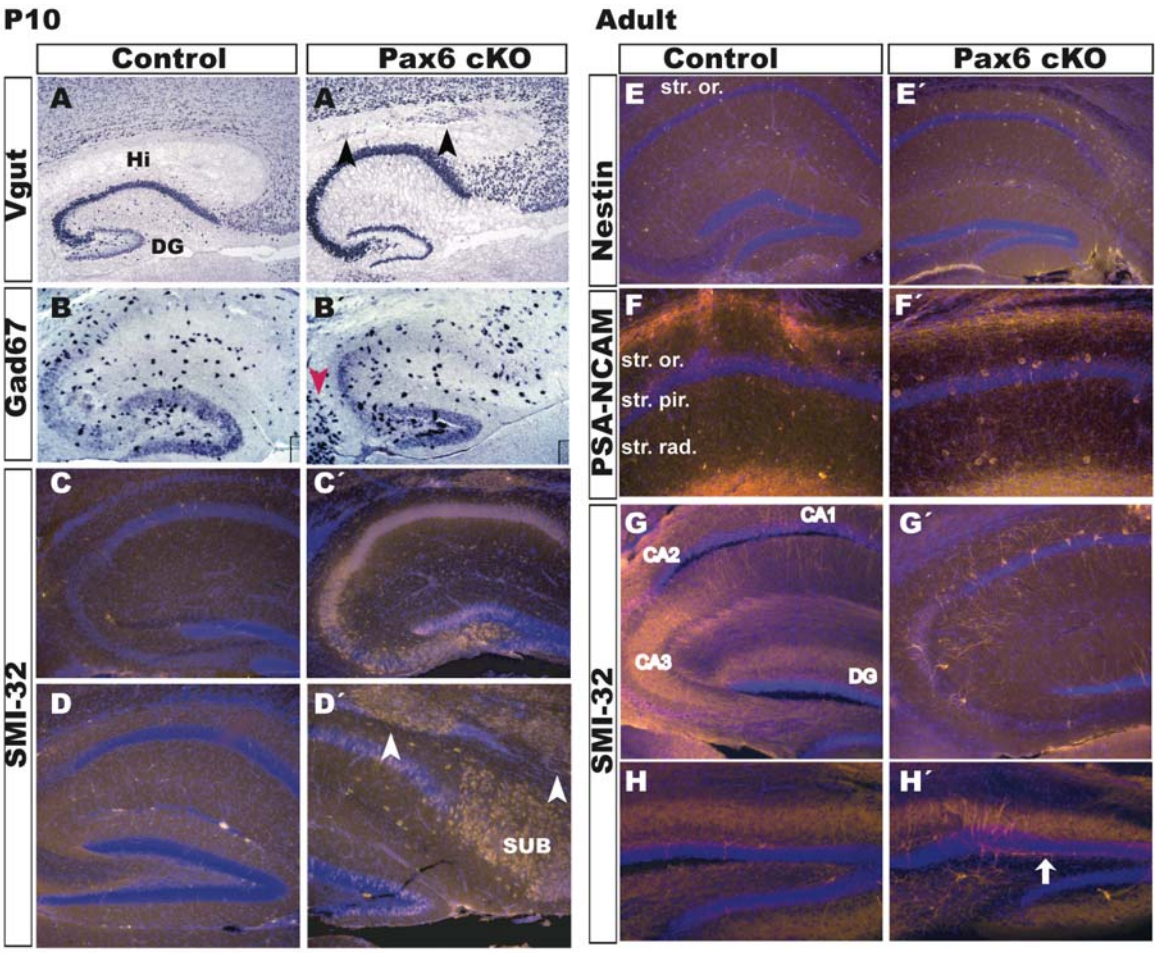

Figure 15. Impairment of hippocampus in *Pax6cKO* brain at P10 and in 7 months old brain

Sagittal sections from P10 brains processed for ISH (A/B´) or IHC (C/H´) with markers as indicated. (A/A´) Stratum pyramidale of hippocampus in *Pax6cKO* is augmented and densely packed with *Vglut1*+ neurons, which are also seen all along the WM above hippocampus (arrowheads in A´). (B/B´) The enlarged HiSVZ in *Pax6cKO* (arrowhead) contains more *Gad67*+ INs that seems to populate the hilus of the dentate girus (DG). (C/D´) The entire Ammon horn of hippocampus, DG and Subiculum show a strong Smi-32 immunoreactivity in *Pax6cKO*. The arrowheads in (D´) point to Smi-32+ cell masses along the WM above hippocampus. (E/H´) Immunolabelling of sagittal sections from adult brain (7 months old) with antibodies as indicated. Note that the enlarged str. or contains many more Nestin+ cells in Pax6cKO brain (E/E´). Stratum oriens, Stratum pyramidale of CA1, and Stratum radiatum in the mutant contain enlarged set of differentiating PSA-NCAM+ neurons

(F/F´). The entire ammon horn of the *Pax6cKO* hippocampus is densely populated by Smi-32+ pyramidal cells, which branch extensively into Stratum oriens and Stratum radiatum (G/G´). In the mutant, the subgranular germinative zone (arrow) contains more Smi-32+ neuronal cell bodies, extending processes (H/H´). DG, Dentate girus; Hi, hippocampus; Sub, Subiculum; str. or, Stratum oriens; str. pir, Stratum pyramidale; str. rad, Stratum radiatum;

2.9. The *Pax6cKO* cortex shows molecular caudalization but normal thalamocortical targetings

Analyses of the cortical phenotype of *Sey/Sey* embryos suggest that the robust rostro-lateral^{high} to caudo-medial^{low} gradient of *Pax6* in RG progenitors plays an essential role in the functional arealization of the developing cortex (Bishop et al., 2000, 2002; Muzio et al., 2002). In contrast to the *Small eye* mutant, the sensory thalamus in the *Pax6cKO* mice is not affected, giving us the unique opportunity to directly examine whether *Pax6* function in the cortex is autonomously required in establishment of area identity.

We first studied the molecular regionalization of the *Pax6cKO* cortex at P10. Most of the known genes that outline borders between distinct cortical areas show regionalized expression in the SGLs and therefore have limited value in studying the molecular regionalization of the cortex in the *Pax6cKO* mice. Notably, in addition to their expression in SGLs, both C*adherin8* and *Id2* are strongly expressed in L5 of the caudal cortex with a rostral limit within the SS cortex. As expected, the expression of both markers extends ectopically beyond the assumed M/SS border in the mutant (Fig. 16A/B´). The SS area, as revealed by histochemsitry for cytochrome oxydase in a flatmount preparation, seemed to have similar size in both genotypes, but in the mutant cortex the SS domain appeared to be located at a slightly more rostral position as compared to the control (data not shown). Notably, the rostral *EphA7* +domain, normally confined to the Fr cortex (Garel et al., 2003), looked diminished in the *Pax6cKO* brain (Fig.16C/C´), and the expression of both *EphA7* and *RZRß* in the occipital cortex was shifted rostrally (Fig.16C/D´). Thus, in accordance with previous data for *Small eye*, *Pax6cKO*

mice also exhibit a reduction of the Fr cortex and a complimentary expansion of the regionalized expression of caudal cortical markers.

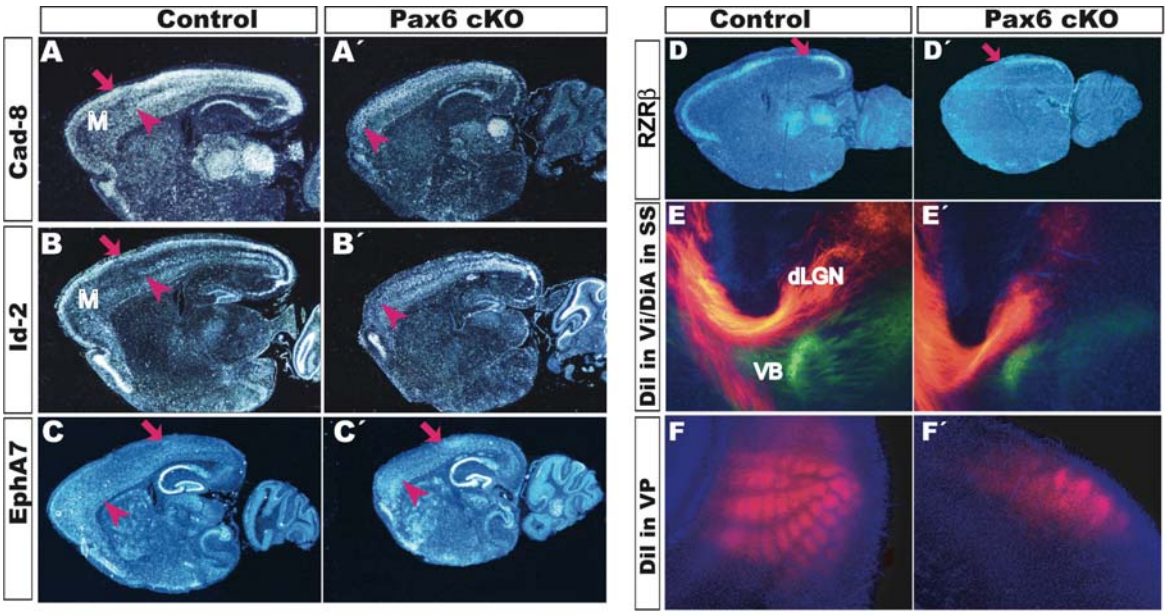

Figure 16. Pax6LOF causes molecular caudalization of the cortex without change of the cortical area identity

(A/D´) ISH analysis on sagittal sections from P10 brains was used with regional markers, as indicated. (A/B) In the controls, the strong expression of *Cad-8* and *Id2* in SGL of the motor (M) cortex (arrows) and in L5 (arrowheads) marks a border between the M and SS areas. (A´/B´, arrowheads) in *Pax6cKO*, the expression of both markers in SGLs is not detectable, however the rostral limit of their expression in L5 extends ectopically from somatosensory (SS) into the M cortex. (C/C´) The regionalized expression of *EphA7* confined to the M cortex outlines a smaller territory in the *Pax6cKO*. The relative size of the caudal *EphA7+* and *RzRß+* domains appeared enlarged in the *Pax6cKO.* The arrows and the arrowheads indicate the limits of the gene expression in the caudal or rostral cortex, respectively (C/D´). (E/F´) Topographic organization of TCA projections in *Pax6cKO* mutant is preserved. (E/E´) After placement of DiI (red) and DiA (green) crystal in the visual (Vi) or SS cortex, the dye diffusion correctly labels the dLGN or VB in both control and KO brains. (F/F´) After DiI crystal placement in the VP nuclei of the thalamus, the barrel field pattern is partially preserved in *Pax6cKO*. dLGN, Dorsal lateral geniculate nucleus; M, motor cortex; SS, somatosensory cortex; TCA, thalamocortical axon; Vi, visual cortex; VP, Ventroposterior;

To directly assess the area identity in the *Pax6cKO* mice we traced the thalamocortical axon (TCA) projections using retrograde labeling (in collaboration with Dr. Zoltan Molnar, Oxford University). Surprisingly, despite the change in the expression of area specific markers, when carbocyanine dye crystals (DiI and DiA) were placed in the putative motor (M1), somatosensory (S1), or visual (V1) cortical areas, TCA projections correctly targeted the ventroanterior (VA), ventroposterior (VP) nuclei, and the dorsal lateral geniculate nucleus (dLGN) of thalamus respectively (Fig.16E/E´). The same pathways were evident when the carbocyanine crystals were placed in different thalamic nuclei (VA, VP, dLGN) and retrograde labeled cells were found in the correspondent cortices (M1, S1 or V1, respectively). After placement of DiI crystals in the VP nucleus of thalamus, clusters of labeled terminals were found in the residual L4 of the barrel field of S1 in the mutant, although not entirely separated as in the control animals (Fig.16F/F´).

These findings indicate that despite the observed caudalization of the molecular properties of the cortex, the cortical areal identity as well as the cortical module arrangement is unaltered in *Pax6cKO* mice.

2.10. Trim11 interacts with Pax6

Previous evidence indicated a dependence of the eye and cortical phenotype on Pax6 dosage (Hill et al., 1991; Schedl et al., 1996; Berger et al., 2007; Manuel et al., 2007, see discussion). Given the important functions of Pax6 during corticogenesis as described in this work, we were further interested to study some molecular mechanisms that control the Pax6 expression in the cortical cells. To identify proteins that interact with Pax6 and possibly modulate its activity, we carried out a two-hybrid screening using *Pax6ΔPD* (Pax6 without PD) as a bait and a cDNA library derived from E15.5 cortex of mouse (Fig.17A). Yeast colonies were selected on plates lacking the leucine, tryptophan and histidine, and supplemented with 65 mM 3-aminotriazole. All these clones were assayed for β-galactosidase activity and confirmed by sequencing. In total of 116 independently positive colonies from $2.5x10^6$ library transformants, four sequences were found to encode for Trim11, the reported ubiquitin E3 ligase of neuroprotective peptide humanin (Niikura et al.,

2003). Sequences of two colonies cover the full-length of Trim11 cDNA with a point mutation at C-terminal. The shortest sequence corresponds to the full coiled-coil domain, flanked by the partial B-box and B30.2 domain (Fig.17B). The characterization of the other sequences encoding different potential interacting proteins of Pax6 is in progress.

To validate our two-hybrid screen result we performed a pull-down assay using full-length of the purified GST-fused Trim11 and a cell lysate containing the full-length Pax6 protein. As shown in Fig.17C, Pax6 binds physically to Trim11

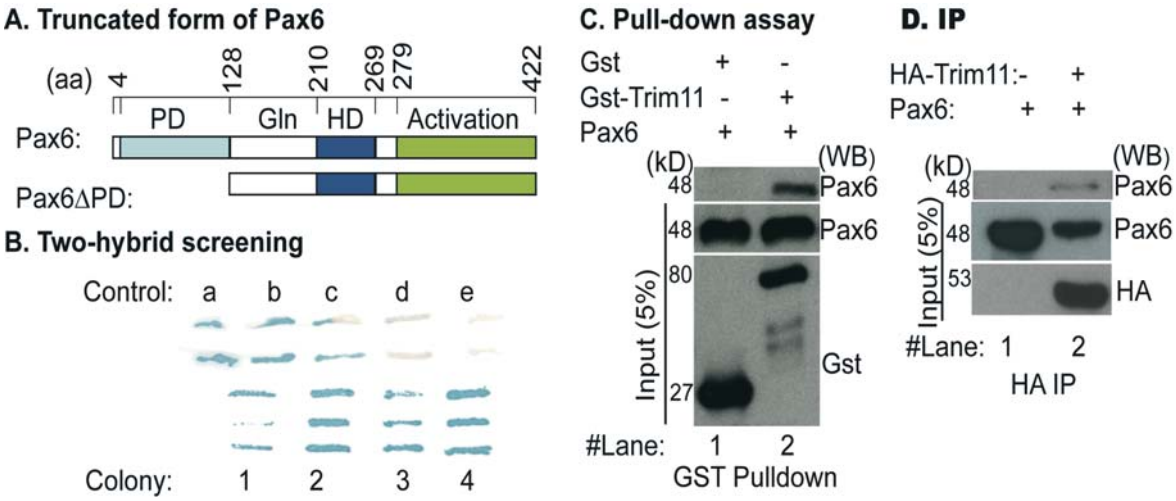

Figure 17. Pax6 interacts physically with Trim11

(A) The schematic representation of the functional domains of Pax6 which contains the two DNA-binding domains the pair domain (PD) and the homeobox domain (HD), the glycine-rich region (Gln) and the activation C-terminal domain. Construct of Pax6 without the pair domain (Pax6ΔPD) was used in the yeast two-hybrid screening. (B) Five different controls (a-e) are shown according to the supplier ´s manual. Four independently positive colonies revealed potential interactions of Pax6 and Trim11 in the yeast two-hybrid assay. (C/D) The interaction of Trim11 and Pax6 were assessed by the pull-down assay (C) and immunoprecipitation assay (D). The upper, middle and lowest blots show the elutants from the pull-down or immunoprecipitation assay and the amount of proteins (input) used in the experiments, respectively. Note that the experiments were performed in the presence of 20 μM MG132 proteasome inhibitor (C/D).

(lane 2), and does not bind to GST alone, which was used as a negative control (lane 1). To confirm the interaction of Trim11 with Pax6 in mammalian cells, a plasmid for N-terminal HA-tagged Trim11 (*HA-Trim11*) or the backbone plasmid (negative control) were transiently transfected with an expression plasmid for mouse *Pax6* cDNA (*CMV-Pax6*) in Hela cells. In accordance with the finding in the pull-down assay, HA-Trim11 was specifically coimmunoprecipitated with Pax6, which only marginal band was seen with the negative control (Fig.17D). In consistence with previous data, the performed analysis of the Trim11 subcellular localization indicated that HA-tagged Trim11 distribute diffusely between the nucleus and cytoplasm in Hela cells (Fig.18E/F´; Reymond et al., 2001; Niikura et al., 2003). *Trim11* transcripts are ubiquitously distributed in developing mouse tissue at E12.5, but most abundantly they are presented in the CNS (central nervous system). In the telencephalon at E12.5, the expression of *Trim11* is mostly confined to cells in VZ of the neuroepithelium (Reymond et al., 2001), where Pax6 is strongly expressed as well, suggesting that these proteins might interact *in vivo*. In this line of evidence, immunostaining for Pax6 and Trim11 of Hela cells, cotransfected with *CMV-Pax6* and *HA-Trim11*, showed a colocalization of both proteins in the nucleus (Fig.18E/F´, pointed by arrowheads in F´).

2.11. Trim11 induces ubiquitination and affects the steady-state levels of Pax6 protein

Finding the interaction between Pax6 and Trim11, an E3 ubiquitin ligase of Humanin peptide (Niikura et al., 2003), prompted us to investigate whether Trim11 also has a role in controlling the degradation of Pax6 through the ubiquitin-proteasome system (UPS).

We first analyzed the half-life of Pax6 in the presence or absence of Trim11 by using cycloheximide-chase experiments. This approach is widely used for study the protein stability (Obrig et al., 1971). Shortly, after a cycloheximide-dependent inhibition of translation of the protein biosynthesis by binding with the 80S ribosome of the cells, the half-life of the questioned protein is determined. As shown in Fig.18A, a dramatic decrease of Pax6 half-life in the presence of Trim11 was observed. After 90 min of the chase

experiment, more than 90% of the Pax6 protein was degraded. Under similar experimental conditions, but in the absence of Trim 11, the half-life of the Pax6 was only slightly affected (Fig.18A, lower diagram represents for amount of proteins in different time points in lower blots).

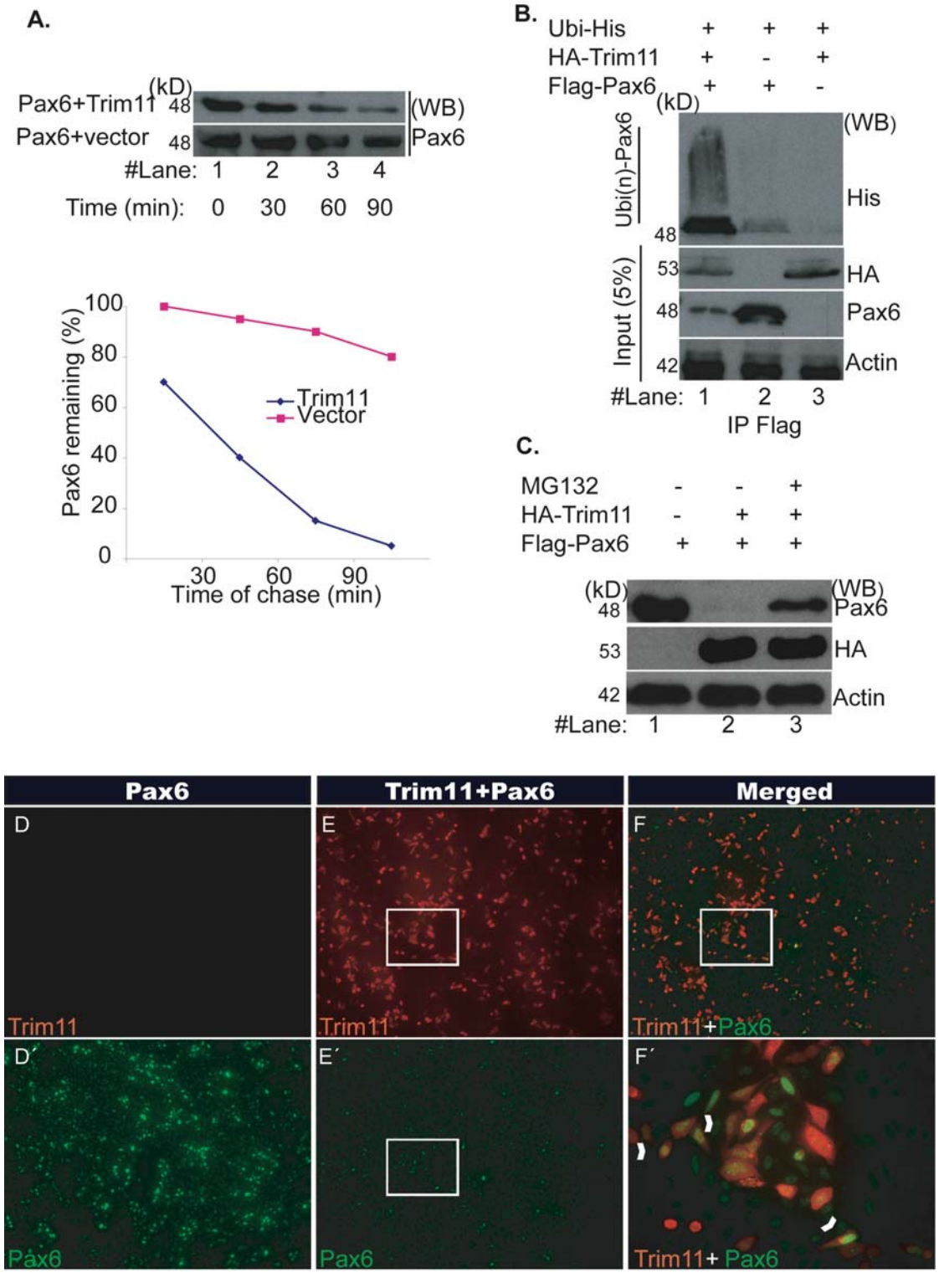

Figure 18. **Trim11 induces ubiquitylation and affects the steady-state levels of Pax6 protein**

(A) Cycloheximide–chase assay was used to assess the effect of Trim11 on the steady-state level of Pax6. Upper and lower blots show the levels of Pax6 in Hela cells after transfection with *CMV-Pax6* construct together with either *HA-Trim11* or with the empty vector, respectively. The quantification of Pax6 protein levels at different time points in cycloheximide–chase assay is also presented as a diagram. (B) Trim11-mediated ubiquitination of Pax6 was proved using an *in vivo* ubiquitination assay. Hela cells were transfected with plasmids as indicated. The immunoblotting analysis of elutants from the anti-Flag immunoprecipitation using anti-His antibody showed a much stronger smear band for the ubiquitinated Pax6 (lane 1, upper blot) in the presence of Trim11 as compared to controls (in the absence of Trim11 or Pax6, lane 2, 3 of upper blot). Note that in the lower blot using an anti-Pax6 antibody there is a substantial reduction of the Pax6 protein level. (C) The proteasome inhibition assay confirmed the UPS-mediated degradation of Pax6. Hela cells were transfected with plasmids and treated with the proteasome inhibitor (MG132) as indicated. In presence of the MG132, the level of Pax6 was recovered significantly (compare levels of Pax6 protein in lanes 2 and 3 of the upper blot). (B/C) Blots with anti-HA antibody showed an equal amount of the Trim11 protein was used in each experiment. The lowest blots using an anti-Actin antibody shows an equal amount of total protein was loaded for SDS-PAGE. (D/F´) The colocalization of Pax6 and Trim11 and the Trim11-mediated degradation of Pax6 were confirmed by double ICC analyses using HA and Pax6 antibodies. Hela cells were transfected with CMV-Pax6 plasmid alone (D/D´) or together with HA-Trim11 (E/E´). In the presence of Trim11, the number of Pax6-imunoreactive cells was severely diminished and the expression level of Pax6 in some Pax6-remaining cells was decreased as illustrated by a much less dense staining (E/E´) when compared to the control (D/D´, without Trim11). Overlay images of Trim11 and Pax6-immnoreactive cells showed the colocalization of Trim11 and Pax6 in transfected Hela cells (E/F´ and F´ which is a higher magnification image of the rectanglor block in E, E´, F).

To confirm that the decrease in the half-life of Pax6 is dependent upon the activation of Trim11 expression, we performed cotransfection of Hela cells

with plasmids of *CMV-Pax6* and *HA-Trim11.* Western blot analysis revealed the level of Pax6 was severely diminished in the presence of Trim11 when compared to control (Fig.18B, lane 1-2; Fig.18C, lane 1-2). Next we tested whether the activation of *Trim11* could also mediate the degradation of endogenous Pax6 protein. For that, we utilized a primary cortical cell culture system. In our system we used primary cells originating from tissues of E12.5 mouse cortex. After electroporating cells with *CMV-Trim11,* they were cultured for 3 days *in vitro* (3DIV), in a chemically defined culture medium (see Material and Method; Bottenstein & Sato, 1979). Under these culture conditions, progenitor proliferation and neuronal differentiation *in vitro* mimic those *in vivo* (Qian et al., 2000). Consistently, the overexpression of Trim11 (through *CMV-Trim11*) led to a substantial reduction of endogenous Pax6 as indicated by the decreased number of Pax6-positive cells in primary culture (Fig.19A/C´, see in detail below).

In vertebrates, two Pax6 isoforms are active, Pax6 and Pax6(5a) (Fig.7; Carriere et al., 1995; Richardson et al., 1995; Zaniolo et al., 2004). To determine whether the decrease of Pax6-positive cells might involve down-regulation of *Pax6* transcription, we performed quantitative PCRs to determine the mRNA levels of *Pax6* and *Pax6(5a)*. Samples were isolated from 3DIV cortical primary cultures after electroporation with the plasmid *CMV-Trim11* plasmid or the backbone plasmid (negative control). In contrast to the decrease in the level of Pax6 protein revealed by ICC detection, we did not observe any significant change in the mRNA level of either *Pax6* or *Pax6(5a)* (data not shown). Thus the enhanced expression of *Trim11* accelerates the degradation of Pax6 protein, but does not affect the transcription of both *Pax6* isoforms.

We next assessed whether Pax6 can serve as a substrate for the ubiquitin ligase activity of Trim11. For this purpose, we overexpressed *Trim11* together with *Pax6*, and His-tagged Ubiquitin (*His-Ub*) in the presence of the proteasome inhibitor MG132 and analyzed the appearance of Ub-conjugated forms of Pax6 (Fig.18B). After immunoprecipitation of Flag-Pax6, blotting using anti-His antibody revealed a large amount of Pax6 was ubiquitinated in the presence of Trim 11, (Fig.19B, lane 1). This band was very faint in the

absence of Trim11 (Fig.18B, lane 2) or Pax6 (Fig.18B, lane 3), indicating that Trim11 mediates the ubiquitination of intracellular Pax6.

Proteasomes are large protein complexes, located in the nucleus and the cytoplasm of all eukaryotes. The main function of the proteasome is to degrade unneeded or damaged proteins by proteolysis, a chemical reaction that breaks peptide bonds. Tagged proteins for degradation are normally labeled by ubiquitin in the reaction chains of ubiquitination (Hochstrasser, 2006). As Pax6 is extensively ubiquitinated by Trim11, we next examined whether the degradation of Pax6 is truly mediated by Trim11 through the ubiquitin proteasome system (UPS). We compared the expression level of Pax6 in Hela cells after cotransfection of *Pax6* and *Trim11* in the presence or absence of the proteasome inhibitor, MG132. Consistently Trim11 could ablate almost completely of Pax6 protein in comparison with the negative control (Fig.18C, lane 1, 2), however in the presence of the proteasome inhibitor, the level of Pax6 was recovered significantly (Fig.18, lane 3). Collectively our data indicate that that Trim11 indeed mediate the degradation of Pax6 via UPS.

2.12. The degradation of Pax6 by overexpression of Trim11 results in repression of neurogenesis

As decribed above, we examined the effect of overexpression of Trim11 in E12.5 cortical primary cultures. Three days after culturing *in vitro* (3 DIV) in a chemically defined culture medium (see material and method; Bottenstein & Sato, 1979), the overexpression of Trim11 (via the expression vector *CMV-Trim11*) led to a decrease in the number of cells immunoreactive for endogenous Pax6 (*CMV-Trim11* transfected cells contained 9.8%±0.4% Pax6-immunoreactive cells; 191 Pax6-immunoreactive cells/1939 total cells/in 5 times of 20x objective) as compared to controls (22.4%±0.5% Pax6 positive cells; 481 Pax6-immunoreactive cells/2147 total cells/in 5 times of 20x objective; $P<0.005$; Fig.19A/C).

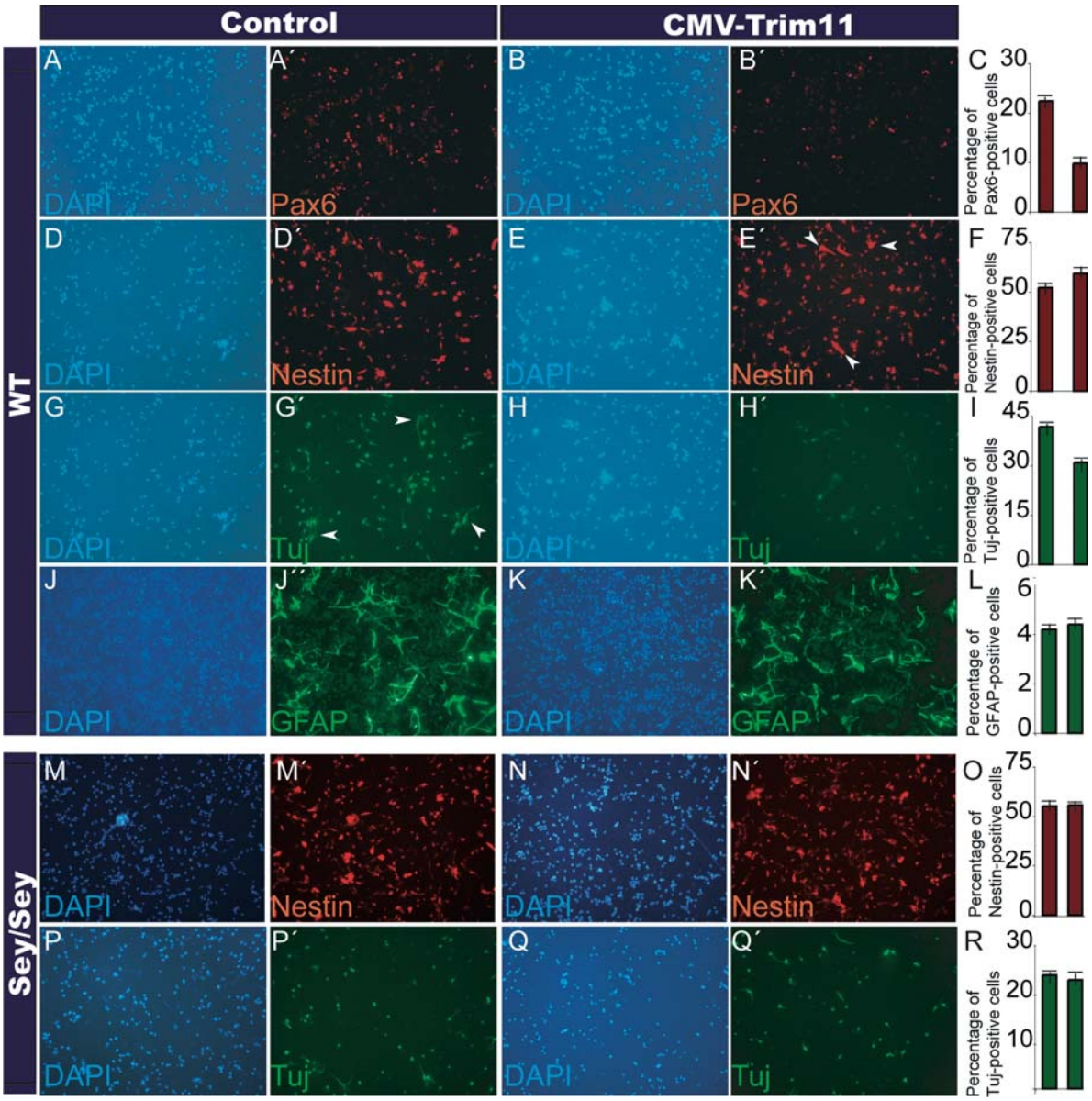

Figure 19. Suppression of cortical neurogenesis after overexpression of Trim11

Primary cells derived from E12.5 WT cortical tissues (A/K´) or *Sey/Sey* (M/Q´) were electroporated with either an empty vector (controls, in A/P´) or with a construct to overexpress Trim11 (CMV-Trim11 in B/Q´). After 3 DIV, ICC analyses were performed with Pax6 antibody (A´/B´) and different antibodies to identify either progenitors (Nestin+ cells, in D/E´, M/N´), neurons (Tuj+ cells in G/H´, P/Q´) or astrocytes (GFAP+ cells in J/K´). DAPI staining is represented on the left side of each of the immunostained slides. Graphs on the right side show results from the quantitative analysis of expression for these markers. Error bars give standard deviations (s.d.).

Immunostaining with a marker for progenitor cells (Nestin+) indicated a slight enhancement of the number of Nestin+ cells in the *CMV-Trim11* transfected cells (57.6%±2.1%; 738 Nestin-immunoreactive cells/1282 total cells/in 5 times of 20x objective) as compared to the control cultures (52.7%±1.7% ; 782 Nestin-immunoreactive cells/1485 total cells/in 5 times of 20x objective) in the control P<0.005 ; Fig.19D/F). On the contrary, the labeling with Tuj1, a marker for postmitotic neurons, indicated that *CMV-Trim11* transfected cells contain less neurons (30.9%±2% Tuj1-immunoreactive cells; 396 Tuj1-immunoreactive cells/1282 total cells/in 5 times of 20x objective) as compared to the controls (41.7%±0.9%; 619 Tuj1-immunoreactive cells/1485 total cells/in 5 times of 20x objective; P<0.005, Fig.19G/I). Notably, while the Nestin+ cells had mostly bipolar morphology, Tuj1+ cells had branched processes in *CMV-Trim11* transfected cells (Fig.19E´/G´, with arrowheads). In addition, we found that the overexpression of Trim11 did not affect the number of GFAP-positive cells, when electroporated cells were cultured for 3-5DIV in Sato medium or for 5-7DIV in a condition for astrocyte differentiation (see Mateial and Method; Fig.19J/L).

We asked further whether the observed inhibition of neurogenesis after the overexpression of Trim11 was specifically due to degradation of Pax6 alone. We performed a similar experiment for overexpression of Trim11 in cortical primary cultures that originated, however, from *Sey/Sey* cortex, which is completely devoid of Pax6 (Hill et al., 1991). Remarkably, no significant change in the number of Tuj- and Nestin-positive cells was detected in these experiments (Fig.19M/R). These results are in full agreement with the detected enhancement of progenitor proliferation and abrogation of neuronal differentiation when Pax6 is not functional *in vivo*, as shown in the *Sey/Sey* cortex (Gotz et al., 1998; Heins et al., 2002). Together, these findings indicate that in addition to the intrinsic role of Pax6 in endowing the radial glial cells with neurogenic features (Heins et al., 2002), possibly the Pax6-interacting partner Trim11 modulates indirectly the neuronal cell fate decision by facilitating the degradation of Pax6.

2.13. Trim11 is a potential direct downstream gene of Pax6

We recently generated a mouse line to allow us to study the effect of overexpression of Pax6 in transgenic mice *in vivo* (Berger et al., 2007). A construct was generated, in which a DNA sequence encoding for GFP, was flanked by two loxP sites and placed in front of the Pax6 cDNA. In the absence of Cre activity, CMV promoter drives the expression of GFP in all body regions of these transgenic mice. However the presence of Cre activity leads to excision of the sequence between the two LoxP sites, allowing the activation of Pax6. In order to conditionally activate the expression of Pax6 in cortical progenitors and postmitotic neurons, respectively (Berger et al., 2007), we used different cell lineage-specific Cre lines, Emx1Cre (Gorsky et al., 2002) and NexCre (Goebbels et al., 2006)

To study whether Trim11 might not only act upstream, but also downstream of Pax6, we examined Trim11 RNA levels in embryonic cortex isolated from transgenic mice after overexpression of *Pax6* in cortical progenitors at the onset of neurogenesis at E9.5 (*Emx1Cre,JoP6*) or in cortical postmitotic neurons (*NexCre,JoP6*) and corresponding controls (Berger et al., 2007). Surprisingly, qPCR analysis showed a substantial increase in *Trim11* transcripts in both experimental conditions, when compared to controls (Fig.21A). We observed 1.9 and 1.7 fold higher levels of Trim11 RNA in samples isolated from *Emx1Cre;JoP6* at E12.5 and *NexCre;JoP6* at E15.5, respectively (Fig.21A). Interestingly, examination of a genomic sequence, including the 5 kb upstream of the starting codon of *Trim11* revealed the presence of multiple putative Pax6 binding sites. Band shift and super-shift assays (similarly to those performed in the study of the Er81 promoter) showed that Pax6 does indeed bind strongly to three synthesized double-stranded oligos corresponding to putative Pax6-binding sites out of the eight tested ones (lane 4-5, 12-13, 18-19; probe a, e, h; Fig.20B/B´). Even though further experiments are required to confirm a direct interaction, our preliminary data suggest that Pax6 might directly regulate the expression and activity of Trim11. Thus, our findings also suggest the existence of an autoregulatory loop between Pax6 and Trim11.

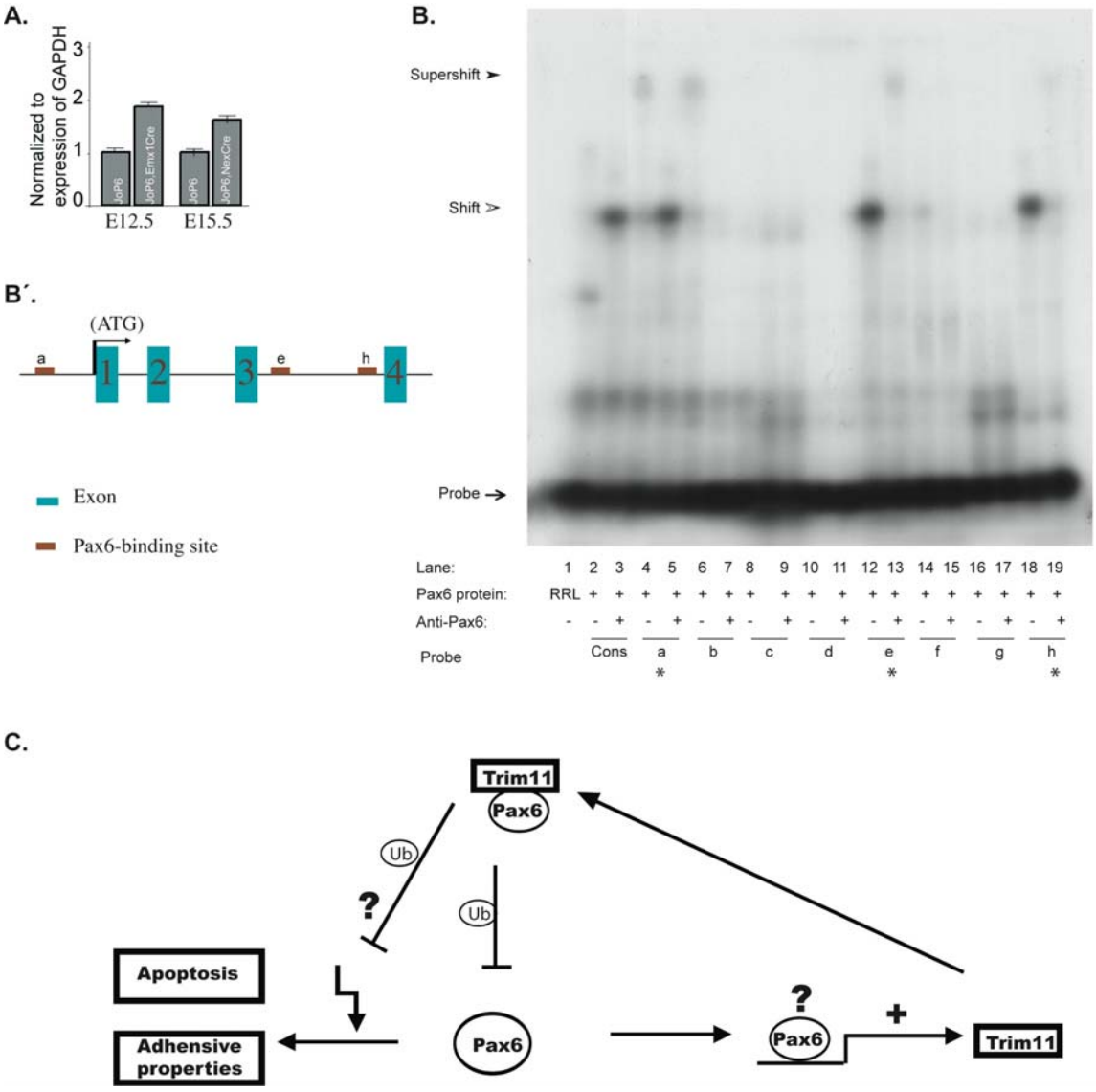

Figure 20. Potential autoregulatory feedback loop regulates the activity of Pax6 and Trim11.

(A). qPCR analysis performed with cortical samples isolated from transgenic mice after overexpression of Pax6 (as described in Berger et al., 2007) in cortical progenitors (*JoP6;Emx1Cre*) or in postmitotic neurons (*JoPax6;NexCre*) showed elevated expression levels of Trim11 when compared to the corresponding control. (B) EMSA assay (similar to that described for the *Er81* promoter) demonstrated that Pax6 binds strongly to three out of the eight putative binding sites for Pax6. (B´) Pax6-binding sites are located in the 5´ upstream region of the starting codon and a genomic region inbetween exons 3-4 of *Trim11*. (D) Schema presents an assumed model of the genetic interaction between Pax6 and Trim11, possibly forming an autroregulatory feedback loop. On the one hand Trim11 protein binds to Pax6 and acts as a Pax6-specific E3 ubiquitin ligase, which attaches ubiquitin residues onto

Pax6 and send it for degradation by the 26S proteasome. On the other hand, Trim11 gene is a downstream target for positive transcriptional activation by Pax6. This interplay between Pax6 and Trim11 defines a basal Pax6–Trim11 loop. As long as the loop is fully close, the balance seems to be in favor of the Pax6 level and maintenance in a biological state. Any shift in this balance, such as in over-dosage of Pax6 would result in abnormal cellular responses such as apoptosis and changing of adhesive properties (Berge et al., 2007; Manuel et al., 2007). To limit such harmful conditions, an auto-regulatory feedback program in cells could response by activating Trim11 in order to repress the over-dosage of Pax6.

3. Discussion

The aims of this project were to get conclusive results on the proposed (but not confirmed) regulatory role of *Pax6* in the specification of neurons of distinct cortical layers, area formation, and to attempt to identify molecular mechanisms regulating the expression level of the neurogenic factor Pax6 in cortical progenitors. Firstly, we have demonstrated that *Pax6* has a crucial role for the correct differentiation of the late RG and thus for the specification of SGL neurons. Secondly, in contrast to previous suggestions we found that *Pax6* is not involved in the generation of IGL neurons, rather we showed that Pax6 affects the migration, and the pool size of subsets of IGL neurons. In further support of this idea, we provided evidence that Pax6 directly regulates the activity of the transcription factor *Er81*, a putative instructive factor for layer 5 neurons, in the pallial progenitors. Thirdly, we found while it is expressed in a prominent rostral-high to caudal-low expression gradient in the cortical progenitors, Pax6 affects the molecular regionalization of the cortex, but does not influence the establishment of cortical area identity. Finally, we demonstrated that the E3 ubiquitin ligase Trim11 controls the stability and may be modulate the expression level of Pax6 protein in cortical progenitors. We further presented evidence for a possible interplay between Pax6 and Trim11, possibly forming an autoregulatory feedback loop that controls *Pax6* function during neurogenesis and developing cortex.

3.1 Pax6 in the neuronal differentiation and formation of cortical layers

Mammalian corticogenesis is a process in which progenitor cells generate neurons destined for specific cortical layers, depending on the expression of layer-determinant genes and environmental cues. The mechanisms underlying the formation of cortical layers have been recently explored by analyzing a single or combination of mutants of neuronal determinant factors. The current view suggests that distinct genetic programs operate at different stages of corticogenesis to specify neurons of different cortical layers (Fig.6;

reviewed by Campbell, 2005; Guillemot et al., 2006). Recent data suggested that generation and specification of the early-born IGL neurons is largely dependent on the function of *Foxg1, Tbr1* and the proneural genes *Ngn1/2*, while the late-born cortical neurons of SGLs are specified in an *Ngn*-independent pathway, requiring the synergistic activities of *Pax6* and the orphan nuclear receptor *Tlx* (Schuurmans et al., 2004; Schmahl et al., 1993; Caric et al., 1997; Land and Monaghan, 2003). However our present findings indicate that *Pax6* plays a crucial role in the neuronal generation of both IGLs and SGLs (see the proposed model in Fig.21).

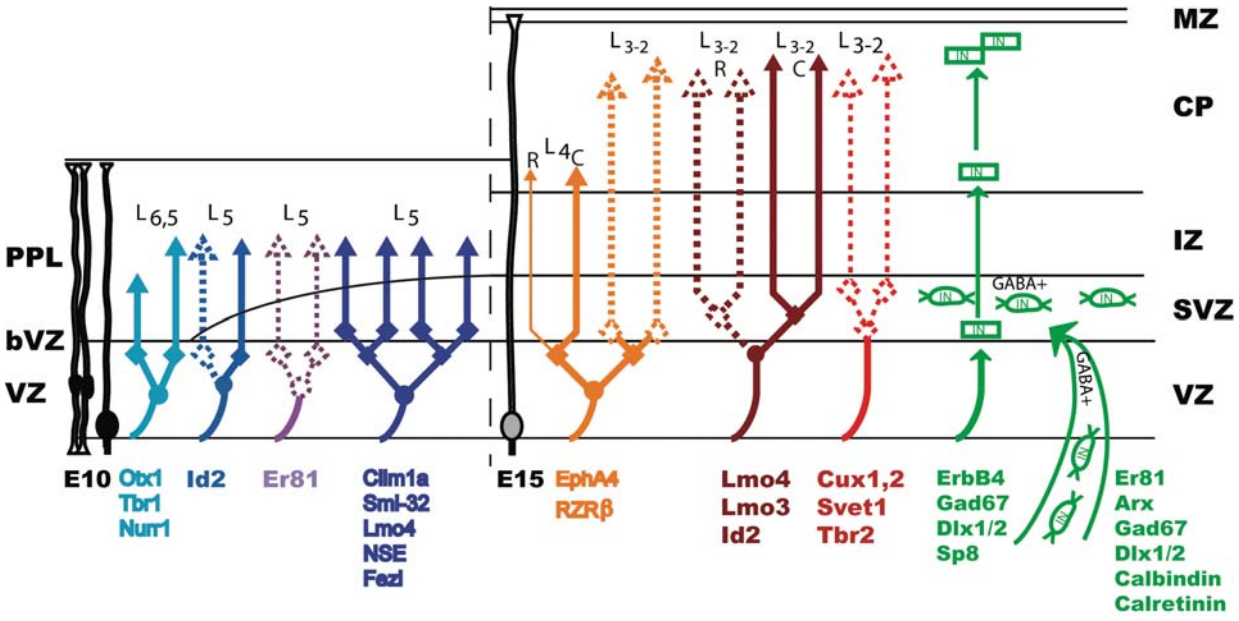

Figure 21. A proposed model of the Pax6-dependant molecular mechanism in mammalian corticogenesis

The model is based mainly on results of the cortical phenotype of *Pax6cKO* mutant postnatally in this study, and published data for the *Sey/Sey* embryos (Tarabykin et al., 2001; Zimmer el al., 2004; Schuurmans et al., 2004). Initially the NE cells (black) divide symmetrically that leads to an increase in the germinative pool of the pallium. Around E12.5 in mouse, a substantial portion of NE cells start to transform into radial glia (RG) pluripotent progenitors that can generate both, neuronal and glial cells (Heins et al., 2002). More than 90% of the early RG cells (E12-E14) express Pax6 at a high level as intrinsic determinant of their fate (Götz et al., 1998). The RG cells divide both symmetrically and asymmetrically at the apical surface of the VZ,

generating both IGL neurons and intermediate progenitors (IP), also named basal progenitors (BPs) (see also Fig.5). These IPs undertake symmetrical division at the basal surface of VZ forming after E13.5 the SVZ, a second proliferative zone of the cortex that produces exclusively SGL neurons (reviewed by Kriegstein et al, 2006). Expressed at a high level in the early RG progenitors, Pax6 controls the specification of sub-lineages of IGL neurons by a direct transcriptional control on the expression of the IGL determinant genes *Ngn2* (for L6, L5; Scardigli et al 2003; Schuurmann et al., 2004) or *Er81* (for L5, this work) in a region restricted manner. Our present results further show that Pax6 is involved in determining the neuronal outcome of some IGL sub-lineages (e.g. for *Clim1a+, Fezl+, Smi32+, Lmo+4, NSE+* L5 neurons) or their migratory ability (e.g. for *Vglut1+, Clim1a+, Lmo3+, Lmo4+, Fezl+, Slap1+, NSE+*). The available data allows to assume that while the first effect, including Pax6-dependent, direct control on the cell cycle parameters of IGL sub-lineages, the migratory deficiency affects neuronal subpopulations that are specified in a Pax6—Ngn2 dependent pathway in a region specific manner (mostly in the rostrolateral cortex). At late developmental stages (after E14.5), the diminished pools of RG progenitors is misspecified and fail to produce both correctly specified IP in the SVZ and SGL in absence of Pax6 (this work, Tarabykin et al., 2001; Nieto et al., 2001). *Pax6* is expressed at low level in the late RG progenitors and only transiently in the IPs suggesting that Pax6-dependent program might specify environmental cues that determine the fate of the SGLs in IPs. Furthermore, the widely documented molecular ventralization of the NE at the PSPB (Stoykova et al., 1996; 2000;Toresson et al., 2000; Yun et al., 2001; Muzio et al., 2002; Kroll and O´Leary, 2005) leads to the massive invasion of GABAergic INs into the pallial SVZ prior to the SGL formation in the *Pax6* mutants possibly contributing to the inhibition of proliferation of the late progenitors in the SVZ (Haydar et al., 2000; Liu et al., 2005), thus hampering in addition the acquisition of the late neuronal cell fate. Another possibility is that the low level of Pax6 in the late RG progenitors might regulate specific sets of still not identified determinants for acquiring of the IGL cell fate. CP, Cortical plate; bVZ, Basal ventricular zone; IZ, Intermediate zone; MZ, Marginal zone; PPL, Preplate; VZ, ventricular zone;

The first conclusion from our analysis of the cortical phenotype in *Pax6cKO* mice is that *Pax6* has an intrinsic role in the specification of SGL neurons. Previous analyses of *Sey/Sey* embryos suggested the involvement of *Pax6* in the formation of SGL (Schmahl et al., 1993; Caric et al., 1997;

Schuurmans et al., 2004) and data from BrdU labeling and transplantation experiments suggested migration defects as a possible reason for the mis-building of SGLs in *Sey/Sey* cortex CP (Caric et al., 1997). The fact that *Pax6cKO* mice reach adulthood helped us to gain a more definitive answer to this important question. Our expression analysis showed a complete or almost full loss of the expression of molecular markers for SGL neurons in *Pax6cKO* cortex (Fig.9). However we did not observed any mis-allocation or an ectopic expression of correctly molecularly specified SGL neurons in the postnatal *Pax6cKO* cortex (Fig.9, see discussion below). Furthermore, the expression analysis at stage E17.5 and P10 revealed severe expression gaps in the rostral mutant cortex for *Id2* and *Lhx2*, two factors strongly expressed in the SGL neurons, suggesting a deficit in the generation of these SGL neuronal lineages (Fig.9G/J´). In addition, BrdU labeling at two stages during generation of the SGL (E16.5 and E18.5), revealed almost a complete loss of upper cortical neurons in *the Pax6cKO* cortex at P10, and an enhanced number of BrdU+ cells within the enlarged VZ/SVZ of the mutant. Interestingly, however these preserved progenitors seemed to have the capacity to produce enlarged sets of olidodendrocytes and INs, possibly even after birth (Fig.13). Thus, when *Pax6* is not functional, the SGL neurons are absent not because of migratory defects or a delay of the RG differentiation, but because of a failure in the specification of the late RG that leads to the generation of SGL neurons. We conclude therefore, that Pax6 has a pivotal role in initiating differentiation of the late RG towards SGL neuronal cell fate. Intriguingly evidence has been proposed that, the neurons of SGLs appear to be selectively activated in the process of remote memory recall (Frankland et al., 2004). In line with this, a selective deficiency in remote memory recall was observed in *Pax6cKO* mice (Raduschkin and Stoykova unpublished data).

The early RG cells generate the majority of the lower cortical layers and the BPs/IPs located in the SVZ. This second proliferative zone is evident after E12.5 in the mouse and is assumed to generate predominantly upper cortical layer neurons (Fig.5; Fig.21; Noctor et al., 2004; Haubensak et a., 2004; Tarabykin et al., 2001; Zimmer et al., 2004). During early corticogenesis the pluripotent RG progenitors in the pallial VZ express Pax6 at a high level,

which progressively declines after stage E15.5 (Walther and Gruss, 1991; Stoykova et al., 2000). The low expression level of Pax6 however seems important for specification of the late RG cells. In fact the forced elevation of the Pax6 expression level in cortical progenitors in transgenic mice causes much more profound diminishing of the upper, when compared with the lower layer neurons (Berger et al., 2007; Manuel et al., 2007).

Another possibility might be that *Pax6* plays an essential role in formation of the second germinative zone of the pallium, the SVZ. As recently suggested, progenitors of the SVZ might play a pivotal role in the generation of the most of the upper layer neurons (Tarabykin et al., 2001). *Pax6* is expressed only transiently in a subpopulation of BPs in the SVZ (Englund et al., 2005), but it seems to be required for their proper specification, possibly by controlling the expression of neuronal identity genes. The present understaanding suggests that *Cux1/2* (Nieto et al., 2004; Zimmer et al., 2004), *Svet1* (Tarabykin et al., 2001), and *Tbr2* (Englund et al., 2005; Quinn et al., (2006), genes that are specifically expressed in both BPs in SVZ and in SGL neurons in *Pax6*-dependent manner and are possible candidates to play a role in this process.

Our analysis discovered a novel role of Pax6, namely involvement in determination of migratory ability and the neuronal output of several subpopulations of IGL neurons. We found (mostly in the rostral cortex) that several subpopolations of IGL neurons (*Vglut1+, Clim1a+, Lmo3+, Lmo4+, Fezl+, Slap1+, NSE+*) have correct molecular specification but are mis-allocated to a lower than normal position in the CP and/or ectopically distributed in GE of the HiSVZ and pPv in the *Pax6* mutant. Similarly, migratory defects of IGL neuron subtypes have been reported in the *Ngn2* mutant and *Ngn2/Ngn1* double mutant (Schuurmans et al., 2004). Given that *Ngn2* acts as a direct downstream of Pax6 in the corticogenesis (Scardigli et al., 2003), these findings suggest possibly that a *Pax6-Ngn2* dependent mechanism modulate the migratory property of these IGL cell lineages.

Moreover we observed an enhancement in the pool size of IGL neuronal sub-lineages (*Clim1+, Lmo4+, Fezl+, Smi-32+*). The preformed BrdU-birthdating analysis during late developmental stages (E16.5 when the

SGL are born) with ISH for early-born L5 neuronal markers (*Fezl, Clim1a*) excluded the possibility that the RG progenitors keep producing early IGL neuronal fate at late developmental window. Thus, we assume that while expressed at a high level in the early RG progenitors, Pax6 could control the neuronal output of IGLs, possibly regulating the mitotic parameters of IGL neuronal sub-lineages. This is in accordance with previous data indicating that only the early progenitors exhibit defects in their proliferative properties in *Sey/Sey* embryos (Gotz et al., 1998; Estivill-Torruset al., 2002). Furthermore, in chimeric *Pax6-/-; Pax6+/+* brain, a bigger proportion of the *Pax6-/-* progenitors exit from the mitotic cycle early in development, leading to a diminished progenitors pool for late neurogenesis (Quinn et al., 2006).

Given that progenitors in the pallial VZ generate the majority of IGL neurons, transcriptional factors expressed both in VZ progenitors and IGL neurons such as Er81 are candidates for instructive factors for specifying IGL neuronal fate. Similarly as for *Ngn2,* we demonstrated in this study that Pax6 directly regulates the expression of *Er81* only at high dosage both *in vitro* and *in vivo*. Accordingly, we show that in the absence of *Pax6* function the expression of *Er81* is severely affected in the ventrolateral VZ and CP at the mid-gastation stage as well in L5 of the parietal cortex at the postnatal stage. This supports the idea that *Pax6* regulates the specification of subpopulations of IGL neuron by controlling the instructive factors of these neuronal subtypes.

Previous data indicated that in absence of Pax6, the pallial progenitors are progressively ventralized, acquiring ectopic expression of subpallial markers that causes a partial transformation of the glutamatergic pallial into the fate of subpallial progenitors, generating GABAergic INs (Stoykova et al., 2000; Toresson et al., 2000; Yun et al., 2001 Kroll and O´Leary, 2005). As a novel characteristic of this phenotype we demonstrated here that during development *Er81* exhibits ectopic and enhanced expression in the pallial SVZ/IZ obviously connected with the olfactory bulb. Furthermore, the enlarged SVZ of the forebrain at rostralmost level seems to generate more *GAD65*+ and Calbindin+ INs, invating the PFC and Fr cortex of the mutant possibly even postnatally. It is interesting to note that GABA signaling is emerging as an essential signaling in modulating progenitor proliferation in the VZ/SVZ of

cortex (Haydar et a., 2000; Liu et al., 2005). It fits well with the reported increased numbers of cycling cells in SVZ of the *Pax6* mutant (Toresson et al., 2000 and Yun et al., 2001). Therefore the widespread ventral misspecification, leading to ectopic GABA signaling in VZ/SVZ in the *Pax6* mutants may determine or contribute to the loss of SGL neurons. We found that the most severely affected domain of the *Pax6cKO* cortex at adulthood is the frontal cortex, which contains an enlarged set of INs, IGL neuronal subpopulation, but completely missing SGLs. The medial PFC, the frontal, and the cingulate cortices integrate information from the sensory, motor, and limbic areas (Uylings et al., 2003; Miashita, 2004) and such integrative function of PFC appears to be essential for remote memory recall (Maviel et al., 2004). In fact *Pax6cKO* mice showed that the PFC and Fr cortex are the most severely affected regions in *Pax6cKO* brain in which the SGL are abrogated. MRI studies on *Aniridia* patients also revealed a reduced gray matter (especially of the anterior cingulate cortex), a dysgenesis of corpus callosum, and absence or hypoplasia of anterior commissure (Ellison-Wright et al., 2004; Sisodiaya et al., 2001). We also found these defects in the *Pax6cKO* mutant (Fig.14). Thus, anatomical defects and related behavior deficits of mutant brains are similar to those of *Aniridia* patients suggesting that the cortex specific *Pax6cKO* mouse line is an ideal model to study aspects of this inherited disorder of humans.

3.2 Pax6 in cortical arealization

Previous studies demonstrated that the frontal cortex of *Sey/Sey* embyo is diminished and molecular markers for caudal cortical domains expand rostrally, implicating *Pax6* in the acquisition of cortical area identity (Bishop et al., 2000, 2002; Muzio et al., 2002). The severe dysgenesis of the diencephalon in both *Sey/Sey* (Stoykova et al., 2000, Hevner et al., 2000) and conventional *Pax6KO (*Jones et al., 2002) embryos hampered so far the study of cortical area identity in these mutants. However, in the cortex-specific *Pax6cKO* these investigations became possible. Our results indicate that the frontal cortex in the *Pax6cKO* is also diminished and mispatterned, the SGLs including layer 4 are severely underrepresented, and there is a rostral shift of caudal borders along the AP axis of the neocortex (Fig.16A/D´). Surprisingly,

however, the TCA and CTA projections from the M, SS and, Vi domains with the correspondent sensory nuclei of thalamus were preserved, indicating that cortical area identity is largely unaffected in a lack of Pax6 in the pallial progenitors (Fig.16E/F´). This is in line with recent results from *Pax6* gain-of-function experiments with PAX77 YAC transgenic mice, carrying several copies of human *PAX6*, that showed also a normal thalamocortical connectivity (Manuel et al., 2007). It is generally assumed that establishment of topographic projections is regulated by cues located within developing cortex (such as *COUP-TF1* and *Emx2* with a regionalized expression in occipital cortex and intermediate structures as internal capsule (Bishop et al., 2000, Zhou et al., 2001). Similarly to *Pax6cKO* mice, *FGF8* hypomorphic mutants display molecular caudalization of the rostral cortex with apparently normal thalamocortical connectivity (Garel et al., 2003). Furthermore, the *Ebf1* and *Dlx1/2* double *KO* mice demonstrate thalamocortical shift without gene expression shift (Garel et al., 2002), while in *Mash1* and *Gbx2 KO* mice where early thalamocortical projections do not reach to the cortex, embryonic cortical gene expression patterns are not affected (Miyashita-Lin et al., 1999; Nakagawa et al., 1999). Together with our new finding for *Pax6cKO,* these results support the view that that molecular regionalization and thalamic connectivity are possibly not strictly interdependent processes (Garel et al., 2002).

3.3 Pax6 in neurogenesis of the adult hippocampus

We were very much intrigued by the fact that the CA1-CA3 regions of the hippocampus in *Pax6cKO* mutant contained enlarged set of pyramidal cells at adulthood. Moreover, Hi in the mutant appeared to have more progenitors-like (Nestin+ cells in str. or) and newborn neurons (PSA-NCAM+ in the ammon horn). Although this phenotype is not a subject of a detailed analysis in the present study, these interesting findings deserve attention.

Previous studies revealed that in the hippocampus, glutamatergic pyramidal cells and cortical GABAergic INs are divergent in both their sources of genesis and their mode of migration. Hippocampal pyramidal neurons are known to originate from distinct components, constituting the hippocampal neuroepithelium (HiSVZ) at the embryonic stage and from a few precursor

cells in the subgranular layer (SGL) of the dentate gyrus, which are able to generate new granule neurons even at the adult stage (reviewed by Kempermann et al., 2004; Liedo et al., 2006). Hippocampal pyramidal neurons also originate from the neuroepithelium in VZ of the dorsal telencephalon, especially from the posterior periventricular zone (pPv), from where they migrate to distinct hippocampal regions (Nakatomi et al., 2002). In contrast to hippocampal pyramidal neurons, the origin of hippocampal INs is still under debate (Kempermann et al., 2004; Liedo et al., 2006). The current view of neurogenesis assumes that the generation of new neurons occurs at low levels in several neurogenic niches in the adult brain (Gross, 2000, Alvarez-Buylla & Lim et al., 2004; Liedo et al., 2006). Developmental signals like Notch, BMPs, Eph/ephrins, Nogging and Shh seem to play important roles in maintaining adult neurogenic niches (reviewed by Alvarez-Buylla and Lim, 2004; Liedo et al., 2006). Recently Wnt and GABA signaling were shown as determinants for various processes during the development, including proliferation, differentiation and maturation of stem cells and their progeny (Kleber and Sommer, 2004; Ge et al., 2007; Jagasia et al., 2006; Tozuka et al., 2005). Several genes encoding for components of the Wnt signaling such as *Wnt3, Wnt7, Fz3, Dvl1* express in the dentate gyrus or coexpress with the neural stem cell marker, *GFAP* (Lie et al., 2005; Maekawa et al., 2005). Recently Lie et al (2005) demonstrated both *in vitro* and *in vivo* that the forced expression of *Wnt3* is sufficient to increase neurogenesis from adult hippocampal progenitors. By contrast, the blockage of Wnt signaling led to the abolishment of neurogenesis in this sub-region.

Thus, several reasons for the observed enhanced presence of pyramidal neurons in Hi of the adult *Pax6cKO* cortex should be considered. Previous data indicates that *Wnt8* and *Wnt3a*, two factors known to promote Hi morphogenesis (Galceran et al., 1999; Lee et al., 2000), are overexpressed in the caudomedial cortical primordium in *Sey/Sey* leading to an expansion of the caudomedial pallium, including the hippocampal anlage (Muzio et al., 2002a). Interestingly, results from MRI indicate a local excess of gray matter volume in Hi from *Aniridia* patients (Ellison-Wright et al., 2004). Indeed, we found at P10 that the subiculum and the Ammon horn of *Pax6cKO* contain a

surplus of *Vglut1+,* NSE+, and Smi-32+ pyramidal neurons. Most intriguingly, we observed that the Hi of the adult brain is not only augmented, but the str. oriens is abundantly populated by Nestin+ cells, and the CA1-CA3 and DG contain enhanced numbers of young differentiating PSA-NCAM+ neurons. Judged by the enhancement of Smi-32+ pyramidal neurons with extensively branched processes, such young neurons appear to differentiate successfully at maturity in the mutant Hi. In adult brain *Pax6, Emx2,* and *Mash1* are expressed in distinct small subpopulations of progenitors in the subgranular layer of DG, HiSVZ and pPv, regions considered to be the neurogenic zones of the adult brain (Gross, 2000, Alvarez-Buylla & Lim et al., 2004; Liedo et al., 2006). We do not know the consequences of the functional ablation of the function of *Pax6* on the expression of *Emx2* and *Mash1* in pPv of Hi. However, our present results allow us to suggest that after birth, a set of newly generated neurons in pPv and/or HiSVZ possibly invade DG and Hi in the *Pax6cKO.* It is conceivable that the addition of new neurons into the already established hippocampal circuits of the adult brain could disrupt specifically Hi-dependent cognitive functions (McClelland et al., 1995). Indeed the *Pax6cKO* mice show a specific defect in contextual recent memory recall (Raduschkin and Stoykova unpublished data)

3.4 Trim11 controls the stability of Pax6

It is becoming clear that transcription factors do not act alone but are dependent on interactions with other proteins in order to fulfill fully their physiological function. These interactions modulate the specificity and regulatory function of the transcription factors on their targets. Previous evidence demonstrated direct interactions of Pax6 with the transcription factor Sox2 on the lens-specific enhancer element of the *∂-crysta*llin gene (Kamachi et al., 2001); Cdx-2/3 and p300 on the *G 1* promoter element of the *proglucagon* gene (Hussain et al., 1999); transcription factor Maf on the *glucagons* promoter; AP-2α on the *gelB* promoter in the corneal epithelium (Sivak et al., 2004). The biochemical dissection of the Pax6 domains had shown that both PD and HD bind to DNA in a specific manner (Fig.7; Epstein et al., 1994b; Czerny et al., 1995; Kozmik et al., 1997; Jun et al., 1998). However, the regulatory elements of almost all identified target genes for

Pax6 binds to the PD of Pax6 (reviewed by Simpson & Price, 2002), while most of the reported Pax6 protein partners bind to the HD or at least to regions out of the PD of Pax6 (Kamachi et al., 2001; Hussain et al., 1999; Planque et al., 2001a,b; Tominaga et al., 2002; Cvekl et al., 1999; Sivak et al., 2004). This raises the possibility that Pax6 exerts its physiological function by using the PD and HD preferably for DNA-binding or protein-protein binding, respectively. In this line of evidence recent analyses of transgenic mice with specific defects in PD or HD of Pax6 revealed that these Pax6 domains contribute differentially to brain development (Haubst et al., 2004). Furthermore numerous C-terminal *Pax6* mutations have been described in patients with different developmental anomalies (Ellison-Wright et al., 2004; Heyman et al., 1999; Singh et al., 2001; Sisodiya et al., 2001; Mitchell et al., 2003). The interaction between Pax6 and its recently identified partners, Homer3 and Dncl1, is ablated by such C-terminal Pax6 mutations (Cooper & Hanson, 2005). Therefore some of the developmental malformation in patients with *Pax6* mutations could be explained by disrupted protein-protein interactions.

Given the neurogenic function of Pax6 for RG progenitors (Heins et al., 2002) and its important role in the generation of neurons with distinct neuronal fate as described in this work, one of our goals was to identify Pax6–interacting partners that modulate the neurogenic role of Pax6 during corticorgenesis. By above objectives, we used mouse Pax6 cDNA, lacking a fragment encoding for the PD (Pax6ΔPD) to screen a cDNA library made from isolated E15.5 mouse cortex (Fig.17A). Out of 116 independent positive colonies, sequences of four corresponded to the cDNA sequence of *Trim11.* During the progression of this study, Cooper & Hanson (2005) presented preliminary data for the identification of Pax6-interacting partners using the cDNA library of the mouse adult brain with Pax6-PST and Pax6-CTP, containing the whole PST domain (amino acid residues 278-422) and the C-terminal peptide (amino acid residues 391-422) from the human Pax6 cDNA. Trim11 is one of the potential Pax6-interacting partners (Cooper & Hanson, 2005). We verified that Trim11 indeed interacts with Pax6 by utilizing different biochemical approaches such as the pull-down, immunoprecipitation assay

and cellular colocalization analysis (Fig.17 and 18). Trim11 acts as an E3 ligase and regulates the intracellular level of Humanin, a peptide with neuroprotective activities against Alzheimer ´s disease (Niikura et al., 2003). Our results indicate that Pax6 is another substrate for the E3 ligase activity of Trim11 (Fig.18). Firstly, the co-expression of Trim11 and Pax6 in Hela cells and the overexpression of Trim11 in cortical primary cells drastically reduce the stability of Pax6 protein. Secondly, Trim11 catalyzes the reaction responsible for forming the Ub-conjugated Pax6. Thirdly, treatment of Trim11 and Pax6-expressing cells with a proteasome inhibitor significantly inhibits the Trim11-mediated degradation of Pax6.

In addition to the common role that E3 ubiquitin ligases play in the degradation pathway, various members of Trim/RBCC family has shown more complex functions, such as those involved in epigenetic control, gene–silencing or control of transcription *(*Meroni & Diez-Roux, 2005; Hirose et al., 2003; Le Douarin et al., 1996; Shimono et al., 2000; Friedman et al., 1996; Cammas et al., 2000; Peng et al., 2002; Wang et al., 2004). By using gain-of-function experiments in cortical primary culture, we showed a corresponding decrease of the Pax6 protein level which is not due to transcriptional regulation of *Pax6* and *Pax6(5a)* mRNA. Thus, our present data demonstrate the exclusive role of Trim11 in controlling the stability of Pax6 protein in cortical progenitors.

There is increasing evidence about the important role of UPS in cortical neurogenesis. Several molecules that are important in this developmental process such as P35, Dab1 and Notch are substrates of UPS (Arnaud et al., 2003; Bock et al., 2004; Patrick et al., 1998; Qiu et al., 2000). Recent analysis revealed that knocking-out the function of UBR1 and UBR2, E3 ubiquitin ligases of N-end rule pathway, causes impairment of neurogenesis (An et al., 2006). In addition, Ubiquitin C-terminal hydrolase L1 affects the morphology of the neural progenitor cells and modulates their differentiation (Sakurai et al., 2006). We found that the overexpression of Trim11 not only mediates the degradation of Pax6 protein, but also inhibits specifically the neurogenic role of Pax6.

3.5 The expression level of Pax6 and Trim 11 possibly involves an autoregulatory feedback loop

Collective data from functional studies on Pax6 has highlighted the fact that different levels of Pax6 play essential roles in different aspects of mammalian development. Thus, homozygous *Sey/Sey* mouse embryo have no eyes, whereas the obvious defects in the heterozygous (*Sey/+*) embryos are the smaller eyes with various ocular abnormalities, suggesting that the function of Pax6 depends on a defined threshold (Hill et al., 1991). Accordingly, transgenic mice carrying multiple copies of human Pax6 on a WT background show similar phenotyes to the *Sey/Sey* ocular abnormalities (Schedl et al., 1996). Thus, the level of Pax6 in the developing eye is crucial, with both reduced and increased gene dosages, causing profound developmental defects in this organ. Also in developing cortex, the difference of the spatiotemporal expression level of Pax6 seems to play specific roles. Thus, abolishment of the rostral-high to caudal-low expression gradient of Pax6 in the cortical progenitors results in severe shrinkage of the rostral cortex specifically (Bishop et al., 2000, 2002; Muzio et al., 2002). Similarly, the high expression level of Pax6 in progenitors of VP and LP is important for the specification of several amygdalar nuclei that originate from these restricted progenitors domains (Tole et al., 2005).

Pax6 is a neurogenic factor for cortical progenitors (Heins et al., 2002) expressed at a high and low level in the early and late progenitors, respectively. It appears to regulate different aspect of corticogenesis, as shown in this present study. It is interesting to note that both, the Pax6 loss-of-function (this work) as well as Pax6 gain-of-function in cortical progenitors (Berger et al., 2007, Manuel et al., 2007) indicated that the specification of SGL neurons is more severely affected. Together, the available data suggest that the maintenance of the correct level of Pax6 in distinct cortical domains and at different time windows has a pivotal role in correct neurogenesis.

Both biological and non-biological studies have shown the establishment of auto-regulatory feedback loops between developmental regulators is important in many systems (Hasty et al., 2002). In living cells,

transcriptional factors and UPS show a “cross-talk” through the formation of an auto-regulatory feedback loop which balance their activities (Wu et al., 1993; Leng et al., 2003). Our results strongly suggest that Trim11, an E3 ligase for Pax6, functions as a negative regulator of Pax6 expression in cortical progenitors. Although further work is necessary to confirm whether Pax6 could directly activate the expression of *Trim11*, we suggest that Pax6 and Trim11 possibly participate in an autoregulatory feedback mechanism, that regulating their expression levels and activities during corticogenesis (see the schema in Fig.20)

Thus our results demonstrate for the first time that the expression of Pax6 is not only regulated at transcriptional level, but also includes post-translational modifications involving the ubiquitin-proteosome system. The data further implicate that Trim11 as being a modulator, thus contributing to the establishment of the correct physiological function of Pax6 transcription factor during mammalian corticogenesis.

4. Summary

Pax6 is a key transcription factor involved in the organogenesis of the eye, pancreas, and brain. In developing cortex, Pax6 has been implicated to play a role in regionalization, neurogenesis, layer formation, and axonal path finding. Mice deficient for Pax6 die before these processes are accomplished, having multiple brain defects, thus precluding further studies on the consequence of Pax6 deficiency on cortical layering, arealization, and brain function. To determine roles of *Pax6* in these key events of cortical patterning, we generated a *Pax6* conditional knockout mouse (*Pax6cKO*) that reachs adulthood, in which the function of Pax6 is ablated at the onset of corticogenesis only in the radial glia (RG) or cortical progenitors. We show that deletion of Pax6 specifically abrogates the differentiation of the late RG progenitors into upper cortical layer neurons. Instead, the RG cells accumulate in an enlarged pool along the corticostriatal border overproducing interneurons and oligodendrocytes. Furthermore we found that *Pax6* function is essential for the normal output of correctly specified subpopulations of the lower cortical layer neurons and their migratory ability. Moreover, we present evidence that Pax6 directly regulates the expression of the transcription factor *Er81* in layer 5 neurons. In the absence of *Pax6*, there is a rostral shift of caudal molecularly defined borders across the AP axis of the cortex, however the area identity and the major connectivity patterns are surprisingly normal. Many morphological defects of mutant brains displayed are similar to those of *Aniridia* patients, suggesting that the cortex specific *Pax6cKO* mice might be helpful to study aspects of this genetic disorder in humans.

Given the essential role of *Pax6* in neurogenesis, we attempted to study mechanisms regulating Pax6 activity in the developing cortex. We searched for proteins interacting with Pax6 by using the yeast two-hybrid screen approach and found that Trim11 interacts with Pax6. Our analysis indicates that Trim11 regulates the intracellular Pax6 level through the ubiquitin-proteasomal degradation pathway. Accordingly, we show that overexpression of Trim11 causes inhibition of neurogenesis due to the

degradation of Pax6. Our results further indicate that Trim11 might participate in an autoregulatory feedback loop that controls *Pax6* function.

5. Materials and Methods

5.1. Oligos, antibodies, plasmids and animals

5.1.1. Oligos

PCR primers for PCR, qPCR, ChIP, EMSA were ordered from IBA (Göttingen, Germany) and Qiagen (Hilden, Germany). The name, sequence (or catalog) and usage of oligos are described in table 2.

Oligo name	Sequence (5´→3´) or catalog number (Qiagen)	Usage
ChIP/Con/F	CCGTCTCTTTAGTCCCGTTAGGTGAAA	ChIP
ChIP/Con/R	GCTCTTGCATTTGCATAGCTAATTACCCT	ChIP
ChIP/P6/81F	CTTTTCTCTACCTTTGACCCGGAGTCCA	ChIP
ChIP/P6/81R	CCTCTCAGCACTCTCCAGGATGAATCT	ChIP
E/P6/Er81	TAGAAGCAGCTTCTCCCGCTTGCTTTCCTTACAATAT	EMSA
E/P6/Er81/M	TAGAAGCAGCTTTTCCCGAGTGCTTTCCTTACAATAT	EMSA
E/P6/Cons	AATTTTCACGCTTGAGTTCACAGCT	EMSA
E/P6/Trim11a	TAATAATAAATCTTTAGGCCAGAGTGAGCAGGGACTG	EMSA
E/P6/Trim11b	TGCACACAAATCAGTGAAAGATGAGTCTTTGCTCTTT	EMSA
E/P6/Trim11c	GGCCGCTGCAGACGCAGGCTGGAGTGCGTTCCGGCTC	EMSA
E/P6/Trim11d	TCTGAGCAGCTCAGGGCTGCCTGTAACTCCAGCTGTA	EMSA
E/P6/Trim11e	ACTTTGATGTGCATTGGAGGGAGACATTCAAACTGTA	EMSA
E/P6/Trim11f	AGTGGGGTGTTCAGAGATGAGTGAAGACAGAAGCCCG	EMSA
E/P6/Trim11g	GAGACCTCCATCTTCTCCCATGTTCTCACCCGTCACT	EMSA
E/P6/Trim11h	CTAGGGGTACTTACTTAAGCCTGAGGCTCCAACAGCC	EMSA
q18S	QT01036875	QPCR
qPax6(5a)/F	CACAGCGGAGTGAATCAGCTT	QPCR
qPax6(5a)/R	GCACCTGGACTTTTGCATCTG	QPCR
qPax6/F	CCTGGTTGGTATCCCGGGA	QPCR
qPax6/R	CCGCTTCAGCTGAAGTCGCA	qPCR
qTrim11/F	GCAGAAATGGCACGACGCCT	qPCR
qTrim11/R	GGAACAGCATTGCGTCCTCCA	qPCR

Table 2. List of oligos

5.1.2. Antibodies

The name, origin, host, source and dilution of antibodies are described in table 3.

Name	Origin	Host	Supplier	Dilution	
				IHC/ICC	WB
Primary Antibody					
Calbindin	Human	Rabbit	Dako	1:2500	
Calretinin	Human	Mouse	Dako	1:2000	

Cre	Peptide	Rabbit	Covance		1:1000
Er81	Chick	Mouse	DSHB	1:3000	
GAD67	Mouse	Mouse	Sigma	1:2000	
GFAP	Peptide	Mouse	Chemicon	1:100	
GFP	Peptide	Mouse	Chemicon	1:500	
GST	Peptide	Mouse	Zymed		1:500
HA	Peptide	Rat	Roche	1:50	1:500
His	Peptide	Mouse	Novagen		1:1000
Luciferase	Peptide	Goat	Abcam	1:100	
Nestin	Peptide	Mouse	Chemicon	1:300	
NeuM	Peptide	Rabbit	Chemicon	1:300	
Pax6	Chick	Mouse	DSHB	1:300	1:500
Pax6	Peptide	Rabbit	BABCO	1:300	1:1000
PSA-NCAM	Peptide	Mouse	Chemicon	1:100	
Smi-32	Peptide	Mouse	Sternerberger	1:2500	
ß-Actin	Peptide	Rabbit	Sigma		1:1000
Tuj	Peptide	Mouse	Chemicon	1:200	
Secondary antibodies (peroxidase-conjugated)					
IgG	Rabbit	Goat	Covance		1:10000
IgG	Mouse	Goat	Covance		1:5000
IgG	Rat	Goat	Covance		1:10000
IgG	Mouse	Goat	Bio-Rad		1:5000
Secondary antibodies (Alexa)					
Alexa 488	Rabbit	Goat	Molecular Probe	1:400	
Alexa 488	Mouse	Goat	Molecular Probe	1:400	
Alexa 568	Mouse	Goat	Molecular Probe	1:400	
Alexa 568	Rabbit	Goat	Molecular Probe	1:400	
Alexa 594	Chick	Goat	Molecular Probe	1:400	
Alexa 594	Rabbit	Goat	Molecular Probe	1:400	
Alexa 594	Mouse	Goat	Molecular Probe	1:400	
Alexa 594	Rat	Goat	Molecular Probe	1:400	

Table 3. List of antibodies

5.1.3. Anti-sense probes for ISH

The name, preparation (linearization, transcription of plasmid templates) and source of anti-sense probes for ISH are described in table 4.

Gene	Probe preparation		Source
	RE	Polymerase	
Arx	HindIII	T3	Lab stock
Cad-8	HindIII	T3	Lab stock
Clim1a	SalI	T7	I. Bach
Cux2	XbaI	T3	J. Liu
Dlx1	XbaI	T3	M. Price
EphA4	EcoRI	T7	R. Klein
ER81	ApaI	SP6	V. Tarabykin
Gad67	XhoI	T3	Lab stock

ID2	SalI	T3	R. Benezra
Lhx2	NotI	T7	G. Bernier
Lmo3	EcoRI	T7	B. Anderson
Lmo4	SacI	T3	B. Anderson
Msi1	SacI	T3	H. Okano
Oligo2	EcoRI	T7	D. Anderson
Otx1	EcoRI	SP6	Lab stock
PLP/DM20	BamHI	T3	Lab stock
RzR-ß	EcoRI	T3	C. Kaznovski
Slap1	EcoRI	T3	Lab stock
Tbr1	HindIII	T3	J. Rubenstein
Vglut1	EcoRI	T3	Lab stock

Table 4. List of anti-sense probes for ISH

5.1.4. Plasmids

The name, insert, backbone vector, references for plasmids are listed in table 5. All plasmids generated in this study are described in detail below.

Name	Insert	Backbone vector	Reference
Pax6ΔPD	Pax6ΔPD	pBDLeu (Invitrogen)	This study
CMV-Pax6	Pax6	PCMV	Walther and Gruss, 1991
Flag-Pax6	Pax6	pCS2-MT	Lab stock
GST-Trim11	Trim11	pGEX (Pharmacia)	This study
HA-Trim11	Trim11	pHA-CMV (Clontech)	This study
Er81-Luc	Er81 promoter	pGL3 (Promega),	This study
Er81Cre	Er81 promoter	Cre backbone	This study
PSP64-Pax6	Pax6	PSP64	Marquardt et al., 2001
CMV-Gfp	Gfp	CMV-Gfp (Clontech)	
Ubi-His			Treier et al., 1994

Table 5. List of plasmids

5.1.5. Animals

Small-eye (Sey), *Pax6 flox* and *Emx1Cre*, *NexCre, Er81Cre JoP6* mice were maintained in a C57BL6/J background. Cortical primary cells were derived from the mouse strain CD1. Chick eggs were ordered from Lohmann Animak health GmbH (Cuxhaven, Germany).

5.2. Methods for DNA study

5.2.1. Standard polymerase chain reaction and genotyping

Primers were designed with length around 20-26 nucleotides with Tm=55-60°C. The reaction mixture contained 1 µl template DNA (10 pg-1 ng plasmid DNA, or 200 ng genomic DNA), 1 µl 10 pmol/µl forward primer, 1 µl 10 pmol/µl reverse primer, 1x PCR Buffer, 4-8 µl 2.5 mM dNTPs, and 0.5 µl *Taq* Polymerase (5U/µl) in a total volume of 30 µl. The thermocycling program (Table 6) was carried out using PTC-200 thermal cycle (Perkin Elmer).

Step	Temperature	Duration
1. Initial denaturation	94 °C	4 minute
2. Denaturation	94 °C	30 seconds
3. Annealing	50-55 °C	30 seconds
4. Elongation	72 °C	(About 1 minute/kb)
5. Go to step 2, repeat 29 to 39 times (30-40 cycles)		
6.Final elongation 72 °C		10 minutes
7. Incubation	4 °C	Unlimited

Table 6. The thermocycling program for a standard polymerase chain reaction (PCR)

5.2.2. Purification of PCR products

PCR products were purified using QIAquick PCR Purification Kit (Qiagen) as described by the manufacturer.

5.2.3. DNA electrophoresis and purification from the agarose gel

0.5-2% agarose gel was prepared by melting agarose (Invitrogen) in 1x TBE Buffer (90 mM Tris-borate, 2 mM EDTA, pH 8.0) and subsequently adding ethidium bromide to a final concentration of 0.3 µg/ml. DNA sample was mixed with 5x DNA loading buffer (25% Ficoll, 100 mM EDTA, 0.05% Bromophenol Blue), and electrophoresis was performed under 1-7 v/cm in 1xTBE buffer. For fragment purification, the band was excised from the gel. DNA was extracted using QIAquick Gel Extract Kit (Qiagen) as described by the manufacturer.

5.2.4. DNA digestion with restriction enzymes

1-10 µg DNA was incubated with 20-80 U of the approate restriction enzyme(s) at 37°C for 2 hours or overnight. For end-cutting of the PCR product, crude PCR product was purified with a PCR Purification Kit (Qiagen) and then incubated with 30-60 U restriction enzyme(s) at 37 °C overnight.

5.2.5. Dephosphorylating or blunting the ends of DNA fragments

Dephosphorylation of DNA 5'-end was performed by directly adding 1 µl Alkaline Phophatase (1U/µl, Roche) into the restriction enzyme digestion mixture and incubating at 37 °C for 1 hour.

DNA polymerase I large fragment (Klenow fragment) (5U/µl, NEB) was used to fill-in the ends of overhang-5' DNA fragment. DNA in restriction enzyme NEB buffer supplemented with 33 µM dNTPs was incubated with Klenow at a concentration of 1U per µg DNA at 25 °C for 30 minutes.

3'-overhang DNA fragment was made blunt using Pwo DNA Polymerase (5U/µl, Roche), 0.5 µl of which was mixed with 5 µl 10x conc. PCR buffer with 20 mM $MgSO_4$ (Roche), 0.5 µl 20 mM dNTPs, 4 µl H_2O, and 40 µl DNA fragment in a total volume of 50 µl, then incubated at 72°C for 15 minutes to achieve the reaction.

5.2.6. Ligation

25-100 ng purified vector fragment was mixed with a 5 fold excess (molecular ratio) of purified insert fragment, 1x T4 DNA ligase buffer (MBI Fermentas), and 1 µl T4 DNA ligase (3 U/µl) (MBI Fermentas) in a total volume of 10 µl. This ligation mixture was incubated at RT for at least 2 hours or at 4^{o}C overnight.

5.2.7. Preparation of electrocompetent cells

Preparation of electrocompetent cells was performed as described in table 7.

1. Inoculate a single colony of *E. coli* (DH5α, DH10B, XL10gold) into 10 ml LB medium and cultured at 37°C shaking overnight (250 rpm).
2. Inoculate the 2-10 ml overnight cultures into 2x1 liter prewarmed LB medium and culture them at 37°C shaking until the O.D.600 reached

0.6-0.8 (about 3 hours).
3. Chill the cells on ice for 10-30 minutes.
4. Centrifuge at 5000 rpm at 4°C for 20 minutes to harvest the cells.
5. Discard the supernatant, wash each pellet from 1 liter culture with 1 liter prechilled water (1:1 wash), then centrifuge at 5000 rpm at 4°C for 20 minutes.
6. Discard the supernatant, wash each pellet with 100 ml prechilled 10% glycerol (1:10 wash), then centrifuge at 6000 rpm (Sorvall HS-4 rotor) at 4°C for 10 minutes.
7. Discard the supernatant, wash each pellet with 20 ml prechilled 10% glycerol (1:50 wash), then centrifuge at 6000 rpm at 4°C for 10 minutes.
8. Discard the supernatant, wash each pellet with 2 ml prechilled 10% glycerol (1:500 wash), then centrifuge at 6000 rpm at 4°C for 5 minutes.
9. Aspirate the supernatant, resuspend each pellet in 2-3 ml 10% glycerol. 50 µl or 100 µl resuspension was aliquoted into each tube on ice, frozen in liquid nitrogen, and stored at –80°C.

Table 7. Preparation of electrocompetent *E. coli* cells.

5.2.8. Preparation of competent cells for heat shock transformation

Competent cells for heat shock transformation were prepared as described in table 8.

1. Inoculate a single colony of *E. coli* (DH5α or XL-1 Blue, XL10gold) in 50 ml LB medium and culture at 37°C shaking overnight (250 rpm).
2. Transfer 4 ml of the overnight culture into 400 ml LB medium and incubate at 37°C shaking to an O.D.600 of 0.35-0.4.
3. Make aliquots of the cultured medium into eight 50 ml prechilled sterile polypropylene tubes (BD Falcon), and incubate them on ice for 5-10 minutes.
4. Centrifuge at 1600 g (3,000 rpm, Sorvall HS-4 rotor) at 4°C for 7 minutes.
5. Discard the supernatants, gently resuspend each pellet in 10 ml

prechilled CaCl2 solution (60 mM CaCl2, 15% glycerol, 10 mM PIPES, pH 7.0), and centrifuge at 1100 g at 4°C for 5 minutes.
6. Discard the supernatants, resuspend each pellet in another 10 ml prechilled CaCl2 solution, and incubate them on ice for 30 minutes.
7. Centrifuge at 1100g at 4°C for 5 minutes.
8. Discard the supernatants, and resuspend each pellet completely in 2 ml prechilled CaCl2 solution.
9. Aliquot 200 µl into each tube on ice, freeze immediately in liquid nitrogen, and store them at –80 °C.

Table 8. Preparation of chemical competent *E. coli* cells.

5.2.9. Transformation of E. coli by electroporation

50 µl competent cells were thawed on ice and transferred in a prechilled 0.1 cm electrode Gene Pulser Cuvette (Bio-Rad). 1 µl DNA solution (1 ng/µl) or 1.5 µl ligation product was added directly to the competent cells and mixed well by gently flicking. Then, the surface of the cuvette was completely dried and the electroporation was performed using a Gene Pulser (Bio-Rad) with following setting, 1.8 kV voltage, 200 Ω resistance, 25 µF capacitance. Afterwards, 960 µl prewarmed LB medium was immediately supplied to the electroporated *E. coli* for recovery. The cells were recovered at 37°C rotating for 1 hour, followed by plating 100 µl and 900 µl on separate plates.

5.2.10. Transformation of E. coli by heat shock

50-100 µl competent cells were thawed on ice and transferred into a Falcon polypropylene tube (BD Falcon). 10 ng pure DNA or 10 µl ligation product was directly added to the competent cells and mixed well by gently flicking. The mixture was incubated on ice for 30 minutes, heat shocked at 42°C for 45 seconds, and incubated on ice for another 2 minutes. Then, 900 µl prewarmed LB or SOC medium (Invitrogen) was supplied to the heat shocked cells, and incubated at 37°C rotating for 1 hour. These cells were subsequently spun down at 3000 rpm for 2 minutes, resuspended in 200 µl medium and plated.

5.2.11. Plasmid DNA isolation from E. coli

DNA from *E.coli* was purified using QIAGEN Plasmid Mini, Midi, Maxi, Mega, Giga Kit (Qiagen), as described by the manufacturer.

5.2.12. Genomic DNA extraction from mammalian cells or mouse tissues

Cultured mammalian cells in a 10 cm dish were trypsinized and washed twice with PBS. Cell pellet was then resuspended in 1 ml cell lysis buffer (100 mM Tris, pH 8.0, 200 mM NaCl, 5 mM EDTA, 0.2% SDS, freshly added 100 µg/ml Proteinase K) and incubated at 50°C shaking for 6 hours. Then, the lysis product was extracted with 1 volume of phenol/chloroform/isoamylalcohol (25:24:1) twice, and precipitated with 1 volume of isopropanol plus 0.1 volume of 3 M NaAc, pH 5.2. The precipitated pellet was washed with 500 µl 70% ethanol, air dried, and dissolved in 50 µl millipore H_2O. The mouse tissue was washed once with PBS before digestion in 500 µl tissue lysis buffer (100 mM Tris, pH 8.5, 200 mM NaCl, 5 mM EDTA, 0.2% SDS, freshly added 250 µg/ml Proteinase K) at 55°C with overnight shaking. Treatments were the same as described above in mammalian cells.

5.2.13. Generation of a Er81Cre transgenic mouse line

The 2 kb upstream from the starting codon of mouse *Er81* gene were amplified by the Expand Long Template PCR kit (Roche) as a NheI/Not fragment, then cloned in Cre-IRES-GFP-Intron-pA plasmid (Ashery-Padan et al., 2000; Berger et al., 2004) in pSL1180 (Pharmacia). The *Er81Cre* mice were generated by pronuclear microinjection. Transgenic mice were identified by PCR analysis or GFP-fluorescence.

5.3. Method for RNA study

5.3.1. Total RNA isolation from eukaryotic cells or embryos

Total RNA from cultured cells or mouse tissues was isolated using RNeasy Mini Kit (Qiagen), as described by the manufacturer.

5.3.2. qRT-PCR

qRT-PCR (qPCR) analysis was performed using a QuantiTect Rev. Transcription and QuantiTect SYBR Green PCR Kit (Qiagen) with a qPCR Mastercycler (Eppendorf) according to manufacture ´s instructions. The assay was done in triplicate and normalized to internal 18S (data in means ± s.d.). The sequences of primers for qPCR are listed in table 2.

5.4. Methods for protein study

5.4.1. Expression and purification of GST-fused recombinant protein

GST-fused Trim11 protein was expressed in *E. coli* and purified as described table 9.

1. Mouse *Trim11* cDNA was inserted into *pGEX-KG* vector (Amersham) between XhoI and HindIII sites in frame with *GST*.
2. Heat shock transformed the *pGEX-KG-Trim11* construct into BL21 DE3 C41 competent cells. Inoculate a single colony into 100 ml LB medium with 50 µg/ml ampicillin, and culture at 37°C shaking overnight.
3. Add prewarmed LB medium with 50 µg/ml ampicillin into the 100 ml overnight culture up to 1 liter, and continuously incubate at 37°C shaking to an O.D.600 of 0.7-0.8 (about 1 hour).
4. Add IPTG to a final concentration of 1 mM to induce the protein expression at 25°C shaking for 6 hours (or at 37°C shaking for 2 hours).
5. Centrifuge at 5000 rpm at 4°C for 25 minutes to harvest the cells.
6. Briefly discard the supernatant, resuspend the pellet with the remaining medium, and transfer the resuspension into a 50 ml Falcon tube.
7. Centrifuge at 4000 rpm at 4°C for 30 minutes. Discard the supernatant and freeze the pellet at –20°C overnight.
8. Resuspend the pellet with 40 ml resuspension buffer (50 mM Tris, pH 7.5, 500 mM NaCl, 2 mM EDTA, freshly added protease inhibitor tablet) on ice.
9. Sonicate the resuspension on ice for 5 x 1 minute with 1 cm tip using Cell Disruptor B15 (Branson Sonifier) under the condition of Output

Option 7 and 50 % Duty Cycle.
10. Ultracentrifuge in a vacuum environment at 25000 rpm at 4°C for 25 minutes using L7 Ultracentrifuge (Beckman).
11. Collect the supernatant, add 500 µl prewashed Glutathione Sepharose 4B (Amersham), and incubate at 4°C rotating for at least 1 hour.
12. Centrifuge at 800 rpm at 4°C for 1 minute and discard the supernatant.
13. Wash with 15 ml prechilled washing buffer (50 mM Tris, pH 7.5, 1000 mM NaCl, 2 mM EDTA, freshly added protease inhibitor) twice. Centrifuge at 800 rpm at 4 °C for 1 minute and discard the supernatant in between.
14. Resuspend the beads with 5 ml washing buffer and transfer them into a 5 ml column (Pierce). Flow through the buffer and wash the beads in the column once more with 4 ml washing buffer column (Pierce). Flow through the buffer and wash the beads in the column once more with 4 ml washing buffer.
15. Elute the GST-Trim11 fusion protein by incubating the beads with 1.2 ml 20 mM Glutathione (Sigma) at 4 °C rotating for 1 hour. Collect the elution.
16. Further elute the protein from the beads with another 2 ml 20 mM Glutathione at 4°C rotating for another 1 hour. Collect the elution.
17. Measure the protein concentration with Bradford Assay (Bio-Rad), in which 1 µl of protein elution was mixed with 800 µl H_2O and 200 µl Bradford Reagent was added. Then, the O.D.595 of the sample was measured and the concentration of protein was determined according to the standard curve.
18. Aliquot the purified protein, freeze them in liquid nitrogen and store at –80°C.

Table 9: Expression and purification of GST-fused Trim11 protein from *E. coli*.

5.4.2. Total protein extraction from mouse embryos

Mouse corties were homogenized briefly with a pipette, and sonicated on ice with continuous pulses for 3-4x10 seconds in 100 µl/cortex lysis buffer 2 (20 mM HEPES, pH 7.85, 30 mM NaCl, 10% glycerol, 0.2 mM EDTA, 1 mM DTT,

and freshly added protease inhibitor) using a Cell Disruptor B15 and 3 mm tip. The protein concentration of the soluble extracts was measure at an absorbance of 280 nm using BioPhotometer (Eppendorf) and normalized using BSA standards. The total protein extracts were aliquoted, frozen in liquid nitrogen, and stored at –80°C.

5.4.3. In vitro transcription/translation

The reaction was performed using a TNT Reticulocyte Lysate System (Promega). The reaction mixture contained 2 µg maxiprep DNA, 4 µl TNT reaction buffer, 2 µl amino acids mixture without methionine, 2 µl amino acids mixture without Leusine, 1.5 µl RNasin, 1.5 µl TNT SP6 or T3 or T7 RNA polymerase, 50 µl reticulocyte lysate, and the approrate volume of DEPC treated H_2O to a total volume of 100 µl was mixed well by flicking and incubated at 30°C for 2 hours.

5.4.4. Western blotting

Total protein extracts of mouse cortex or cultured cells were obtained by either sonification or heating in SDS-PAGE sample buffer (2% SDS, 9 mM Tris-HCl at pH 6.8, 20% glycerol, 0.02% bromophenol blue, 0.1 M DTT) with a cocktail of protease inhibitors (Roche). The supernatant from the soluble fraction was collected after centrifugation at 10000 g for 2 min. The protein concentration was estimated by the Bradford procedure (BioRad). Proteins (20-50 µg) were fractionated by SDS-PAGE and blotted onto transfer membranes (Millipose) for western blot analysis. Membranes were incubated with antibodies against primary and secondary antibodies (table 3). Antibodies were detected by chemiluminescence kit from Pierce. Quantifications were normalized to the level of actin. Blots were re-used by using a re-BlotWestern Blot Recycling kit (Chemicon).

5.4.5. Luciferase assay

NIH-3T3 and Hela cells or the cortex primary cells were lysed and used for Luciferase activity quantification with a luciferase assay system (Promega) and Lumat LB9501 luminometer (Berthold), according to manufacturer `instructions.

5.5. Methods for study of protein-protein interaction

5.5.1. Yeast two-hybrid screening

The yeast-two-hybrid screening was performed using the ProQuest two-hybrid system (Invitrigen).

5.5.1.1. Construct for the two-hybrid screening

The Sal1/NotI cDNA fragment of *Pax6ΔPD,* which encodes murine Pax6 without the pair domain was cloned into the pDBLeu vector (Invitrigen) in frame with the GAL4 DNA binding domain (Fig.18A). The cloning and expression of recombinant protein in yeast were verified by sequencing and western blot analysis, respectively.

The *pDBLeu-Pax6ΔPD* construct was used as a bait plasmid in the yeast two-hybrid screening. A cDNA library of the E15.5 Mouse cortex is harbored in the *pEXP-AD502* vector (EvoQuest Custom cDNA library, Invitrogen) to be expressed as a transactivation domain fusion protein.

5.5.1.2. Evaluation of transformation efficiency of MaV203 competent cells

The cotransformation efficiency of *MaV203* competent cells was evaluated as described in table 10.

1. Thaw the PEG/LiAc (Invitrogen) solution at RT and mix the solution well before dispensation.
2. Thaw the *MaV203* competent yeast cells (library scale, Invitrogen) in a 30°C incubator for 90 seconds (or less). Invert the tube several times immediately, and transfer 100 µl into a 1.5 ml eppendorf tube.
3. Add 1 µg pDBLeu- *Pax6ΔPD* and 1 µg *pEXP-AD502* vector to the competent cells, mix well by flicking the tube.
4. Add 600 µl PEG/LiAc solution into the mixture, mix well by inverting the tube until the competent cells are totally homogenous
5. Incubate in a 30°C incubator for 30 minutes, inverting the tube every 10 minutes.
6. Add 35.5 µl DMSO and mix well by inverting the tube.

7. Heat shock the cells at 42°C for 20 minutes, inverting the tube occasionally.
8. Centrifuge the tube at 2000 rpm for 5 seconds and aspirate the supernatant.
9. Resuspend the pellet in 1 ml autoclaved H_2O and make 1:10, 1:100 and 1:1000 dilutions.
10. Plate 100 µl from the crude resuspension and each dilution onto the selection medium plate SD-L-W (21.36 g SD medium (Clontech), 0.512 g DO-Leu-Trp (Clontech), 17.6 g Agarose (Invitrogen) in a total volume of 800 ml, autoclaved, 25 ml/dish). Medium plate SD-L-W (21.36 g SD medium (Clontech), 0.512 g DO-Leu-Trp (Clontech), 17.6 g Agarose (Invitrogen) in a total volume of 800 ml, autoclaved, 25 ml/dish).
11. Incubate the plate upside down at 30°C for 72 hours.

Table 10. Evaluation of the cotransformation efficiency of *MaV203* yeast competent cells

5.5.1.3. Determination of the 3-Amino-1,2,4-Triazole (3AT)

3AT was used to inhibit background colonies during the first round of library screenning. 2 single yeast colonies from five control strains a-e (Fig.18; Invitrogen) as well as yeast cotransformed with *pDBLeu-Pax6ΔPD* and *pEXP-AD502* vector on SD-L-W plates were patched onto SD-L-W-H plates (8.01 g SD medium, 0.186 g DO-Leu-Trp-His (Clontech), 6.6 g agarose in a total volume of 300 ml, autoclaved, 25 ml/dish) supplemented with different concentrations of 3AT (0 mM, 10 mM, 25 mM, 50 mM, 60 mM, 75 mM, 100 mM, diluted from 2 M stock). After incubation for 18 hours at 30°C, the highest 3AT concentration inhibiting the growth of control strain e and permitting the growths of other control strains was selected for the library screen. 60 mM 3AT was used in this study.

5.5.1.4. Extraction of total protein from yeast

Yeast total protein was extracted as described in table 11.

1. Inoculate a single colony into 5 ml proper broth and incubate at 30°C shaking overnight.

2. Check the O.D.600 of overnight culture, and apply 5 O.D. yeast cells for the protein extraction (If O.D.600=1.0, use 5 ml cultured cells; If O.D.600=2.0, use 2.5 ml).
3. Centrifuge at 13000 rpm for about 10 seconds to pellet the cells.
4. Aspirate the supernatant, resuspend the pellet in 180 µl 2 M NaOH containing 5% β-mercaptoethanol, and incubate on ice for 10 minutes.
5. Add 20 µl 110% TCA (w/v) to precipitate the proteins and incubate on ice for 10 minutes.
6. Centrifuge at 13000 rpm for 1 minute and carefully remove the supernatant.
7. Neutralize the pellet by resuspending it in 100 µl 1 M Tris, pH 11.0.
8. Centrifuge at 13000 rpm for 1 minute and carefully remove the supernatant.
9. Resuspend the pellet in 100 µl 2x SDS loading buffer, incubate at 95°C for 5 minutes.
10. 5-10 µl (0.25-0.5 O.D.) sample was subjected to SDS-polyacrylamide gel electrophoresis and western blotting.

Table 11. Extraction of total protein from yeast cells

5.5.1.5. cDNA library screen on histidine minus medium

The first round of the cDNA library screen was performed on plates lacking leucine, tryptophan and histidine, and supplemented with 60 mM 3AT as described in table 12.

1. Heat shock transform the *MaV203* competent yeast cells with *pDBLeu-Pax6ΔPD* as described above, then plate on SD-L medium (8.01 g SD medium, 0.207 g DO-Leu (Clontech), 6.6 g agarose, autoclaved, 25 ml/dish) and incubate for 48 hours.
2. Inoculate a single *pDBLeu-Pax6ΔPD* transformant into 100 ml SD-L broth, and incubate at 30°C overnight.
3. Check the O.D.600 of the inoculated SD-L broth (1:5 dilution)
4. For good competent cells, the O.D.600 of the starting culture in YEPG broth (10 g Yeast extract, 20 g Peptone 140, 20 g D-glucose, 20 mg uracil, 20 mg adenine sulphate in a total volume of 1 liter, autoclaved)

should be 0.2-0.3.
5. Incubate at 30°C for 4.5 hours with shaking.
6. Centrifuge 200 ml culture at 2,500 rpm for 2 minutes, discard the supernatant and wash cells with 10 ml LTS buffer (10 mM Tris, pH 7.4, 1 mM EDTA, 0.1 M LiAc, 1 M Sorbitol).
7. Centrifuge at 2,500 rpm for 2 minutes, discard the supernatant, resuspend the cells in 1.1 ml LTS buffer, and equally distribute into 22 tubes each with 50 µl.
8. Centrifuge at 13,000 rpm for about 10 seconds, and aspirate the supernatants.
9. Add 250 µl 50% PEG 4000, 36 µl 1 M LiAc, 20 µl 2 mg/ml carrier Salmon Sperm DNA (Stratagene) into each tube.
10. Add 50 µl DNA solution containing 5 µg maxipreped library DNA into each tube. Then use a pipette to destroy the pellet slightly, and mix well by vortexing.
11. Incubate at 30°C for 45 minutes, inverting the tubes occasionally.
12. Heat shock at 42°C for 20 minutes, inverting the tubes occasionally.
13. Centrifuge at 13000 rpm for about 10 seconds, and aspirate the supernatants.
14. Wash each pellet with 100 µl H_2O or TE buffer (10 mM Tris, pH 7.4, 1 mM EDTA) without destroying the pellets.
15. Resuspend each cell pellet in 0.5 ml YEPG broth and recover the transformed yeast cells at 30°C for 3 hours with shaking.
16. Centrifuge at 13,000 rpm for about 10 seconds, aspirate 0.3 ml medium, and resuspend the pellet in the remaining 0.2 ml medium.
17. Plate each resuspension onto a 15 cm SD-L-W-H plate supplemented with 60 mM 3AT (40 ml medium per 15 cm dish). Incubate the plates at 30°C for 72 hours.
18. One tube was reserved to check the transformation efficiency before the last centrifugation. 20 µl from the 500 µl resuspension was diluted 1:10, 1:100, 1:1000, and 200 µl of each dilutions was then plated onto a SD-L-W plates.

Table 12. The first round of cDNA library screen on histidine minus medium

5.5.1.6. cDNA library screen by X-gal assay

The second round of the cDNA library screen, a X-gal assay, was performed as described in table 13.

1. Inoculate positive colonies from the first round of screen onto numbered SD-L-W plates. Also inoculate all these colonies onto Nytran nylon transfer membranes (Schleicher&Schuell BioScience) that were wet and tightly attached to SD-L-W medium. Incubate the inoculated plates at 30 °C overnight.
2. Proper amount of X-gal (Applichem) was dissolved in 100 µl DMFA, and then diluted in 7 ml Z-Buffer (16.1 g $Na_2HPO_4.7H_2O$ (or 10.7 g $Na_2HPO_4.2H_2O$), 5.5 g $NaH_2PO4.H_2O$, 0.75 g KCl, 0.25 g $MgSO_4.7H_2O$ in a total volume of 1 liter) to a final concentration of 0.3-1 mg/ml.
3. Distribute the 7 ml X-gal in Z-Buffer onto a Whatman paper in a 9 cm dish.
4. Freeze the nylon membrane with yeast colonies inoculated in liquid nitrogen for 1 minute.
5. Place the frozen membrane onto the Whatman paper, and incubate at 30°C.
6. Check the X-gal staining of the colonies after 10 minutes to overnight incubation.

Table 13. The second round of cDNA library screen using X-gal assay

5.5.1.7. DNA extraction from yeast cells

1.5 ml overnight culture was pelleted by centrifugation at 13000 rpm for about 10 seconds, and resuspended in 30 µl STES buffer (100 mM Tris, pH 8.0, 1 mM EDTA, 100 mM NaCl, 0.1% SDS). The resuspension was vortexed, spun down at 13000 rpm for about 10 seconds, and resuspended in another 30 µl STES buffer. Acid washed glass beads were added to 80% volume, followed by vortexing the sample for 5x1 minute. Then, 200 µl TE buffer was added, and DNA was recovered by phenol/chloroform/isoamylalcohol (25:24:1) extraction and isopropanol precipitation. For the isolation of a certain plasmid, the extracted DNA was transformed into *E. coli* and selected on an ampicillin or kanamycin plate.

5.5.2. Analysis of protein-protein Interaction

5.5.2.1. GST pull-down assay

Trim11 or GST protein (control) was incubated with 50 µl of the pre-washed Glutathione Sepharose 4B beads in 500 µl pull-down binding buffer containing 20 mM Tris (pH 7.5), 150 mM NaCl, 1 mM EDTA, 0.1% NP-40, proteinase inhibitors (Roche) at 4°C with rotating overnight for coupling. Hela cells were transfected with *CMV-Pax6*. After 48 hours of culturing, proteins were extracted in the M-PER mammalian protein extraction reagent (Pierce). Equal amounts of mammalian expressed proteins were added to bead-coupled GST or GST-Trim11 and incubated for 2 h at 4^{o}C in pull-down buffer. Afterwards beads were washed three times with a pulldown washing buffer, containing 20 mM Tris (pH 7.5), 100 mM NaCl, 1 mM EDTA, 0.1% NP-40, proteinase inhibitor (Roche) at 4°C. Bound proteins subsequently were eluted from the beads with 40 µl 2xSDS loading buffer by heating at 95°C for 5 minutes, then centrifuged at 13 000 rpm for 1 minute.

5.5.2.2. Immunoprecipitation

For immunoprecipitation experiments, *CMV-Pax6* and *HA-Trim11* were transiently cotransfected and harvested after 48 hours. The immunoprecipitation was performed using the ProFound HA Tag IP/Co-IP kit (Pierce), according to the manufacturer ´s instruction. The experiments were carried out in the presence of the proteasome inhibitor MG132 (20 µM). Elutants from the pull-down and the immunoprecipitation assays and corresponding inputs were electrophoresed using SDS-PAGE and subjected to western blot analyses with approriate antibodies.

5.6. Methods for study of protein-nuclei acids association

5.6.1. Electrophoretic mobility shift assay (EMSA)

EMSA was performed as described by Bäumer et al (2003) with some modifications. Briefly, Pax6 proteins were overexpressed using the TNT *in vitro* transcription and translation system (Promega) according to the manufacturer's instruction. Double-stranded oligonucleotides (see table 2) were end-labeled using polynucleotide kinase and gramma-^{P32}ATP. The

binding reaction was performed for 1 hour on ice in a binding buffer (25 mM HEPES pH7.4, 10% glycerol, 75 mM NaCl, 0.25 mM EDTA, 10 µg/ml, 1 mM DTT, 0.1% Nonidet P-40, 1 mM $MgCl_2$, protease inhibitor cocktail) with 5 µg poly-dI-dC, 25000 cpm of the double-stranded oligonucleotide and 5 µl of Pax6 TNT protein. For the antibody shift analysis 0.5 µl of Pax6 polyclonal rabbit antibodies (Babco) were added and samples incubated for an additional 15 min. Samples were load on 4% TAE polyacrylamide gel. Complexes were separated at 10V/cm. The gel was dried and processed for autoradiography.

5.6.2. Chromatin immunoprecipitation (ChIP) assay

Chromatin extraction was prepared from E15.5 mouse cortices. Immunoprecipitation was performed using a ChIP assay kit according to the manufacture's instruduction (Upstate Biotechnology). Polyclonal Pax6 antibodies (BABCO) or pre-immune serum (as control) were used for immunoprecipitation (10 µg antibody per immunoprecipitation). Amplification was performed using primer pairs listed in the table 2.

5.7. Methods for study of protein ubiquitylation

5.7.1. Measurement of the protein half-life

24 hour after transfection with the indicated combination of plasmids, cycloheximide (20 µg/ml) was added to the Hela cells (Fig.19A). Protein levels were determined by collecting cells at the different time points and performing immunoblotting as described above. The relative amount of Pax6 protein was evaluated by densitometry.

5.7.2. In vivo ubiquitylation assay

Hela cells were transiently transfected with plasmids of *His-Ub*, *HA-Trim11* and *Flag-Pax6* as indicated in Fig.19B. 40 hours after transfection, cells were treated with MG132 (20 µM) for an additional 8 hours and harvested. The harvested cells were used for immunoprecipitatation using the FLAG Tagged Protein Immunoprecipitation Kit (Sigma), according to the manufacturer ´s instroduction. Elutants of the immunoprecipitation and Inputs were served for the immunoblot analysis.

5.7.3. Steady-state protein level analysis

Hela cells were cotransfected with *CMV-Pax6* and either *HA-Trim11* or an empty plasmid. 24 hours after transfection cells were treated with MG132 (20 µM) for additional twenty-four hours. Cell lysates were subjected to western blotting. PAX6 proteins were detected by using an anti-Pax6 antibody. The same blots were re-probed with anti-ß-Actin antibody as a loading control.

5.8. Methods for cell culture

5.8.1. Cell culture and cell transfection

NIH-3T3 and Hela, Neuro2A cells were maintained and cultured in DMEM medium plus 10% FCS. Cells were transfected by using Lipofectamine 2000 (Invitrogen) according to supplier´s instroduction.

5.8.2. Primary culture of cortical cells and cell electroporation

The two telencephalic hemispheres were isolated under sterile conditions in Ca^{2+}/Mg^{2+}-free HBSS containing 10 mM HEPES. After twice washing with fresh Ca^{2+}/Mg^{2+}-free HBSS containing 10 mM HEPES, cells were incubated for 18 min at 37°C in 0.25% Trypsin/EDTA (Sigma). The tissue was then dissociated mechanically with a fire-polished Pasteur pipette coated with serum, centrifuged for 5 min at 1000 rpm, washed and resuspended in DMEM medium plus 10% FCS. Cortical primary cells were electroporated with the nucleotransfection device (Amaxa). Electroporated cells were cultured in different conditions. Dissociated cells were cultured on coverslips coated with poly-D-lysine and with Sato medium (DMEM, 100 µg/ml albumin, 100 µg/ml apo-transferrin, 16 µg/ml putrescine, 0.06 ng/ml progesterone, 40 ng/ml selenium, 5 µg/ml insulin, 1 mM sodium pyruvate, 2 mM L-glutamine) for 3 days for cortical progenitors (Nestin and Pax6-positive cells) and neuron differentiation (Tuj-positive cells) (Fig.20, Bottenstein & Sato, 1979). To obtain mature neurons dissociated cells were cultured in either the Sato medium or the mature neuron medium (Neurobasal-A medium supplemented with 10 mg insulin, 10 mg transferrin, 5% FCS, 2% B27, 2 mM GlutaMAX, 5 µM cytosine arabinoside). Cells were cultured on coverslips coated with poly-L-ornithine and with Sato medium or D-MEM medium containing 1g/l D-Glucose plus 10

mM HEPES and 10% FCS for astrocyte differentiation.

5.9. Methods for histological study

5.9.1. Manipulation of the mouse embryo and brain

Pregnant mice with the desired stage of embryos or postnatal mice were killed. Embryos or brains were washed in ice-cold PBS. Additionally, a tissue sample from either the yolk sack or tail was taken from each individual specimen and processed for the extraction of genomic DNA and genotyping. Mouse embryos and brains were fixed in 4% PFA and washed in PBS before embedding.

5.9.2. Cryo embedding and sectioning

Mouse embryos and brains were incubated in 30% Sucrose/PBS for cryo-protection. The specimens were thenembedded in blocks. Sectioning was performed with a cryostat (CM 3050 S, Leica). After cutting, sections were allowed to dry on a 28°C-heating plate for 30 min. Afterwards, the slides were stored at –20°C to –80°C.

5.9.3. Paraffin embedding and sectioning

Mouse embryos and brains were dehydrated in an ascending stepwise of ethanol and incubated overnight in isopropanol. They after that were incubated in 25% Toluol/Isopropanol, 50% Toluol/Isopropanol, 75% Toluol/Isopropanol and 100% Toluol for 1 hour for each step. Then, the samples were incubated in liquid paraplast at 60°C for three days (changing the wax every day). The samples were embedded in appropriate paraplast-filled blocks. The blocks were stored at RT. Paraffin-sections were performed with a microtome (Leica). Sections with thicknesses from 5 µm to 10 µm were transferred to a heated water-bath (43°C). After sections had spread, they were collected on glass slides. Slides were then dried overnight at 37°C. The dried sections were stored at 4°C.

5.9.4. Cresylviolet staining

Paraffin-sections were dewaxed in histoclear and rehydrated in decreasing concentrations of ethanol. After incubating the sections for 15 minutes in 50%

K_2SO_3 and rinsing in H_2O, the samples were stained for 15 minutes in 1,5% Cresylviolet (Sigma) in 10 mM Sodium acetate/10mM Acetic acid (Acetate buffer). The sections then were incubated in Aceteate buffer (three times for one minute) and washed in H_2O. After excess Cresylviolet was removed by incubation in 70% Ethanol for 1 minutes, the sections were dehydrated in 100% Ethanol and cleared in Histoclear (5 minutes each step). Stained sections were then mounted on a glass coverslip (Marienfeld), using Eukitt (Kindler) mounting medium.

5.9.5. Insitu hybridization

10-20 µg plasmid DNA was linearized by incubating with 40 u restriction enzyme at 37 °C for 3 hours, purified with the phenol extraction or the PCR Purification Kit (Qiagen), and eluted in 10 µl TE. 1 µl elution was loaded on an agarose gel to check the linearization efficiency. Plasmids for probes and restriction enzymes for plasmid linearization are listed in table 4.

5.9.5.1. Dig-labeling insitu hybridization

Linearized template-DNA was transcribed *in vitro* to generate the anti-sense-mRNA probes, by using Digoxygenin-labelled (DIG) UTP´s. The *in vitro*-transcription reaction contain: 14 µl of DEPC-treated H_2O, 2 µl of 10X transcription buffer (Roche), 2 µl of DIG-Nucleotide mix (Boehringer), 1 µg of linearized template DNA, 0.5 µl of RNAse inhibitor (Promega), 1 µl of RNA polymerase (Roche). The reaction was incubated for 2 hours at 37°C. Afterwards (in order to check the efficency of anti-sense mRNA synthesis) an aliquot was run on a 1% Agarose gel. The reaction-mix was further incubated with 2 µl/reaction DNAse I for 15 minutes at 37°C (to degrade excessive template DNA). The reaction was then diluted with 100 µl TE, 10 µl 4M LiCl and the RNA was precipitated by adding 300 µl 100% Ethanol, followed by incubation at –20°C for 2 hours. After spinning the tubes for 20 minutes at 13000 rpm at 4°C, the pellet was washed in 70% Ethanol and briefly air-dried. The RNA-pellet was then resuspended in 50 µl DEPC-treated H_2O and kept at –20°C. ISH with DIG-labeled probe was performed as described in the table 13.

Treatment and solution	Condition	Duration

1st Day		
For Cryo-sectioning slide		
4% PFA	RT	15 min
PBS x 2	RT	5 min x 2
Proteinase K (50ml of 1M Tris-Cl pH 8.0, 10ml of 0.5 EDTA, add to 1l Milipore water, 0.5ml of Proteinase K (10mg/ml) (add fresh)	37^{o}C	4 min
For Paraffin-sectioning slide		
Histoclear x 3	RT	7 min x 3
100% Ethanol	RT	2 min x 2
96% Ethanol	RT	1 min
90% Ethanol	RT	1 min
70% Ethanol	RT	1 min
50% Ethanol	RT	1 min
Proteinase K at 37^{o}C	37^{o}C	20 min
Steps for both Cryo-sectioning and Paraffin-sectioning slides		
Glycin (250 ml of PBS, 2.5ml of 20% glycine)	RT	5 min
PBS x 2	RT	5 min x 2
Postfixation (250ml of 4% PFA, 1ml of 50% Glutaraldehyde)	RT	5 min
PBS x 2	RT	5 min x 2
Prehybridization (50ml of formamide, 25ml of 20 x SSC pH4.5, 1g of blocking powder (Boehringer), 1ml of 0.5M EDTA, 1ml of 100 mg/ml tRNA, 0.1ml of 100 mg/ml Heparin, 0.1ml of Tween-20, 1ml of 10% CHAPS, add DEPC-water to 100ml)	70^{o}C	>2 hours
Probe in hybridization buffer	70^{o}C	ON
2nd day		
2xSSC (25ml of 20xSSC pH4.5, add milipore water to 250 l)	RT	5 min
2x SSC/50% Formamide x 3	65^{o}C	30 min x 3
KTBT (100ml of 1M Tris-HCl pH7.5, 60ml of 5M NaCl, 20ml of 1M KCl, 20ml of Tween-20, add water	RT	10 min

to 2l, autocalave all components, and mix before using)		
Blocking Reagent (8ml KTBT, 2ml Sheep Serum	RT	>2 hours
Anti-DIG antibody (Roche) in Blocking Reagent (1:2000)	4°C	ON
3rd day		
KTBT x 3	RT	5 min x 3
KTBT x 3	RT	30 min x 3
NTMT plus Levamisole x 3 (NTMT: 100ml of 1M Tris pH 9.5, 20ml of 5M NaCl, 50ml of 1M $MgCl_2$, 1ml of Tween-20, add water to 1l; add freshly 0.24 g Levamisole	RT	5 min x 3
NTMT plus Levamisole/ NBT/BCIP (10ml NTMT, 2.4 mg Levamisole, 0.2ml NBT/BCIP (Roche).	RT	As desirable
PBT x 4	RT	5 min x 4
Mounting in Mowiol		

Table 13. Procedure for ISH with DIG-labeled probe, (x: repeated time)

5.9.5.2. Radioactive-labeling insitu hybridization

For the synthesis of radioactively labelled mRNA probes, the linerarized template-DNA´s (Table 4) were transcribed in a reaction containing: 10 µl of DEPC-treated H_2O, 2 µl of 10X transcription buffer (Roche), 100 µM of DTT (Boehringer), 80 µCi of ^{35}S-UTP (Amersham), 1µg of linearized template DNA, 10 U of RNAse inhibitor (Promega), 10 U RNA polymerase (Roche). The reaction mix was incubated for 60 minutes at 37°C. Afterwards, 1 µl yeast tRNA (10 mg/ml) and 2 µl DNAse I (Promega) were added and incubated for 15 minutes at 37°C. The reaction-mix was then purified using G50 columns (Amersham) and the final volume was adjusted to 50% Formamide/50 mM DTT. The radioactivity of the probe was measured in a scintilation counter (Beckmann) and contained at least $2x10^7$ cpm. ISH with radioactively labelled probe was performed as described in table 14.

Treatment and solution	Condition	Duration
1st Day – Prehybridization and hybridization		

Histoclear x 2	RT	7 min x 2
100% Ethanol	RT	2 min
96% Ethanol	RT	2 min
90% Ethanol	RT	2 min
70% Ethanol	RT	2 min
50% Ethanol	RT	2 min
30% Ethanol	RT	2 min
Saline	RT	5 min
PBS	RT	5 min
PFA	RT	20 min
PBS x 2	RT	5 min x 2
Proteinase K	RT	7 min
PBS x 2	RT	5 min x 2
PFA	RT	5 min
PBS	RT	5 min
Acetylation mix (6.25 ml Triethanolamine, 1.25 ml Acetic acid, add milipore water to 500 ml)	RT	10 min
Saline	RT	5 min
PBS	RT	5 min
30% Ethanol	RT	2 min
50% Ethanol	RT	2 min
70% Ethanol	RT	2 min
90% Ethanol	RT	2 min
96% Ethanol	RT	2 min
100% Ethanol	RT	2 min
Probe ($5x10^4$ cpm/µl) in hybridization buffer (0.2 g PVP, 0.2 g Ficoll, 1.38 g NaH_2PO_4 pH 6.8, 50 mM EDTA, 3 M NaCl, 0.1 M Tris pH 8, 1ml of formamide, 0.2 ml of 1M DTT, 0.4 ml of 50% dextransulfate, 1 µl of tRNA, plus water to 2 ml)	50^oC	ON
2^{nd} day: Washes		
50% Formamid/2xSSC/β-Mercaptoethanol	37^oC	15 min

50% Formamid/2xSSC/β-Mercaptoethanol	65°C	30 min
	37°C	2 hours
NTE	37°C	15 min
NTE plus RNAse	37°C	15 min
NTE	37°C	15 min
50% Formamid/2xSSC/β-Mercaptoethanol	37°C	30 min
2 x SSC	RT	15 min
0.1 x SSC	RT	15 min
30% Ethanol	RT	2 min
50% Ethanol	RT	2 min
70% Ethanol	RT	2 min
90% Ethanol	RT	2 min
96% Ethanol	RT	2 min
100% Ethanol	RT	2 min
3rd Day: Dipping		
Dipping solution	42°C in dark	
4th Day: Dipping		
1% Acetic acid	RT	1 min
30% Sodiumthiosulphate	RT	3 min
dH_2O x 3	RT	1 min x 3
dH_2O x 3	42°C	1 min x 3
Giemsa staining-solution (4% Giemsa stock-solution plus 40 mM Sodium phosphate buffer, pH6)	RT	30 min
In tap dH_2O	RT	30 min
Mounting in Eukitt mounting medium		

Table 14. Procedure for ISH with radioactive-labeled probe, (x: repeated time)

5.9.6. Immunostaining

5.9.6.1. Immunohistochemistry (IHC)

Paraffin-sections were dewaxed in Histoclear (Vogel), rehydrated in a seria of ethanol solution containing decreasing amount of alcohol and rinsed in PBS.

Cryosections were washed in PBS and afterwards postfixed in 4% PFA/PBS for 10 minutes. With some primary antibodies section were boiled in Antigen-Unmasking solution (Vector). The sections were then blocked in a solution containing PBT (PBS + 0,1% Triton 100) and 10% FCS for 2 hours. Diluted primary antibodies were incubated on the slides for overnight at 4°C in blocking solution. After rinsing in PBT, the sections were incubated in diluted secondary antibodies in blocking solution for 1-2 hours at room temperature. Before mounting, the sections were rinsed again in PBT and sealed with Vectashield mounting-medium, containing DAPI or Propidium Iodide (as nuclear counterstain) (Vector). The mounted sections were kept at 4°C, protected from light.

5.9.6.2. Immunofluorescence and index of the counted cells

Cells grow on cover slips were fixed in 4% PFA, permeabilized with 0.5% Triton X-100 in PBS, and blocked with 10% FCS in PBT. Cells were then incubated overnight in primary antibodies followed by 1 h in secondary antibodies. Cover slips were mounted onto glass slides by using the Vectashield mounting medium with DAPI (Vector laboratories).

To compare the index of the counted cells for different markers in the experiment of the overexpression of Trim11 and the corresponding controls, cortical primary cells were stained with antibodies as described and counterstained with the nuclei marker DAPI. Images with objective of 20x were taken using BX60 fluorescence microscope. Antibody-positive cells and total cells as DAPI-positive were counted and processed using analysis software. The index of markers was calculated by dividing the total number antibody-positive cells by the total number cells showing overexpression of Trim11 and the corresponding controls. Data shown as means ± s.d. P values were evaluated by using a Student ´s t-test.

5.9.7. In ovo chick electroporation

Fertilized chick eggs were incubated at 38°C in a humid incubator for 36-44 hours to reach stage HH9-11 (Hamburger and Hamilton, 1951). 2.5 µg/µl DNA *Er81-Luc* plus 2.5 µg/µl of *CMV-Pax6* or *CMV-Gfp* in PBS supplemented with 1 mM $MgCl_2$ and 25-50 ng/µl Fast Green were pipetted into a microinjection

glass needle. The needle then assembled in Pneumatic PicoPump PV820 pump system (World Precision Instruments). After incubation, an egg was held on a stand oriented so that the embryo sits on the top of the yolk. A 5 ml syringe (Terumo) was used to aspirate 2.5 ml albumin from the egg. About 2 cm^2 of shell above the embryo was removed. Some drops of 1xTyrode buffer (8 g NaCl, 0.2 g KCl, 0.271 g $CaCl_2.2H_2O$, 0.05 g $NaH_2PO_4.2H_2O$, 0.2 g $MgCl_2.6H_2O$, 1 g glucose in a total volume of 1 liter) were applied on the embryo to prevent drying, and 1:75 diluted black ink (Higgins) in 1xTyrods buffer was injected with a 1 ml syringe (Terumo) into the yolk right beneath the embryo to visualize it. Subsequently, a small hole was carefully made in the vitelline membrane using a 0.125 mm diameter wolfram-draht needle (Agar Scientific) making the neural tube accessible. A parallel platinum electrode (Aldrich) with 5-6 mm length, 0.25 mm diameter, and 7 mm distance between two electrodes was placed onto the vitelline membrane flanking the embryo in parallel with neural tube, pressed down to the same horizontal level with the neural tube, and several drops of 1xTyrods buffer were applied on each electrode. Afterwards, DNA solution was injected into the neural tube, and 5 square electric pulses were giving by a Electro Square Porator ECM830 electroporator (BTX) with following setting of 33 V, 50 miniseconds/pulse with 950 miniseconds intervals. Finally, the window on the shell was tightly sealed with tape, and the electroporated embryo was further incubated for 48 hours to reach stage HH18-20. The surviving embryos were collected and analyzed by immunohistochemistry. At least 10 electroporated embryos were analysed in each experiment.

5.9.8. X-Gal staining

Mouse brains were prepared and fixed in fixing solution (37% formaldehyde, 25% glutaldehyde, 10% NP-40, 20x PBS). X-Gal staining was performed on whole brain. The ß-galactosidase-activity was developed in staining solution (PBS, 1 mg/ml X-Gal, 2mM $MgCl_2$, 0,01% SDS, 0,02% NP40, 5 mM $K_3Fe(CN)_6$, 5mM $K_4Fe(CN)_6$), for several hours to overnight at 30°C and protected from light. The samples were washed in PBS and stored in 80% glycerol at 4°C.

5.9.9. BrdU labelling

BrdU (Sigma) uptake experiments were done by intraperitoneal injection (100 µl of 0.014 g BrdU in 1 ml PBS /10 g body weight) into pregnant mice. For pulse-labelling of SGL neurons, pregnant mice were injected at E16.5 (time point of the generation of SGL peaks) or E18.5 (predominantly L2-3 are born). Newborns of the injected mice were sacrificed at P10. Brains of newborns were then dissected and embedded. Sections were cut and then used for immunohistochemistry

Abbreviations

Short name	Full name
3AT	3-Amino-1, 2, 4-Triazole
AVE	Anterior visceral endoderm
bHLH	Basic helix-loop-helix
BPs	Basal progenitors
CC	Corpus callosum
CGE	Caudal ganglionic eminence
ChIP	Chromatin immunoprecipitation
cKO	Conditional knockout
CNS	Central nervous system
CP	Cortical plate
CR	Cajal-Retzius
CSMN	Corticospinal motor neurons
D/V	Dorsoventral
DG	Dentate girus
DIG	Digoxygenin
DIV	Days of *in vitro* culture
dLGE	Dorsal lateral ganglionic eminence
dLGN	Dorsal lateral geniculate nucleus
DP	Dorsal pallium
EMSA	Electrophoretic mobility shift assay
Fr	Frontal cortex
GE	Germinative epithelium
H&E	Haematoxilin & eosin
HD	Homeobox domain
Hi	Hippocampus
HiSVZ	Hippocampal SVZ
ICC	Immunocytochemistry
IGL	Infragranular layer

IHC	Immunohistochemistry
INs	Interneurons
IPs	Intermediate progenitors
ISH	*Insitu* hybridization
IZ	Intermediate zone
L1-6	Layer1-6
LGE	Lateral ganglionic eminence
LMS	Lateral migratory streams
LOF	Loss-of-function
LP	Lateral pallium
MGE	Media ganglionic eminence
MP	Medial pallium
MZ	Marginal zone
NE	Neuroepithelial cells
OB	Olfactory buld
Oc	Occipital
Par	Parietal cortex
PD	Pair domain
POA	Preoptic Area
PP	Preplate
pPv	Posterior periventricular zone
pPV	Posterior periventricular region
PSPB	Pallial-subpallial border
PTM	Post-translation modification
qPCR	Quantitative RT-PCR
RG	Radial glia
RMS	Rostral migratory streams
RT	Room temperature
Sey	Small eye
SGL	Subgranular layer
SGZ	Subgranular zone
shRNA	Short hairpin RNA interference

smRNA	Small modulatory RNA
SS	Somatosensory
Str.L.M	Stratum lacunosum-moleculare
Str.M	Stratum moleculare
Str.or	Stratum oriens
Str.Pir	Stratum pyramidale
Str.Rad	Stratum radiatum
SVZ	Subventricular zone
UPS	Ubiquitin-proteasome system
vLGE	Ventral lateral ganglionic eminence
VP	Ventroposterior
VZ	Ventricular zone
WB	Western blot
WM	White matter

References

Alifragis, P., Molnar, Z., and Parnavelas, J. G. (2003). Restricted expression of Slap-1 in the rodent cerebral cortex. Gene Expr Patterns 3, 437-440.

Alvarez-Buylla, A., and Lim, D. A. (2004). For the long run: maintaining germinal niches in the adult brain. Neuron 41, 683-686.

An, J. Y., Seo, J. W., Tasaki, T., Lee, M. J., Varshavsky, A., and Kwon, Y. T. (2006). Impaired neurogenesis and cardiovascular development in mice lacking the E3 ubiquitin ligases UBR1 and UBR2 of the N-end rule pathway. Proc Natl Acad Sci U S A 103, 6212-6217. Epub 2006 Apr 6210.

Anderson, T. R., Hedlund, E., and Carpenter, E. M. (2002). Differential Pax6 promoter activity and transcript expression during forebrain development. Mech Dev 114, 171-175.

Andrews, G. L., and Mastick, G. S. (2003). R-cadherin is a Pax6-regulated, growth-promoting cue for pioneer axons. J Neurosci 23, 9873-9880.

Anthony, T. E., Klein, C., Fishell, G., and Heintz, N. (2004). Radial glia serve as neuronal progenitors in all regions of the central nervous system. Neuron 41, 881-890.

Arlotta, P., Molyneaux, B. J., Chen, J., Inoue, J., Kominami, R., and Macklis, J. D. (2005). Neuronal subtype-specific genes that control corticospinal motor neuron development in vivo. Neuron 45, 207-221.

Arnaud, L., Ballif, B. A., and Cooper, J. A. (2003). Regulation of protein tyrosine kinase signaling by substrate degradation during brain development. Mol Cell Biol 23, 9293-9302.

Ashery-Padan, R., Marquardt, T., Zhou, X., and Gruss, P. (2000). Pax6 activity in the lens primordium is required for lens formation and for correct placement of a single retina in the eye. Genes Dev 14, 2701-2711.

Ballas, N., Grunseich, C., Lu, D. D., Speh, J. C., and Mandel, G. (2005). REST and its corepressors mediate plasticity of neuronal gene chromatin throughout neurogenesis. Cell 121, 645-657.

Baumer, N., Marquardt, T., Stoykova, A., Spieler, D., Treichel, D., Ashery-Padan, R., and Gruss, P. (2003). Retinal pigmented epithelium determination requires the redundant activities of Pax2 and Pax6. Development 130, 2903-2915.

Bayer, S. A., and Altman, J. (1991). Neocortical Development.

Berger, J., Eckert, S., Scardigli, R., Guillemot, F., Gruss, P., and Stoykova, A. (2004). E1-Ngn2/Cre is a new line for regional activation of Cre recombinase in the developing CNS. Genesis 40, 195-199.

Berger, J., Berger, S., Tuoc, T. C., D'Amelio, M., Cecconi, F., Gorski, J. A., Jones, K. R., Gruss, P., and Stoykova, A. (2007). Conditional activation of Pax6 in the developing cortex of transgenic mice causes progenitor apoptosis. Development 28, 28.

Bertrand, N., Castro, D. S., and Guillemot, F. (2002). Proneural genes and the specification of neural cell types. Nat Rev Neurosci 3, 517-530.

Bishop, K. M., Goudreau, G., and O'Leary, D. D. (2000). Regulation of area identity in the mammalian neocortex by Emx2 and Pax6. Science 288, 344-349.

Bishop, K. M., Rubenstein, J. L., and O'Leary, D. D. (2002). Distinct actions of Emx1, Emx2, and Pax6 in regulating the specification of areas in the developing neocortex. J Neurosci 22, 7627-7638.

Bock, H. H., Jossin, Y., May, P., Bergner, O., and Herz, J. (2004). Apolipoprotein E receptors are required for reelin-induced proteasomal degradation of the neuronal adaptor protein Disabled-1. J Biol Chem 279, 33471-33479. Epub 32004 Jun 33472.

Bottenstein, J. E., and Sato, G. H. (1979). Growth of a rat neuroblastoma cell line in serum-free supplemented medium. Proc Natl Acad Sci U S A 76, 514-517.

Britanova, O., Akopov, S., Lukyanov, S., Gruss, P., and Tarabykin, V. (2005). Novel transcription factor Satb2 interacts with matrix attachment region DNA elements in a tissue-specific manner and demonstrates cell-type-dependent expression in the developing mouse CNS. Eur J Neurosci 21, 658-668.

Brown, T. A., and McKnight, S. L. (1992). Specificities of protein-protein and protein-DNA interaction of GABP alpha and two newly defined ets-related proteins. Genes Dev 6, 2502-2512.

Bulchand, S., Subramanian, L., and Tole, S. (2003). Dynamic spatiotemporal expression of LIM genes and cofactors in the embryonic and postnatal cerebral cortex. Dev Dyn 226, 460-469.

Callaerts, P., Halder, G., and Gehring, W. J. (1997). PAX-6 in development and evolution. Annu Rev Neurosci 20, 483-532.

Callaerts, P., Leng, S., Clements, J., Benassayag, C., Cribbs, D., Kang, Y. Y., Walldorf, U., Fischbach, K. F., and Strauss, R. (2001). Drosophila Pax-6/eyeless is essential for normal adult brain structure and function. J Neurobiol 46, 73-88.

Cammas, F., Mark, M., Dolle, P., Dierich, A., Chambon, P., and Losson, R. (2000). Mice lacking the transcriptional corepressor TIF1beta are defective in early postimplantation development. Development 127, 2955-2963.

Campbell, K., and Gotz, M. (2002). Radial glia: multi-purpose cells for vertebrate brain development. Trends Neurosci 25, 235-238.

Campbell, K. (2005). Cortical neuron specification: it has its time and place. Neuron 46, 373-376.

Caric, D., Gooday, D., Hill, R. E., McConnell, S. K., and Price, D. J. (1997). Determination of the migratory capacity of embryonic cortical cells lacking the transcription factor Pax-6. Development 124, 5087-5096.

Carriere, C., Plaza, S., Caboche, J., Dozier, C., Bailly, M., Martin, P., and Saule, S. (1995). Nuclear localization signals, DNA binding, and transactivation properties of quail Pax-6 (Pax-QNR) isoforms. Cell Growth Differ 6, 1531-1540.

Chalepakis, G., Tremblay, P., and Gruss, P. (1992). Pax genes, mutants and molecular function. J Cell Sci Suppl 16, 61-67.

Chalepakis, G., Wijnholds, J., Giese, P., Schachner, M., and Gruss, P. (1994). Characterization of Pax-6 and Hoxa-1 binding to the promoter region of the neural cell adhesion molecule L1. DNA Cell Biol 13, 891-900.

Chapouton, P., Gartner, A., and Gotz, M. (1999). The role of Pax6 in restricting cell migration between developing cortex and basal ganglia. Development 126, 5569-5579.

Chauhan, B. K., Reed, N. A., Yang, Y., Cermak, L., Reneker, L., Duncan, M. K., and Cvekl, A. (2002). A comparative cDNA microarray analysis reveals a spectrum of genes regulated by Pax6 in mouse lens. Genes Cells 7, 1267-1283.

Chauhan, B. K., Reed, N. A., Zhang, W., Duncan, M. K., Kilimann, M. W., and Cvekl, A. (2002). Identification of genes downstream of Pax6 in the mouse lens using cDNA microarrays. J Biol Chem 277, 11539-11548.

Chauhan, B. K., Zhang, W., Cveklova, K., Kantorow, M., and Cvekl, A. (2002). Identification of differentially expressed genes in mouse Pax6 heterozygous lenses. Invest Ophthalmol Vis Sci 43, 1884-1890.

Colombo, E., Galli, R., Cossu, G., Gecz, J., and Broccoli, V. (2004). Mouse orthologue of ARX, a gene mutated in several X-linked forms of mental retardation and epilepsy, is a marker of adult neural stem cells and forebrain GABAergic neurons. Dev Dyn 231, 631-639.

Cooper, S. T., and Hanson, I. M. (2005). A screen for proteins that interact with PAX6: C-terminal mutations disrupt interaction with HOMER3, DNCL1 and TRIM11. BMC Genet 6, 43.

Coutte, L., Monte, D., Imai, K., Pouilly, L., Dewitte, F., Vidaud, M., Adamski, J., Baert, J. L., and de Launoit, Y. (1999). Characterization of the human and mouse ETV1/ER81 transcription factor genes: role of the two alternatively spliced isoforms in the human. Oncogene 18, 6278-6286.

Cvekl, A., Kashanchi, F., Brady, J. N., and Piatigorsky, J. (1999). Pax-6 interactions with TATA-box-binding protein and retinoblastoma protein. Invest Ophthalmol Vis Sci 40, 1343-1350.

Czerny, T., and Busslinger, M. (1995). DNA-binding and transactivation properties of Pax-6: three amino acids in the paired domain are responsible for the different sequence recognition of Pax-6 and BSAP (Pax-5). Mol Cell Biol 15, 2858-2871.

Czerny, T., Halder, G., Kloter, U., Souabni, A., Gehring, W. J., and Busslinger, M. (1999). twin of eyeless, a second Pax-6 gene of Drosophila, acts upstream of eyeless in the control of eye development. Mol Cell 3, 297-307.

DeDiego, I., Smith-Fernandez, A., and Fairen, A. (1994). Cortical cells that migrate beyond area boundaries: characterization of an early neuronal population in the lower intermediate zone of prenatal rats. Eur J Neurosci 6, 983-997.

Deisseroth, K., and Malenka, R. C. (2005). GABA excitation in the adult brain: a mechanism for excitation- neurogenesis coupling. Neuron 47, 775-777.

Desai, A. R., and McConnell, S. K. (2000). Progressive restriction in fate potential by neural progenitors during cerebral cortical development. Development 127, 2863-2872.

Doetsch, F., Caille, I., Lim, D. A., Garcia-Verdugo, J. M., and Alvarez-Buylla, A. (1999). Subventricular zone astrocytes are neural stem cells in the adult mammalian brain. Cell 97, 703-716.

Duncan, M. K., Cvekl, A., Li, X., and Piatigorsky, J. (2000). Truncated forms of Pax-6 disrupt lens morphology in transgenic mice. Invest Ophthalmol Vis Sci 41, 464-473.

Duncan, M. K., Kozmik, Z., Cveklova, K., Piatigorsky, J., and Cvekl, A. (2000). Overexpression of PAX6(5a) in lens fiber cells results in cataract and upregulation of (alpha)5(beta)1 integrin expression. J Cell Sci 113, 3173-3185.

Edlund, T., and Jessell, T. M. (1999). Progression from extrinsic to intrinsic signaling in cell fate specification: a view from the nervous system. Cell 96, 211-224.

Ellison-Wright, Z., Heyman, I., Frampton, I., Rubia, K., Chitnis, X., Ellison-Wright, I., Williams, S. C., Suckling, J., Simmons, A., and Bullmore, E. (2004). Heterozygous PAX6 mutation, adult brain structure and fronto-striato-thalamic function in a human family. Eur J Neurosci 19, 1505-1512.

Englund, C., Fink, A., Lau, C., Pham, D., Daza, R. A., Bulfone, A., Kowalczyk, T., Hevner, R. F., Miyashita-Lin, E., and Rubenstein, J. L. (2005). Pax6, Tbr2, and Tbr1 are expressed sequentially by radial glia, intermediate progenitor cells, and postmitotic neurons in developing neocortex

Cortical and thalamic axon pathfinding defects in Tbr1, Gbx2, and Pax6 mutant mice: evidence that cortical and thalamic axons interact and guide each other. J Neurosci 25, 247-251.

Epstein, J., Cai, J., Glaser, T., Jepeal, L., and Maas, R. (1994). Identification of a Pax paired domain recognition sequence and evidence for DNA-dependent conformational changes. J Biol Chem 269, 8355-8361.

Epstein, J. A., Glaser, T., Cai, J., Jepeal, L., Walton, D. S., and Maas, R. L. (1994). Two independent and interactive DNA-binding subdomains of the Pax6 paired domain are regulated by alternative splicing. Genes Dev 8, 2022-2034.

Estivill-Torrus, G., Pearson, H., van Heyningen, V., Price, D. J., and Rashbass, P. (2002). Pax6 is required to regulate the cell cycle and the rate of progression from symmetrical to asymmetrical division in mammalian cortical progenitors. Development 129, 455-466.

Farah, M. H., Olson, J. M., Sucic, H. B., Hume, R. I., Tapscott, S. J., and Turner, D. L. (2000). Generation of neurons by transient expression of neural bHLH proteins in mammalian cells. Development 127, 693-702.

Fode, C., Ma, Q., Casarosa, S., Ang, S. L., Anderson, D. J., and Guillemot, F. (2000). A role for neural determination genes in specifying the dorsoventral identity of telencephalic neurons. Genes Dev 14, 67-80.

Frankland, P. W., Bontempi, B., Talton, L. E., Kaczmarek, L., and Silva, A. J. (2004). The involvement of the anterior cingulate cortex in remote contextual fear memory. Science 304, 881-883.

Fremeau, R. T., Jr., Troyer, M. D., Pahner, I., Nygaard, G. O., Tran, C. H., Reimer, R. J., Bellocchio, E. E., Fortin, D., Storm-Mathisen, J., and Edwards, R. H. (2001). The expression of vesicular glutamate transporters defines two classes of excitatory synapse. Neuron 31, 247-260.

Friedman, J. R., Fredericks, W. J., Jensen, D. E., Speicher, D. W., Huang, X. P., Neilson, E. G., and Rauscher, F. J., 3rd (1996). KAP-1, a novel corepressor for the highly conserved KRAB repression domain. Genes Dev 10, 2067-2078.

Galceran, J., Farinas, I., Depew, M. J., Clevers, H., and Grosschedl, R. (1999). Wnt3a-/--like phenotype and limb deficiency in Lef1(-/-)Tcf1(-/-) mice. Genes Dev 13, 709-717.

Garel, S., Yun, K., Grosschedl, R., and Rubenstein, J. L. (2002). The early topography of thalamocortical projections is shifted in Ebf1 and Dlx1/2 mutant mice. Development 129, 5621-5634.

Garel, S., Huffman, K. J., and Rubenstein, J. L. (2003). Molecular regionalization of the neocortex is disrupted in Fgf8 hypomorphic mutants. Development 130, 1903-1914.

Ge, S., Pradhan, D. A., Ming, G. L., and Song, H. (2007). GABA sets the tempo for activity-dependent adult neurogenesis. Trends Neurosci 30, 1-8.

Gehring, W. J., and Ikeo, K. (1999). Pax 6: mastering eye morphogenesis and eye evolution. Trends Genet 15, 371-377.

Gehring, W. J. (2002). The genetic control of eye development and its implications for the evolution of the various eye-types. Int J Dev Biol 46, 65-73.

Glaser, T., Jepeal, L., Edwards, J. G., Young, S. R., Favor, J., and Maas, R. L. (1994). PAX6 gene dosage effect in a family with congenital cataracts, aniridia, anophthalmia and central nervous system defects. Nat Genet 7, 463-471.

Goebbels, S., Bormuth, I., Bode, U., Hermanson, O., Schwab, M. H., and Nave, K. A. (2006). Genetic targeting of principal neurons in neocortex and hippocampus of NEX-Cre mice. Genesis 44, 611-621.

Gorski, J. A., Talley, T., Qiu, M., Puelles, L., Rubenstein, J. L., and Jones, K. R. (2002). Cortical excitatory neurons and glia, but not GABAergic neurons, are produced in the Emx1-expressing lineage. J Neurosci 22, 6309-6314.

Gotz, M., Stoykova, A., and Gruss, P. (1998). Pax6 controls radial glia differentiation in the cerebral cortex. Neuron 21, 1031-1044.

Gotz, M., and Huttner, W. B. (2005). The cell biology of neurogenesis. Nat Rev Mol Cell Biol 6, 777-788.

Gotz, M., and Barde, Y. A. (2005). Radial glial cells defined and major intermediates between embryonic stem cells and CNS neurons. Neuron 46, 369-372.

Goudreau, G., Petrou, P., Reneker, L. W., Graw, J., Loster, J., and Gruss, P. (2002). Mutually regulated expression of Pax6 and Six3 and its implications for the Pax6 haploinsufficient lens phenotype. Proc Natl Acad Sci U S A 99, 8719-8724.

Griffin, C., Kleinjan, D. A., Doe, B., and van Heyningen, V. (2002). New 3' elements control Pax6 expression in the developing pretectum, neural retina and olfactory region. Mech Dev 112, 89-100.

Gross, C. G. (2000). Neurogenesis in the adult brain: death of a dogma. Nat Rev Neurosci 1, 67-73.

Guillemot, F. (2005). Cellular and molecular control of neurogenesis in the mammalian telencephalon. Curr Opin Cell Biol 17, 639-647.

Guillemot, F., Molnar, Z., Tarabykin, V., and Stoykova, A. (2006). Molecular mechanisms of cortical differentiation. Eur J Neurosci 23, 857-868.

Hack, M. A., Sugimori, M., Lundberg, C., Nakafuku, M., and Gotz, M. (2004). Regionalization and fate specification in neurospheres: the role of Olig2 and Pax6. Mol Cell Neurosci 25, 664-678.

Hack, M. A., Saghatelyan, A., de Chevigny, A., Pfeifer, A., Ashery-Padan, R., Lledo, P. M., and Gotz, M. (2005). Neuronal fate determinants of adult olfactory bulb neurogenesis. Nat Neurosci 8, 865-872.

Halder, G., Callaerts, P., and Gehring, W. J. (1995). Induction of ectopic eyes by targeted expression of the eyeless gene in Drosophila. Science 267, 1788-1792.

Hanashima, C., Li, S. C., Shen, L., Lai, E., and Fishell, G. (2004). Foxg1 suppresses early cortical cell fate. Science 303, 56-59.

Hand, R., Bortone, D., Mattar, P., Nguyen, L., Heng, J. I., Guerrier, S., Boutt, E., Peters, E., Barnes, A. P., Parras, C., et al. (2005). Phosphorylation of Neurogenin2 specifies the migration properties and the dendritic morphology of pyramidal neurons in the neocortex. Neuron 48, 45-62.

Hartfuss, E., Galli, R., Heins, N., and Gotz, M. (2001). Characterization of CNS precursor subtypes and radial glia. Dev Biol 229, 15-30.

Hartfuss, E., Forster, E., Bock, H. H., Hack, M. A., Leprince, P., Luque, J. M., Herz, J., Frotscher, M., and Gotz, M. (2003). Reelin signaling directly affects radial glia morphology and biochemical maturation. Development 130, 4597-4609.

Hasty, J., McMillen, D., and Collins, J. J. (2002). Engineered gene circuits. Nature 420, 224-230.

Haubensak, W., Attardo, A., Denk, W., and Huttner, W. B. (2004). Neurons arise in the basal neuroepithelium of the early mammalian telencephalon: a major site of neurogenesis. Proc Natl Acad Sci U S A 101, 3196-3201. Epub 2004 Feb 3112.

Haubst, N., Berger, J., Radjendirane, V., Graw, J., Favor, J., Saunders, G. F., Stoykova, A., and Gotz, M. (2004). Molecular dissection of Pax6 function: the specific roles of the paired domain and homeodomain in brain development. Development 131, 6131-6140.

Haydar, T. F., Wang, F., Schwartz, M. L., and Rakic, P. (2000). Differential modulation of proliferation in the neocortical ventricular and subventricular zones. J Neurosci 20, 5764-5774.

Heins, N., Malatesta, P., Cecconi, F., Nakafuku, M., Tucker, K. L., Hack, M. A., Chapouton, P., Barde, Y. A., and Gotz, M. (2002). Glial cells generate neurons: the role of the transcription factor Pax6. Nat Neurosci 5, 308-315.

Heisenberg, M. (1998). What do the mushroom bodies do for the insect brain? an introduction. Learn Mem 5, 1-10.

Heisenberg, M. (1998). What do the mushroom bodies do for the insect brain? an introduction. Learn Mem 5, 1-10.

Hershko, A., and Ciechanover, A. (1998). The ubiquitin system. Annu Rev Biochem 67, 425-479.

Hevner, R. F., Shi, L., Justice, N., Hsueh, Y., Sheng, M., Smiga, S., Bulfone, A., Goffinet, A. M., Campagnoni, A. T., and Rubenstein, J. L. (2001). Tbr1 regulates differentiation of the preplate and layer 6. Neuron 29, 353-366.

Hevner, R. F., Miyashita-Lin, E., and Rubenstein, J. L. (2002). Cortical and thalamic axon pathfinding defects in Tbr1, Gbx2, and Pax6 mutant mice: evidence that cortical and thalamic axons interact and guide each other. J Comp Neurol 447, 8-17.

Hevner, R. F., Daza, R. A., Rubenstein, J. L., Stunnenberg, H., Olavarria, J. F., and Englund, C. (2003). Beyond laminar fate: toward a molecular classification of cortical projection/pyramidal neurons. Dev Neurosci 25, 139-151.

Hevner, R. F., Daza, R. A., Englund, C., Kohtz, J., and Fink, A. (2004). Postnatal shifts of interneuron position in the neocortex of normal and reeler mice: evidence for inward radial migration. Neuroscience 124, 605-618.

Hevner, R. F., Hodge, R. D., Daza, R. A., and Englund, C. (2006). Transcription factors in glutamatergic neurogenesis: conserved programs in neocortex, cerebellum, and adult hippocampus. Neurosci Res 55, 223-233.

Heyman, I., Frampton, I., van Heyningen, V., Hanson, I., Teague, P., Taylor, A., and Simonoff, E. (1999). Psychiatric disorder and cognitive function in a family with an inherited novel mutation of the developmental control gene PAX6. Psychiatr Genet 9, 85-90.

Hill, R. E., Favor, J., Hogan, B. L., Ton, C. C., Saunders, G. F., Hanson, I. M., Prosser, J., Jordan, T., Hastie, N. D., and van Heyningen, V. (1991). Mouse small eye results from mutations in a paired-like homeobox-containing gene. Nature 354, 522-525.

Hirose, S., Nishizumi, H., and Sakano, H. (2003). Pub, a novel PU.1 binding protein, regulates the transcriptional activity of PU.1. Biochem Biophys Res Commun 311, 351-360.

Hochstrasser, M. (2006). Lingering mysteries of ubiquitin-chain assembly. Cell 124, 27-34.

Holm, P. C., Mader, M. T., Haubst, N., Wizenmann, A., Sigvardsson, M., and Gotz, M. (2007). Loss- and gain-of-function analyses reveal targets of Pax6 in the developing mouse telencephalon. Mol Cell Neurosci 34, 99-119.

Hussain, M. A., and Habener, J. F. (1999). Glucagon gene transcription activation mediated by synergistic interactions of pax-6 and cdx-2 with the p300 co-activator. J Biol Chem 274, 28950-28957.

Inoue, K., Terashima, T., Nishikawa, T., and Takumi, T. (2004). Fez1 is layer-specifically expressed in the adult mouse neocortex. Eur J Neurosci 20, 2909-2916.

Iulianella, A., Vanden Heuvel, G., and Trainor, P. (2003). Dynamic expression of murine Cux2 in craniofacial, limb, urogenital and neuronal primordia. Gene Expr Patterns 3, 571-577.

Ivanova, A., Nakahira, E., Kagawa, T., Oba, A., Wada, T., Takebayashi, H., Spassky, N., Levine, J., Zalc, B., and Ikenaka, K. (2003). Evidence for a second wave of oligodendrogenesis in the postnatal cerebral cortex of the mouse. J Neurosci Res 73, 581-592.

Jagasia, R., Song, H., Gage, F. H., and Lie, D. C. (2006). New regulators in adult neurogenesis and their potential role for repair. Trends Mol Med 12, 400-405.

Jen, Y., Manova, K., and Benezra, R. (1997). Each member of the Id gene family exhibits a unique expression pattern in mouse gastrulation and neurogenesis. Dev Dyn 208, 92-106.

Jones, L., Lopez-Bendito, G., Gruss, P., Stoykova, A., and Molnar, Z. (2002). Pax6 is required for the normal development of the forebrain axonal connections. Development 129, 5041-5052.

Jun, S., Wallen, R. V., Goriely, A., Kalionis, B., and Desplan, C. (1998). Lune/eye gone, a Pax-like protein, uses a partial paired domain and a homeodomain for DNA recognition. Proc Natl Acad Sci U S A 95, 13720-13725.

Kaeser, M. D., and Emerson, B. M. (2006). Remodeling plans for cellular specialization: unique styles for every room. Curr Opin Genet Dev 16, 508-512.

Kamachi, Y., Uchikawa, M., Tanouchi, A., Sekido, R., and Kondoh, H. (2001). Pax6 and SOX2 form a co-DNA-binding partner complex that regulates initiation of lens development. Genes Dev 15, 1272-1286.

Kammandel, B., Chowdhury, K., Stoykova, A., Aparicio, S., Brenner, S., and Gruss, P. (1999). Distinct cis-essential modules direct the time-space pattern of the Pax6 gene activity. Dev Biol 205, 79-97.

Kandel, E. R., Schwartz, J. H., and Jessell, T. M. (2000). Principles of Neural Science.

Kempermann, G., Jessberger, S., Steiner, B., and Kronenberg, G. (2004). Milestones of neuronal development in the adult hippocampus. Trends Neurosci 27, 447-452.

Kessel, M., and Gruss, P. (1991). Homeotic transformations of murine vertebrae and concomitant alteration of Hox codes induced by retinoic acid. Cell 67, 89-104.

Kiecker, C., and Lumsden, A. (2005). Compartments and their boundaries in vertebrate brain development. Nat Rev Neurosci 6, 553-564.

Kim, E. A., Noh, Y. T., Ryu, M. J., Kim, H. T., Lee, S. E., Kim, C. H., Lee, C., Kim, Y. H., and Choi, C. Y. (2006). Phosphorylation and transactivation of Pax6 by homeodomain-interacting protein kinase 2. J Biol Chem 281, 7489-7497.

Kim, J., and Lauderdale, J. D. (2006). Analysis of Pax6 expression using a BAC transgene reveals the presence of a paired-less isoform of Pax6 in the eye and olfactory bulb. Dev Biol 292, 486-505.

Kleber, M., and Sommer, L. (2004). Wnt signaling and the regulation of stem cell function. Curr Opin Cell Biol 16, 681-687.

Kleinjan, D. A., Seawright, A., Childs, A. J., and van Heyningen, V. (2004). Conserved elements in Pax6 intron 7 involved in (auto)regulation and alternative transcription. Dev Biol 265, 462-477.

Kohwi, M., Osumi, N., Rubenstein, J. L., and Alvarez-Buylla, A. (2005). Pax6 is required for making specific subpopulations of granule and periglomerular neurons in the olfactory bulb. J Neurosci 25, 6997-7003.

Kozmik, Z., Czerny, T., and Busslinger, M. (1997). Alternatively spliced insertions in the paired domain restrict the DNA sequence specificity of Pax6 and Pax8. Embo J 16, 6793-6803.

Kozmik, Z. (2005). Pax genes in eye development and evolution. Curr Opin Genet Dev 15, 430-438.

Kriegstein, A., Noctor, S., and Martinez-Cerdeno, V. (2006). Patterns of neural stem and progenitor cell division may underlie evolutionary cortical expansion. Nat Rev Neurosci 7, 883-890.

Kroll, T. T., and O'Leary, D. D. (2005). Ventralized dorsal telencephalic progenitors in Pax6 mutant mice generate GABA interneurons of a lateral ganglionic eminence fate. Proc Natl Acad Sci U S A 102, 7374-7379. Epub 2005 May 7376.

Krumlauf, R. (1992). Evolution of the vertebrate Hox homeobox genes. Bioessays 14, 245-252.

Krumlauf, R. (1994). Hox genes in vertebrate development. Cell 78, 191-201.

Kudoh, T., Wilson, S. W., and Dawid, I. B. (2002). Distinct roles for Fgf, Wnt and retinoic acid in posteriorizing the neural ectoderm. Development 129, 4335-4346.

Kurusu, M., Nagao, T., Walldorf, U., Flister, S., Gehring, W. J., and Furukubo-Tokunaga, K. (2000). Genetic control of development of the mushroom bodies, the associative learning centers in the Drosophila brain, by the eyeless, twin of eyeless, and Dachshund genes. Proc Natl Acad Sci U S A 97, 2140-2144.

Kuwabara, T., Hsieh, J., Nakashima, K., Taira, K., and Gage, F. H. (2004). A small modulatory dsRNA specifies the fate of adult neural stem cells. Cell 116, 779-793.

Kwan, K. M. (2002). Conditional alleles in mice: practical considerations for tissue-specific knockouts. Genesis 32, 49-62.

Land, P. W., and Monaghan, A. P. (2003). Expression of the transcription factor, tailless, is required for formation of superficial cortical layers. Cereb Cortex 13, 921-931.

Le Douarin, B., Nielsen, A. L., Garnier, J. M., Ichinose, H., Jeanmougin, F., Losson, R., and Chambon, P. (1996). A possible involvement of TIF1 alpha and TIF1 beta in the epigenetic control of transcription by nuclear receptors. Embo J 15, 6701-6715.

Lee, S. M., Tole, S., Grove, E., and McMahon, A. P. (2000). A local Wnt-3a signal is required for development of the mammalian hippocampus. Development 127, 457-467.

Lefebvre, T., Planque, N., Leleu, D., Bailly, M., Caillet-Boudin, M. L., Saule, S., and Michalski, J. C. (2002). O-glycosylation of the nuclear forms of Pax-6 products in quail neuroretina cells. J Cell Biochem 85, 208-218.

Leng, R. P., Lin, Y., Ma, W., Wu, H., Lemmers, B., Chung, S., Parant, J. M., Lozano, G., Hakem, R., and Benchimol, S. (2003). Pirh2, a p53-induced ubiquitin-protein ligase, promotes p53 degradation. Cell 112, 779-791.

Levison, S. W., and Goldman, J. E. (1993). Both oligodendrocytes and astrocytes develop from progenitors in the subventricular zone of postnatal rat forebrain. Neuron 10, 201-212.

Li, B., Carey, M., and Workman, J. L. (2007). The role of chromatin during transcription. Cell 128, 707-719.

Lie, D. C., Colamarino, S. A., Song, H. J., Desire, L., Mira, H., Consiglio, A., Lein, E. S., Jessberger, S., Lansford, H., Dearie, A. R., and Gage, F. H. (2005). Wnt signalling regulates adult hippocampal neurogenesis. Nature 437, 1370-1375.

Liu, X., Wang, Q., Haydar, T. F., and Bordey, A. (2005). Nonsynaptic GABA signaling in postnatal subventricular zone controls proliferation of GFAP-expressing progenitors. Nat Neurosci 8, 1179-1187.

Lledo, P. M., Alonso, M., and Grubb, M. S. (2006). Adult neurogenesis and functional plasticity in neuronal circuits. Nat Rev Neurosci 7, 179-193.

Lobe, C. G., Koop, K. E., Kreppner, W., Lomeli, H., Gertsenstein, M., and Nagy, A. (1999). Z/AP, a double reporter for cre-mediated recombination. Dev Biol 208, 281-292.

Long, J. E., Garel, S., Alvarez-Dolado, M., Yoshikawa, K., Osumi, N., Alvarez-Buylla, A., and Rubenstein, J. L. (2007). Dlx-dependent and -independent regulation of olfactory bulb interneuron differentiation. J Neurosci 27, 3230-3243.

Lukaszewicz, A., Savatier, P., Cortay, V., Giroud, P., Huissoud, C., Berland, M., Kennedy, H., and Dehay, C. (2005). G1 phase regulation, area-specific cell cycle control, and cytoarchitectonics in the primate cortex. Neuron 47, 353-364.

Luo, L., and O'Leary, D. D. (2005). Axon retraction and degeneration in development and disease. Annu Rev Neurosci 28, 127-156.

Ma, Q., Kintner, C., and Anderson, D. J. (1996). Identification of neurogenin, a vertebrate neuronal determination gene. Cell 87, 43-52.

Maekawa, M., Takashima, N., Arai, Y., Nomura, T., Inokuchi, K., Yuasa, S., and Osumi, N. (2005). Pax6 is required for production and maintenance of progenitor cells in postnatal hippocampal neurogenesis. Genes Cells 10, 1001-1014.

Malandrini, A., Mari, F., Palmeri, S., Gambelli, S., Berti, G., Bruttini, M., Bardelli, A. M., Williamson, K., van Heyningen, V., and Renieri, A. (2001). PAX6 mutation in a family with aniridia, congenital ptosis, and mental retardation. Clin Genet 60, 151-154.

Malatesta, P., Hartfuss, E., and Gotz, M. (2000). Isolation of radial glial cells by fluorescent-activated cell sorting reveals a neuronal lineage. Development 127, 5253-5263.

Malatesta, P., Hack, M. A., Hartfuss, E., Kettenmann, H., Klinkert, W., Kirchhoff, F., and Gotz, M. (2003). Neuronal or glial progeny: regional differences in radial glia fate. Neuron 37, 751-764.

Mallamaci, A., and Stoykova, A. (2006). Gene networks controlling early cerebral cortex arealization. Eur J Neurosci 23, 847-856.

Mann, F., Peuckert, C., Dehner, F., Zhou, R., and Bolz, J. (2002). Ephrins regulate the formation of terminal axonal arbors during the development of thalamocortical projections. Development 129, 3945-3955.

Mansouri, A., Goudreau, G., and Gruss, P. (1999). Pax genes and their role in organogenesis. Cancer Res 59, 1707s-1709s; discussion 1709s-1710s.

Manuel, M., Georgala, P. A., Carr, C. B., Chanas, S., Kleinjan, D. A., Martynoga, B., Mason, J. O., Molinek, M., Pinson, J., Pratt, T., et al. (2007). Controlled overexpression of Pax6 in vivo negatively autoregulates the Pax6 locus, causing cell-autonomous defects of late cortical progenitor proliferation with little effect on cortical arealization. Development 134, 545-555.

Marin, O., Anderson, S. A., and Rubenstein, J. L. (2000). Origin and molecular specification of striatal interneurons. J Neurosci 20, 6063-6076.

Marin, O., and Rubenstein, J. L. (2001). A long, remarkable journey: tangential migration in the telencephalon. Nat Rev Neurosci 2, 780-790.

Marquardt, T., Ashery-Padan, R., Andrejewski, N., Scardigli, R., Guillemot, F., and Gruss, P. (2001). Pax6 is required for the multipotent state of retinal progenitor cells. Cell 105, 43-55.

Maviel, T., Durkin, T. P., Menzaghi, F., and Bontempi, B. (2004). Sites of neocortical reorganization critical for remote spatial memory. Science 305, 96-99.

McClelland, J. L., McNaughton, B. L., and O'Reilly, R. C. (1995). Why there are complementary learning systems in the hippocampus and neocortex: insights from the successes and failures of connectionist models of learning and memory. Psychol Rev 102, 419-457.

McConnell, S. K., and Kaznowski, C. E. (1991). Cell cycle dependence of laminar determination in developing neocortex. Science 254, 282-285.

Meroni, G., and Diez-Roux, G. (2005). TRIM/RBCC, a novel class of 'single protein RING finger' E3 ubiquitin ligases. Bioessays 27, 1147-1157.

Mikkola, I., Bruun, J. A., Bjorkoy, G., Holm, T., and Johansen, T. (1999). Phosphorylation of the transactivation domain of Pax6 by extracellular signal-regulated kinase and p38 mitogen-activated protein kinase. J Biol Chem 274, 15115-15126.

Mikkola, I., Bruun, J. A., Holm, T., and Johansen, T. (2001). Superactivation of Pax6-mediated transactivation from paired domain-binding sites by dna-independent recruitment of different homeodomain proteins. J Biol Chem 276, 4109-4118.

Miller, F. D., and Gauthier, A. S. (2007). Timing Is Everything: Making Neurons versus Glia in the Developing Cortex. Neuron 54, 357-369.

Ming, G. L., and Song, H. (2005). Adult neurogenesis in the mammalian central nervous system. Annu Rev Neurosci 28, 223-250.

Misson, J. P., Edwards, M. A., Yamamoto, M., and Caviness, V. S., Jr. (1988). Identification of radial glial cells within the developing murine central nervous system: studies based upon a new immunohistochemical marker. Brain Res Dev Brain Res 44, 95-108.

Mitchell, T. N., Free, S. L., Williamson, K. A., Stevens, J. M., Churchill, A. J., Hanson, I. M., Shorvon, S. D., Moore, A. T., van Heyningen, V., and Sisodiya, S. M. (2003). Polymicrogyria and absence of pineal gland due to PAX6 mutation. Ann Neurol 53, 658-663.

Miyashita, T., and Williams, C. L. (2004). Peripheral arousal-related hormones modulate norepinephrine release in the hippocampus via influences on brainstem nuclei. Behav Brain Res 153, 87-95.

Miyashita-Lin, E. M., Hevner, R., Wassarman, K. M., Martinez, S., and Rubenstein, J. L. (1999). Early neocortical regionalization in the absence of thalamic innervation. Science 285, 906-909.

Miyata, T., Kawaguchi, A., Okano, H., and Ogawa, M. (2001). Asymmetric inheritance of radial glial fibers by cortical neurons. Neuron 31, 727-741.

Miyata, T., Kawaguchi, A., Saito, K., Kawano, M., Muto, T., and Ogawa, M. (2004). Asymmetric production of surface-dividing and non-surface-dividing cortical progenitor cells. Development 131, 3133-3145.

Mizuguchi, R., Sugimori, M., Takebayashi, H., Kosako, H., Nagao, M., Yoshida, S., Nabeshima, Y., Shimamura, K., and Nakafuku, M. (2001). Combinatorial roles of olig2 and neurogenin2 in the coordinated induction of pan-neuronal and subtype-specific properties of motoneurons. Neuron 31, 757-771.

Molnar, Z., Metin, C., Stoykova, A., Tarabykin, V., Price, D. J., Francis, F., Meyer, G., Dehay, C., and Kennedy, H. (2006). Comparative aspects of cerebral cortical development. Eur J Neurosci 23, 921-934.

Molyneaux, B. J., Arlotta, P., Hirata, T., Hibi, M., and Macklis, J. D. (2005). Fezl is required for the birth and specification of corticospinal motor neurons. Neuron 47, 817-831.

Morgan, R. (2004). Conservation of sequence and function in the Pax6 regulatory elements. Trends Genet 20, 283-287.

Muzio, L., DiBenedetto, B., Stoykova, A., Boncinelli, E., Gruss, P., and Mallamaci, A. (2002). Conversion of cerebral cortex into basal ganglia in Emx2(-/-) Pax6(Sey/Sey) double-mutant mice. Nat Neurosci 5, 737-745.

Muzio, L., DiBenedetto, B., Stoykova, A., Boncinelli, E., Gruss, P., and Mallamaci, A. (2002). Emx2 and Pax6 control regionalization of the pre-neuronogenic cortical primordium. Cereb Cortex 12, 129-139.

Nacher, J., Varea, E., Blasco-Ibanez, J. M., Castillo-Gomez, E., Crespo, C., Martinez-Guijarro, F. J., and McEwen, B. S. (2005). Expression of the transcription factor Pax 6 in the adult rat dentate gyrus. J Neurosci Res 81, 753-761.

Nakagawa, Y., Johnson, J. E., and O'Leary, D. D. (1999). Graded and areal expression patterns of regulatory genes and cadherins in embryonic neocortex independent of thalamocortical input. J Neurosci 19, 10877-10885.

Nakagawa, Y., and O'Leary, D. D. (2003). Dynamic patterned expression of orphan nuclear receptor genes RORalpha and RORbeta in developing mouse forebrain. Dev Neurosci 25, 234-244.

Nakatomi, H., Kuriu, T., Okabe, S., Yamamoto, S., Hatano, O., Kawahara, N., Tamura, A., Kirino, T., and Nakafuku, M. (2002). Regeneration of hippocampal pyramidal neurons after ischemic brain injury by recruitment of endogenous neural progenitors. Cell 110, 429-441.

Navarro-Quiroga, I., Hernandez-Valdes, M., Lin, S. L., and Naegele, J. R. (2006). Postnatal cellular contributions of the hippocampus subventricular zone to the dentate gyrus, corpus callosum, fimbria, and cerebral cortex. J Comp Neurol 497, 833-845.

Neuman, T., Keen, A., Zuber, M. X., Kristjansson, G. I., Gruss, P., and Nornes, H. O. (1993). Neuronal expression of regulatory helix-loop-helix factor Id2 gene in mouse. Dev Biol 160, 186-195.

Nieto, M., Schuurmans, C., Britz, O., and Guillemot, F. (2001). Neural bHLH genes control the neuronal versus glial fate decision in cortical progenitors. Neuron 29, 401-413.

Niikura, T., Hashimoto, Y., Tajima, H., Ishizaka, M., Yamagishi, Y., Kawasumi, M., Nawa, M., Terashita, K., Aiso, S., and Nishimoto, I. (2003). A tripartite motif protein TRIM11 binds and destabilizes Humanin, a neuroprotective peptide against Alzheimer's disease-relevant insults. Eur J Neurosci 17, 1150-1158.

Noctor, S. C., Martinez-Cerdeno, V., Ivic, L., and Kriegstein, A. R. (2004). Cortical neurons arise in symmetric and asymmetric division zones and migrate through specific phases. Nat Neurosci 7, 136-144.

O'Leary, D. D. (1989). Do cortical areas emerge from a protocortex? Trends Neurosci 12, 400-406.

O'Leary, D. D., and Nakagawa, Y. (2002). Patterning centers, regulatory genes and extrinsic mechanisms controlling arealization of the neocortex. Curr Opin Neurobiol 12, 14-25.

Obrig, T. G., Culp, W. J., McKeehan, W. L., and Hardesty, B. (1971). The mechanism by which cycloheximide and related glutarimide antibiotics inhibit peptide synthesis on reticulocyte ribosomes. J Biol Chem 246, 174-181.

Onuma, Y., Takahashi, S., Asashima, M., Kurata, S., and Gehring, W. J. (2002). Conservation of Pax 6 function and upstream activation by Notch signaling in eye development of frogs and flies. Proc Natl Acad Sci U S A 99, 2020-2025.

Parnavelas, J. G., and Nadarajah, B. (2001). Radial glial cells. are they really glia? Neuron 31, 881-884.

Patrick, G. N., Zhou, P., Kwon, Y. T., Howley, P. M., and Tsai, L. H. (1998). p35, the neuronal-specific activator of cyclin-dependent kinase 5 (Cdk5) is degraded by the ubiquitin-proteasome pathway. J Biol Chem 273, 24057-24064.

Peng, H., Feldman, I., and Rauscher, F. J., 3rd (2002). Hetero-oligomerization among the TIF family of RBCC/TRIM domain-containing nuclear cofactors: a potential mechanism for regulating the switch between coactivation and corepression. J Mol Biol 320, 629-644.

Planque, N., Leconte, L., Coquelle, F. M., Benkhelifa, S., Martin, P., Felder-Schmittbuhl, M. P., and Saule, S. (2001). Interaction of Maf transcription factors with Pax-6 results in synergistic activation of the glucagon promoter. J Biol Chem 276, 35751-35760. Epub 32001 Jul 35716.

Planque, N., Leconte, L., Coquelle, F. M., Martin, P., and Saule, S. (2001). Specific Pax-6/microphthalmia transcription factor interactions involve their DNA-binding domains and inhibit transcriptional properties of both proteins. J Biol Chem 276, 29330-29337. Epub 22001 May 29311.

Puelles, L., and Rubenstein, J. L. (1993). Expression patterns of homeobox and other putative regulatory genes in the embryonic mouse forebrain suggest a neuromeric organization. Trends Neurosci 16, 472-479.

Puelles, L., Kuwana, E., Puelles, E., Bulfone, A., Shimamura, K., Keleher, J., Smiga, S., and Rubenstein, J. L. (2000). Pallial and subpallial derivatives in the embryonic chick and mouse telencephalon, traced by the expression of the genes Dlx-2, Emx-1, Nkx-2.1, Pax-6, and Tbr-1. J Comp Neurol 424, 409-438.

Qian, X., Shen, Q., Goderie, S. K., He, W., Capela, A., Davis, A. A., and Temple, S. (2000). Timing of CNS cell generation: a programmed sequence of neuron and glial cell production from isolated murine cortical stem cells. Neuron 28, 69-80.

Qiu, L., Joazeiro, C., Fang, N., Wang, H. Y., Elly, C., Altman, Y., Fang, D., Hunter, T., and Liu, Y. C. (2000). Recognition and ubiquitination of Notch by Itch, a hect-type E3 ubiquitin ligase. J Biol Chem 275, 35734-35737.

Quinn, J. C., Molinek, M., Martynoga, B. S., Zaki, P. A., Faedo, A., Bulfone, A., Hevner, R. F., West, J. D., and Price, D. J. (2006). Pax6 controls cerebral cortical cell number by regulating exit from the cell cycle and specifies cortical cell identity by a cell autonomous mechanism. Dev Biol 22, 22.

Quiring, R., Walldorf, U., Kloter, U., and Gehring, W. J. (1994). Homology of the eyeless gene of Drosophila to the Small eye gene in mice and Aniridia in humans. Science 265, 785-789.

Rajewsky, K., Gu, H., Kuhn, R., Betz, U. A., Muller, W., Roes, J., and Schwenk, F. (1996). Conditional gene targeting. J Clin Invest 98, 600-603.

Rakic, P. (1988). Specification of cerebral cortical areas. Science 241, 170-176.

Reymond, A., Meroni, G., Fantozzi, A., Merla, G., Cairo, S., Luzi, L., Riganelli, D., Zanaria, E., Messali, S., Cainarca, S., et al. (2001). The tripartite motif family identifies cell compartments. Embo J 20, 2140-2151.

Richardson, J., Cvekl, A., and Wistow, G. (1995). Pax-6 is essential for lens-specific expression of zeta-crystallin. Proc Natl Acad Sci U S A 92, 4676-4680.

Roy, K., Kuznicki, K., Wu, Q., Sun, Z., Bock, D., Schutz, G., Vranich, N., and Monaghan, A. P. (2004). The Tlx gene regulates the timing of neurogenesis in the cortex. J Neurosci 24, 8333-8345.

Rubenstein, J. L., Martinez, S., Shimamura, K., and Puelles, L. (1994). The embryonic vertebrate forebrain: the prosomeric model. Science 266, 578-580.

Sakai, M., Serria, M. S., Ikeda, H., Yoshida, K., Imaki, J., and Nishi, S. (2001). Regulation of c-maf gene expression by Pax6 in cultured cells. Nucleic Acids Res 29, 1228-1237.

Sakurai, M., Ayukawa, K., Setsuie, R., Nishikawa, K., Hara, Y., Ohashi, H., Nishimoto, M., Abe, T., Kudo, Y., Sekiguchi, M., et al. (2006). Ubiquitin C-terminal hydrolase L1 regulates the morphology of neural progenitor cells and modulates their differentiation. J Cell Sci 119, 162-171.

Sauer, B., and Henderson, N. (1989). Cre-stimulated recombination at loxP-containing DNA sequences placed into the mammalian genome. Nucleic Acids Res 17, 147-161.

Scardigli, R., Baumer, N., Gruss, P., Guillemot, F., and Le Roux, I. (2003). Direct and concentration-dependent regulation of the proneural gene Neurogenin2 by Pax6. Development 130, 3269-3281.

Schaeren-Wiemers, N., Andre, E., Kapfhammer, J. P., and Becker-Andre, M. (1997). The expression pattern of the orphan nuclear receptor RORbeta in the developing and adult rat nervous system suggests a role in the processing of sensory information and in circadian rhythm. Eur J Neurosci 9, 2687-2701.

Schedl, A., Ross, A., Lee, M., Engelkamp, D., Rashbass, P., van Heyningen, V., and Hastie, N. D. (1996). Influence of PAX6 gene dosage on development: overexpression causes severe eye abnormalities. Cell 86, 71-82.

Schmahl, W., Knoedlseder, M., Favor, J., and Davidson, D. (1993). Defects of neuronal migration and the pathogenesis of cortical malformations are associated with Small eye (Sey) in the mouse, a point mutation at the Pax-6-locus. Acta Neuropathol (Berl) 86, 126-135.

Schuurmans, C., Armant, O., Nieto, M., Stenman, J. M., Britz, O., Klenin, N., Brown, C., Langevin, L. M., Seibt, J., Tang, H., et al. (2004). Sequential phases of cortical specification involve Neurogenin-dependent and -independent pathways. Embo J 23, 2892-2902. Epub 2004 Jul 2891.

Seo, S., Herr, A., Lim, J. W., Richardson, G. A., Richardson, H., and Kroll, K. L. (2005). Geminin regulates neuronal differentiation by antagonizing Brg1 activity. Genes Dev 19, 1723-1734.

Seo, S., Richardson, G. A., and Kroll, K. L. (2005). The SWI/SNF chromatin remodeling protein Brg1 is required for vertebrate neurogenesis and mediates transactivation of Ngn and NeuroD. Development 132, 105-115.

Shimono, Y., Murakami, H., Hasegawa, Y., and Takahashi, M. (2000). RET finger protein is a transcriptional repressor and interacts with enhancer of polycomb that has dual transcriptional functions. J Biol Chem 275, 39411-39419.

Simpson, T. I., and Price, D. J. (2002). Pax6; a pleiotropic player in development. Bioessays 24, 1041-1051.

Singh, S., Tang, H. K., Lee, J. Y., and Saunders, G. F. (1998). Truncation mutations in the transactivation region of PAX6 result in dominant-negative mutants. J Biol Chem 273, 21531-21541.

Singh, S., Chao, L. Y., Mishra, R., Davies, J., and Saunders, G. F. (2001). Missense mutation at the C-terminus of PAX6 negatively modulates homeodomain function. Hum Mol Genet 10, 911-918.

Sisodiya, S. M., Free, S. L., Williamson, K. A., Mitchell, T. N., Willis, C., Stevens, J. M., Kendall, B. E., Shorvon, S. D., Hanson, I. M., Moore, A. T., and van Heyningen, V. (2001). PAX6 haploinsufficiency causes cerebral malformation and olfactory dysfunction in humans. Nat Genet 28, 214-216.

Sivak, J. M., West-Mays, J. A., Yee, A., Williams, T., and Fini, M. E. (2004). Transcription Factors Pax6 and AP-2alpha Interact To Coordinate Corneal Epithelial Repair by Controlling Expression of Matrix Metalloproteinase Gelatinase B. Mol Cell Biol 24, 245-257.

St-Onge, L., Sosa-Pineda, B., Chowdhury, K., Mansouri, A., and Gruss, P. (1997). Pax6 is required for differentiation of glucagon-producing alpha-cells in mouse pancreas. Nature 387, 406-409.

Stenman, J., Toresson, H., and Campbell, K. (2003). Identification of two distinct progenitor populations in the lateral ganglionic eminence: implications for striatal and olfactory bulb neurogenesis. J Neurosci 23, 167-174.

Stern, C. D. (2001). Initial patterning of the central nervous system: how many organizers? Nat Rev Neurosci 2, 92-98.

Stoykova, A., and Gruss, P. (1994). Roles of Pax-genes in developing and adult brain as suggested by expression patterns. J Neurosci 14, 1395-1412.

Stoykova, A., Fritsch, R., Walther, C., and Gruss, P. (1996). Forebrain patterning defects in Small eye mutant mice. Development 122, 3453-3465.

Stoykova, A., Gotz, M., Gruss, P., and Price, J. (1997). Pax6-dependent regulation of adhesive patterning, R-cadherin expression and boundary formation in developing forebrain. Development 124, 3765-3777.

Stoykova, A., Treichel, D., Hallonet, M., and Gruss, P. (2000). Pax6 modulates the dorsoventral patterning of the mammalian telencephalon. J Neurosci 20, 8042-8050.

Stoykova, A., Hatano, O., Gruss, P., and Gotz, M. (2003). Increase in reelin-positive cells in the marginal zone of Pax6 mutant mouse cortex. Cereb Cortex 13, 560-571.

Streit, A., and Stern, C. D. (1999). Neural induction. A bird's eye view. Trends Genet 15, 20-24.

Sun, Y., Nadal-Vicens, M., Misono, S., Lin, M. Z., Zubiaga, A., Hua, X., Fan, G., and Greenberg, M. E. (2001). Neurogenin promotes neurogenesis and inhibits glial differentiation by independent mechanisms. Cell 104, 365-376.

Sur, M., and Rubenstein, J. L. (2005). Patterning and plasticity of the cerebral cortex. Science 310, 805-810.

Takebayashi, H., Yoshida, S., Sugimori, M., Kosako, H., Kominami, R., Nakafuku, M., and Nabeshima, Y. (2000). Dynamic expression of basic helix-loop-helix Olig family members: implication of Olig2 in neuron and oligodendrocyte differentiation and identification of a new member, Olig3. Mech Dev 99, 143-148.

Tang, H. K., Singh, S., and Saunders, G. F. (1998). Dissection of the transactivation function of the transcription factor encoded by the eye developmental gene PAX6. J Biol Chem 273, 7210-7221.

Tarabykin, V., Stoykova, A., Usman, N., and Gruss, P. (2001). Cortical upper layer neurons derive from the subventricular zone as indicated by Svet1 gene expression. Development 128, 1983-1993.

Tole, S., Remedios, R., Saha, B., and Stoykova, A. (2005). Selective requirement of Pax6, but not Emx2, in the specification and development of several nuclei of the amygdaloid complex. J Neurosci 25, 2753-2760.

Tominaga, T., Meng, W., Togashi, K., Urano, H., Alberts, A. S., and Tominaga, M. (2002). The Rho GTPase effector protein, mDia, inhibits the DNA binding ability of the transcription factor Pax6 and changes the pattern of neurite extension in cerebellar granule cells through its binding to Pax6. J Biol Chem 277, 47686-47691. Epub 42002 Sep 47624.

Toresson, H., Potter, S. S., and Campbell, K. (2000). Genetic control of dorsal-ventral identity in the telencephalon: opposing roles for Pax6 and Gsh2. Development 127, 4361-4371.

Tozuka, Y., Fukuda, S., Namba, T., Seki, T., and Hisatsune, T. (2005). GABAergic excitation promotes neuronal differentiation in adult hippocampal progenitor cells. Neuron 47, 803-815.

Uylings, H. B., Groenewegen, H. J., and Kolb, B. (2003). Do rats have a prefrontal cortex? Behav Brain Res 146, 3-17.

Voelker, C. C., Garin, N., Taylor, J. S., Gahwiler, B. H., Hornung, J. P., and Molnar, Z. (2004). Selective neurofilament (SMI-32, FNP-7 and N200) expression in subpopulations of layer V pyramidal neurons in vivo and in vitro. Cereb Cortex 14, 1276-1286.

Walsh, G., and Jefferis, R. (2006). Post-translational modifications in the context of therapeutic proteins. Nat Biotechnol 24, 1241-1252.

Walther, C., and Gruss, P. (1991). Pax-6, a murine paired box gene, is expressed in the developing CNS. Development 113, 1435-1449.

Wang, Y., Li, Y., Qi, X., Yuan, W., Ai, J., Zhu, C., Cao, L., Yang, H., Liu, F., Wu, X., and Liu, M. (2004). TRIM45, a novel human RBCC/TRIM protein, inhibits transcriptional activities of ElK-1 and AP-1. Biochem Biophys Res Commun 323, 9-16.

Warren, N., and Price, D. J. (1997). Roles of Pax-6 in murine diencephalic development. Development 124, 1573-1582.

Warren, N., Caric, D., Pratt, T., Clausen, J. A., Asavaritikrai, P., Mason, J. O., Hill, R. E., and Price, D. J. (1999). The transcription factor, Pax6, is required for cell proliferation and differentiation in the developing cerebral cortex. Cereb Cortex 9, 627-635.

Weinmann, A. S., Yan, P. S., Oberley, M. J., Huang, T. H., and Farnham, P. J. (2002). Isolating human transcription factor targets by coupling chromatin immunoprecipitation and CpG island microarray analysis. Genes Dev 16, 235-244.

Wichterle, H., Garcia-Verdugo, J. M., Herrera, D. G., and Alvarez-Buylla, A. (1999). Young neurons from medial ganglionic eminence disperse in adult and embryonic brain. Nat Neurosci 2, 461-466.

Wichterle, H., Turnbull, D. H., Nery, S., Fishell, G., and Alvarez-Buylla, A. (2001). In utero fate mapping reveals distinct migratory pathways and fates of neurons born in the mammalian basal forebrain. Development 128, 3759-3771.

Wilson, P. A., and Hemmati-Brivanlou, A. (1997). Vertebrate neural induction: inducers, inhibitors, and a new synthesis. Neuron 18, 699-710.

Wonders, C. P., and Anderson, S. A. (2006). The origin and specification of cortical interneurons. Nat Rev Neurosci 7, 687-696.

Wu, X., Bayle, J. H., Olson, D., and Levine, A. J. (1993). The p53-mdm-2 autoregulatory feedback loop. Genes Dev 7, 1126-1132.

Xi, R., and Xie, T. (2005). Stem cell self-renewal controlled by chromatin remodeling factors. Science 310, 1487-1489.

Xu, P. X., Zhang, X., Heaney, S., Yoon, A., Michelson, A. M., and Maas, R. L. (1999). Regulation of Pax6 expression is conserved between mice and flies. Development 126, 383-395.

Yamaguchi, H., Zhou, C., Lin, S. C., Durand, B., Tsai, S. Y., and Tsai, M. J. (2004). The nuclear orphan receptor COUP-TFI is important for differentiation of oligodendrocytes. Dev Biol 266, 238-251.

Yun, K., Potter, S., and Rubenstein, J. L. (2001). Gsh2 and Pax6 play complementary roles in dorsoventral patterning of the mammalian telencephalon. Development 128, 193-205.

Zaniolo, K., Leclerc, S., Cvekl, A., Vallieres, L., Bazin, R., Larouche, K., and Guerin, S. L. (2004). Expression of the alpha4 integrin subunit gene promoter is modulated by the transcription factor Pax-6 in corneal epithelial cells. Invest Ophthalmol Vis Sci 45, 1692-1704.

Zhou, C., Tsai, S. Y., and Tsai, M. J. (2001). COUP-TFI: an intrinsic factor for early regionalization of the neocortex. Genes Dev 15, 2054-2059.

Zimmer, C., Tiveron, M. C., Bodmer, R., and Cremer, H. (2004). Dynamics of Cux2 expression suggests that an early pool of SVZ precursors is fated to become upper cortical layer neurons. Cereb Cortex 14, 1408-1420. Epub 2004 Jul 1406.

Curriculum vitae

Personal data

Surname	:	Tuoc
Forename	:	Tran Cong
Nationality	:	Vietnamese
Birthth	:	28-10-1976
Marital Status	:	Married
Address	:	Department of Molecular Cell Biology, Max-Planck-Institute for Biophysical Chemistry Am Fassberg 11 37077 – Göttingen – Germany
Telephone	:	0049-551-2011469
Fax	:	0049-551-2011504
Email	:	tcong@gwdg.de

Scientific Education

2004-2007	:	PhD student in the Department of Molecular Cell Biology, Max-Planck-Institute for Biophysical Chemistry, Göttingen, Germany
2000-2002	:	Masters study- International Masters program (Major: Biotechnology) - University of Hannover (Germany)
1998-2000	:	Research assistant-Department of Molecular Biology and Genetics engineering-Institute of Biotechnology (IBT)-Vietnamese Academy of Science & Technology
1994-1998	:	B.Sc. Biology- Vietnam National University (Vietnam)

Publications

1. Tuoc, T., Radushkin, K., Pinon, M., Ashery-Padan, R., Molnar, Z., Davidoff, M., Gruss, P and Stoykova, A. Layer-specific defects and behaviour abnormalities in the cortex specific Pax6 knock out mice. Submitted
2. Berger, J., Berger, S., Tuoc, T. C., D'Amelio, M., Cecconi, F., Gorski, J. A., Jones, K. R., Gruss, P., and Stoykova, A. (2007). Conditional activation of Pax6 in the developing cortex of transgenic mice causes progenitor apoptosis. Development 28, 28.